2016

Evaluation of regional, very heavy precipitation events in the upper Mississippi region using climate model ensembles

Sho Kawazoe
Iowa State University

Evaluation of regional, very heavy precipitation events in the upper Mississippi region using climate model ensembles

by

Sho Kawazoe

A dissertation submitted to the graduate faculty

in partial fulfillment of the requirements for the degree of

DOCTOR OF PHILOSOPHY

Major: Meteorology

Program of Study Committee:
William J. Gutowski Jr., Major Professor
Raymond W. Arritt
Kristie J. Franz
Gene S. Takle
Xiaoqing Wu

Iowa State University

Ames, Iowa

2016

TABLE OF CONTENTS

LIST OF FIGURES

Chapter 2:

Chapter 4:

LIST OF TABLES

Chapter 2:

Chapter 3:

Chapter 4:

ACKNOWLEDGMENTS

"A single arrow is easily broken, but not ten in a bundle."- Japanese proverb.

This implies that while one person may have inherent limitations, the support of others can yield great accomplishments. This dissertation is in no part an independent effort, but a culmination of the all the support I've received during my tenure at Iowa State University.

First, I would like to thank my major professor, Dr. Gutowski for his guidance, expertise, and patience for the last 7 years. Regardless of his busy schedule, his assistance was always available, and his promotion to associate dean exemplifies the respect so many have for him. He has been an inspiration, and I am forever grateful for all the opportunity he has given me. It has been an honor to work under his supervision, and I hope that as I advance through my career, I am able to repay the commitment he has shown in me. I will miss our talks, especially during the baseball season.

I would like to thank my committee members for their expertise and suggestions. Their recommendation will go a long way in preparing my material for publication. I would also like to offer my sincere gratitude to all of the faculty members in the meteorology program. They have provided me the fundamental understanding of the physical processes of the atmosphere, and the foundation I've gained from the program is what allowed me to achieve my Bachelors, Masters, and Ph.D degrees. Thank you to my graduate colleagues. Our many conversations and friendships is something I will cherish for the rest of my life. Your dedication to your research was a true motivation for me and kept me focused on the task at hand. This program, and everyone associated with it, will always have a special place in my heart.

Finally, to my parents, Takashi and Mieko, and my brothers, Ko and Sun. As I look back throughout my academic career, your love and support was never wavering. You have been a

true role model, and I have been able to get through my struggles because I knew I could count on each one of you. As I wrap up my career here at Iowa State, my hope is that I have become the son/brother that you can be proud of, just like I am of you. Thank you, from the bottom of my heart.

ABSTRACT

Projected increases in temperature and moisture in future climates promote a more favorable environment for very heavy/extreme precipitation events. Although precipitation events at the highest intensities have increased in the last ~50 years and are projected to continue into the future, climate models can have difficulty replicating very heavy events seen in observations, often due to coarse horizontal and vertical resolutions. Global climate models (GCMs) with horizontal resolution spanning usually around 100~300km may be able to replicate winter storms, which have larger spatial characteristics, but often fail to replicate summer events, as Mesoscale Convective Systems (MCSs) dominate the precipitation characteristics in the central U.S. MCSs often occur at a much small spatial scale than winter storms. High resolution (~50km to finer horizontal resolution) regional climate models (RCMs) may provide a better rendition of MCSs. Climate models provide valuable information to the scientific community, as evidenced by an abundance of peer-reviewed literature evaluating extreme events in climate simulations. Continued improvement in the structure of climate models has produced results more consistent with observations.

GCMs from the Coupled Model Intercomparison Project – Phase 5 (CMIP5), and RCMs from the North American Regional Climate Change Assessment Program (NARCCAP) are used in this study. The domain examined is an upper Mississippi region. In Chapter 2, CMIP5 models are compared with observations during the winter (December-February) months. The analysis reveals that CMIP5 models agree fairly well observations, though coarser resolution GCMs produce a smoother spatial distribution of heavy precipitation. In the remaining studies, NARCCAP RCMs are examined along with observations during the summer months (June – August). Chapter 3 examines the contemporary climate. Results show that while most models

produce credible simulations of widespread very heavy events with respect to observations, biases are present for particular simulations, and is highlighted in this study. In Chapter 4, climate change of summertime widespread very heavy precipitation events is examined. Most models project a decrease in average precipitation but an increase in intensity and frequency of very heavy precipitation. Areas of projected precipitation increase occur in areas where conditions will become more favorable for convective storm development.

CHAPTER 1

GENERAL INTRODUCTION

1. Introduction

Extremely heavy precipitation events, especially those leading to massive flooding, can inflict tremendous stress on the natural and social-economic systems. For the U.S. Midwest, where agricultural farmland covers more than two-thirds of the land use and dominates the regional economy (Pryor et al. 2013), flooding is of heightened concern to the community. Two leading examples are the 1993 Midwest flood (Kunkel et al. 1994; Gumley and King 1995) and the 2008 Midwest flood (Dirmeyer and Kinter 2009; Hoke 2009), which caused an estimated $21 billion and $15 billion in damages, respectively (Lavers and Villarini 2013).

However, the 1993 and 2008 floods are also examples of how difficult forecasting such events can be. The 2008 Midwest floods occurred one month earlier, were shorter lived, and in a slightly different area than the 1998 Midwest floods (Coleman and Budikova 2010). Also, both flooding events were exacerbated by higher than normal precipitation in the late summer to fall of the year before. The abundance of peer-reviewed literature available for these two events alone shows how different environmental conditions can alter the characteristics of very heavy precipitation events.

As the climate rapidly changes, there is increasingly strong evidence from both observations and climate models to suggest that frequency and intensity of extreme/very heavy precipitation events will increase (Emori and Brown 2005; Frei et al. 2006; Wuebbles et al. 2014). This could result in a higher frequency of floods such as those seen in 1993 and 2008. Because these trends are projected to continue, stakeholders and policy makers require

information on expected changes in order to mitigate and adapt to the changing climate. Climate models are used to offer such information, as they provide simulations for both contemporary (past) and scenario (future) climates.

For this dissertation, we will use ensembles of climate simulations from two modeling groups:

- Global climate models (GCMs) from the Coupled Model Intercomparison Project – Phase 5 (CMIP5; Taylor et al. 2012), and
- Regional climate models (RCMs) from the North American Regional Climate Change Assessment Program (NARCCAP; Mearns et al. 2009, 2012).

We will use the multi-model ensemble from CMIP5 and NARCCAP to provide a comprehensive picture of the uncertainties that are present in climate models. Using an ensemble of models that are each structurally different may provide collectively more consistent and reliable simulations (Mailhot et al. 2011).

The goals of this study are to assess the ability climate models collectively to reproduce very heavy precipitation seen in observations, to determine if they produce very heavy precipitation for the same physical conditions as in observations, and to provide a baseline for understanding how very heavy events and its causes processes change under enhanced greenhouse warming scenarios. These goals are guided by our study objective, which is to offer a methodology for assessing the capability of climate models to produce very heavy precipitation events.

We will address these goals by (1) extracting very heavy daily precipitation events in models and observations, (2) evaluating the behavior of the environmental fields leading up to

the very heavy event, and (3) diagnosing if future-scenario simulations produce an environment that is more favorable for stronger storms yielding very heavy precipitation events.

This study builds on our previous manuscripts, which focused on very heavy precipitation events during the winter season in the upper Mississippi basin. Both Gutowski et al. (2010) and Kawazoe and Gutowski (2013) used RCMs from NARCCAP, with the former using monthly time scales, and the latter using daily time scales. Both studies showed that models were able to reproduce widespread, very heavy precipitation events under the same physical conditions seen in observations.

2. Dissertation Organization

This dissertation consists of three manuscripts. Chapter 2 analyzes widespread, very heavy precipitation events using GCMs from CMIP5. The purpose of this study is to determine if CMIP5 ensembles, with their varying horizontal resolutions, are able to replicate both winter (December-February) heavy precipitation and its supporting environmental characteristics seen in observations. Chapter 3 uses RCMs from NARCCAP to study summer, widespread very heavy precipitation events, and to evaluate the performance of climate models to produce very heavy events in under the same physical conditions as observations. Although the goal of this study is similar to Chapter 2, differences in model ensembles and evaluation season, among others, substantially alters the direction of this study compared to Chapter 2. Chapter 4 uses Chapter 3 as its foundation but uses NARCCAP models to examine changes in the scenario climate during the summer season. The performance of contemporary climate simulations gives us insight into the level of confidence we can give to the NARCCAP ensembles.

3. References

Coleman, J.S.M., and D. Budikova, 2010: Atmospheric aspects of the 2008 Midwest floods: a repeat of 1993? *International Journal of Climatology*, **30**, 1645-1667, doi:10.1002/joc.2009.

Dirmeyer, P. A., and J. L. Kinter III, 2009: The "Maya Express": Floods in the U.S. Midwest. *Eos, Trans. Amer. Geophys. Union*, **90**, 101–102, doi:10.1029/2009EO120001.

Emori, S., A. Hasegawa, T. Suzuki, and K. Dairaku. 2005: Validation, parameterization dependence and future projection of daily precipitation simulated with a high-resolution atmospheric GCM. *Geophys. Res. Lett.*, **32**, L06708, doi:10.1029/2004GL022306.

Frei, C., R. Schooll, S. Fukutome, J. Schmidli, and P. L. Vidale, 2006: Future change of precipitation extremes in Europe: Intercomparison of scenarios from regional climate models. *J. Geophys. Res.*, **111**, D06105, doi:10.1029/2005JD005965.

Gumley, L. E., and M. D. King, 1995: Remote sensing of flooding in the U.S. upper Midwest during the summer of 1993. *Bull. Amer. Meteor. Soc.*, **76,** 933–943, doi: 10.1175/1520-0477(1995)076<0933:RSOFIT>2.0.CO;2

Gutowski, W. J., and Coauthors, 2010: Regional extreme monthly precipitation simulated by NARCCAP RCMs. *J. Hydrometeor.,* **11**, 1373–1379, doi:10.1175/2010JHM1297.1.

Hoke, J. E., 2009: The Midwest flooding of June 2008: A National Weather Service assessment. *Proc. Impacts of 2008,* Phoenix, AZ, Amer. Meteor. Soc., 3.1. [Available online at http://ams.confex.com/ams/89annual/techprogram/paper_152059.htm].

Kawazoe, S., and W.J. Gutowski. 2013a: Regional, Very Heavy Daily Precipitation in NARCCAP Simulations. *J. Hydrometeor*., **14**, 1212-1227, doi:10.1175/JHM-D-12-068.1.

Lavers, D. A., and G. Villarini, 2013: Atmospheric rivers and flooding over the central United States. *J. Climate*, **26**,7829–7836, doi:10.1175/JCLI-D-13-00212.1.

Mailhot, A., I. Beauregard, G. Talbot, D. Caya, and S. Biner, 2011: Future changes in intense precipitation over Canada assessed from multi-model NARCCAP ensemble simulations, *Int. J. Climatol*., **32**, 1151-1163, doi:10.1002/joc.2343.

Mearns, L. O., W. J. Gutowski, R. Jones, L.-Y. Leung, S. McGinnis, A. M. B. Nunes, and Y. Qian, 2009: A regional climate change assessment program for North America. *Eos, Trans. Amer.Geophys. Union*, **90,** 311, doi:10.1029/2009EO360002.

Mearns, L.O., and Coauthors, 2012: The North American Regional Climate Change Assessment Program: Overview of Phase I results. *Bull. Amer. Meteor. Soc.*, **93**, 1337–1362, doi:10.1175/BAMS-D-11-00223.1.

Pryor, S. C., R. J. Barthelmie, and J. T. Schoof, 2013: High-resolution projections of climate impacts for the midwestern USA. *Climate Research*, **56**, 61-79, doi:10.3354/cr01143

Taylor, K. E., R. J. Stouffer, and G. A. Meehl, 2012: An overview of CMIP5 and the experiment design. *Bull. Amer. Meteor. Soc*., **93**, 485–498, doi:10.1175/BAMS-D-11-00094.1.

Wuebbles, D. J., K. Kunkel, M. Wehner, and Z. Zobel, 2014: Severe weather in United States under a changing climate, *Eos Trans AGU*, **95**(18), 149–150, doi: 10.1002/2014EO180001.

CHAPTER 2

REGIONAL, VERY HEAVY DAILY PRECIPITATION IN CMIP5 SIMULATIONS

Published in *Journal of Hydrometeorology*, March 2013

Sho Kawazoe and William J. Gutowski Jr.

Abstract

The authors analyze the ability of global climate models (GCMs) from phase 5 of the Coupled Model Intercomparison Project (CMIP5) multimodel ensemble to simulate very heavy daily precipitation and its supporting processes, comparing them with observations. Their analysis focuses on an upper Mississippi region for winter (December–February), when it is assumed that resolved synoptic circulation governs precipitation.

CMIP5 GCMs generally reproduce well the precipitation versus intensity spectrum seen in observations to intensities as strong as 20 mm day^{-1}. Most models do not produce the highest precipitation intensities seen in observations. Models show good agreement at the 95th percentile, while the coarsest resolution models generally show lower precipitation at high-intensity thresholds, such as the 99.5th percentile. There is no dominant month for simulated very heavy events to occur, although observed very heavy events occur most frequently in December. Further analysis focuses on precipitation events exceeding the 99.5th percentile that occur simultaneously at several points in the region, yielding so-called "widespread events." Examination of additional fields during widespread very heavy events shows that the models produce these events under the same physical conditions seen in the observations. The coarsest models generally produce similar behavior, although features have smoother spatial distributions.

However, the resolution in itself could not be identified as a major reason that separates one model from another. The capabilities of the CMIP5 GCMs examined here support using them to assess changes in very heavy precipitation under future climate scenarios.

1. Introduction

With enhancements in climate models' ability to simulate past and future climate, one topic that has gained attention is very heavy events accompanying global climate change. Increased variability in winds, temperature, and precipitation, among others, are of great interest to both the scientific community and the general public because of the social and economic impacts these events can cause. To validate these climate models, simulations need to be compared with observational data to determine if physical behaviors causing these events in models are similar to those in the real world. By using projections based on validated models, one can make analyses and decisions concerning future climate change with greater confidence.

Here we analyze very heavy daily precipitation events, as defined by Groisman et al. (2005), during the winter months in the upper Mississippi region. We use climate simulations produced by 21 global climate models (GCMs) for phase 5 of the Coupled Model Intercomparison Project (CMIP5) multimodel ensemble (Taylor et al. 2012). A major portion of this paper is motivated by previous work by Kawazoe and Gutowski (2013), who focused on very heavy winter precipitation in the same region, but by regional climate models (RCMs) from the North American Regional Climate Change Assessment Program (NARCCAP). The goals of this study are to assess the ability of the CMIP5 models collectively to reproduce very heavy daily precipitation in observations, to produce very heavy precipitation for the same physical conditions as in observations, and to provide a baseline for understanding how very heavy daily

precipitation and its causal processes change under enhanced greenhouse warming scenarios. We note, however, that while this capability is a necessary condition for using the models to assess climate change for very heavy precipitation events, assessment of changes would have to assume that these models capture enhanced greenhouse gas scenarios appropriately.

2. Observations, Simulations, and Analysis Methods

a. Observations

The analysis uses the University of Washington's (UW) gridded precipitation (Maurer et al. 2002) as the primary observational data. This dataset provides observation-based precipitation on a 0.125° grid that covers all of the contiguous United States. Interpolation for this gridded dataset used the scheme of Shepard (1984) as implemented in Widmann and Bretherton (2000). The dataset also uses corrections for systematic elevation effects given by the Parameter-Elevation Regressions on Independent Slopes Model (PRISM; Daly et al. 1994). The dataset in the Network Common Data Form (NetCDF) format covers the period 1950–99.

We use the UW data as the basis for identifying days when very heavy precipitation occurs. For all other fields in the observational analysis, we used the North American Regional Reanalysis (NARR; Mesinger et al. 2006). The fields we use include 500-hPa geopotential heights, 2-m air temperature, 2-m specific humidity, and 10-m horizontal winds. These fields represent key environmental conditions during the development of very heavy precipitation events and are also common to the output archives for most of the models examined here.

b. Simulations

Model output comes from 21 global climate models that simulated the historical period 1850–2005 for CMIP5 (Table 1; Taylor et al. 2012). Analyses of all models are from the

historical experiment using the r1i1p1 ensemble member. The GCMs used in this analysis are models available in archives on 1 June 2012, with an emphasis on models that provided daily precipitation, 500-hPa geopotential heights, 2-m air temperature, 2-m specific humidity, and 10-m horizontal winds.

c. Analysis

We analyzed the period 1980–99, consistent with available UW precipitation data. Our region of interest is the upper Mississippi region, designated here as the region bounded by (37°–47°N, 89°–99°W) and highlighted in Figure 1. Resolution of each model within this region is listed on Table 2. This is the same region used in some of our previous precipitation analyses (Gutowski et al. 2008, 2010; Kawazoe and Gutowski 2013). Our analysis focuses on the winter season [December–February (DJF)], when synoptic dynamics are more important than in the warmer months, when smaller-scale convective events may be more important (e.g., Schumacher and Johnson 2005, 2006). This assumption here is that resolved circulation governs winter events, so that the other model fields we analyze are directly relevant to understanding the physical behavior of very heavy events (e.g., Gutowski et al. 2008).

We converted the original UW output to a 0.5° grid by averaging all original grid points that fell in a 0.5° box centered on the new grid point. We did this to give the dataset the same nominal resolution as the NARR and the highest-resolution GCM.

CMIP5 models are in daily increments from 0000 to 0000UTC (1800–1800 local standard time in the upper Mississippi region). The UW dataset is in daily increments from 0600 to 0600UTC (0000–0000 local standard time in the upper Mississippi region), a factor that may affect some of our results. The analysis examining conditions other than precipitation during

very heavy events used the 0000UTC fields at the start of the day, which provided information on the initial state of the atmosphere.

We defined a precipitation event as precipitation above 0.25 mm day^{-1} recorded for 1 day at one observational or model grid point, which differs with Kawazoe and Gutowski (2013), who defined a precipitation event as all nonzero records. We extracted the top 0.5% of all precipitation events as very heavy daily events. From these events, we then found widespread very heavy events by searching for multiple very heavy events occurring on the same day. The GCMs have a range of different resolutions. To determine widespread very heavy events, we adjusted all GCM output to equivalent 0.5° grid boxes to match the grid we use for the UW data Thus, a 2.5° × 3.75° grid box in the HadCM3 covers roughly (2.5/0.5) × (3.75/0.5) = 37.5 times more area than a 0.5° grid box, so one HadCM3 grid box is the equivalent of 37.5 grid boxes at 0.5°. The nominal area equivalent to 0.5° for the other GCMs is listed on Table 2. For our analysis, we designated simultaneous very heavy events on 15 or more equivalent 0.5° grid boxes as widespread events. Note that for the coarsest models, a widespread event can occur with just one grid box having a very heavy event.

We examined several atmospheric fields, listed earlier, to understand conditions conducive to very heavy events. These fields give insight into the preferred conditions for very heavy precipitation events and become the basis for assessing simulated versus observed processes yielding very heavy precipitation. The 10-m winds is used as our primary indicator of moisture flux. Although it is not perfectly synonymous with moisture flux direction and convergence, it is a low-level circulation field available from all the models. For 500-hPa geopotential heights, 2-m air temperature, and 2-m specific humidity, we examined anomalies. These anomalies are composites of fields on the days of widespread very heavy events minus the

20-yr time average during the winter season. We compute time averages separately for each model and for the observations. To gauge the magnitude of the anomalies, we also computed the 2–5-day variability of the same fields throughout the analysis period, applying to daily time series a Lanczos filter with nine weights and a cutoff frequency of 5 days.

3. Widespread Very Heavy Precipitation

Table 3 shows the average precipitation rate and frequency of daily precipitation events in the upper Mississippi region for the observations and for each model. The numbers in parentheses are the percentage of days with precipitation above 2.5 mm day^{-1}. Other than NorESM1-M and MIROC-ESM-CHEM, the models produce too much precipitation. Other than GFDL CM3, BCC-CSM1.1, and BNU-ESM, the models also produce fewer days with precipitation than observed. Similar to Kawazoe and Gutowski (2013), days with precipitation above 2.5 mm day^{-1} agree well between observations and models. This shows that fewer precipitation events below 2.5 mm day^{-1} occurred in the models than observations, indicating that CMIP5 GCMs produce fewer "drizzle" events than observed, in contrast to the NARCCAP RCMs in Kawazoe and Gutowski (2013). Recall, however, that the definition of a precipitation event in Kawazoe and Gutowski (2013) is any nonzero precipitation, whereas here we count only events with precipitation exceeding 0.25 mm day^{-1}. This difference may account for the different frequency of "drizzle" events between the two studies. The spreads across models in average precipitation rate and days with precipitation do not indicate that resolution in itself is an important factor for differences with observations.

Figures 2 and 3 show histograms of normalized frequency versus intensity in the upper Mississippi region using 2.5 mm day^{-1} bins. Figure 2 contains models with all supporting

environmental fields, and Figure 3 has additional models that did not have all supporting fields, so they are used for the precipitation analysis only. Observations and the models are in relatively good agreement up to around 20 mm day^{-1}. Other than the BNU-ESM, NorESM1-M, and MIROC-ESM-CHEM, the models show a higher frequency of precipitation in bins greater than 20 mm day^{-1} compared to observations, while not producing events at the highest intensity spectrum. MIROC4h agrees well with observations over the whole intensity spectrum, perhaps because it has a resolution similar to the grid for observations.

Table 4 shows precipitation for each model and for the observations at the 95th, 99th, and 99.5th percentiles. The models and observations show fairly good agreement at the 95th percentile. At higher percentiles, finer resolution models have very heavy events that tend to be greater than observations, with MPI-ESM-LR being a slight outlier. Excluding the CanESM2, the coarsest-resolution GCMs show precipitation lower than observations at all percentiles. This suggests that the coarsest-resolution models do not replicate intense, small-scale circulation features that are necessary for producing very heavy events.

Figures 4 and 5 show the distribution of days with simultaneous very heavy events on a given number of grid boxes. Figure 4 contains models with all supporting environmental fields, and Figure 5 has additional models that did not have all supporting fields, so they are used for the precipitation analysis only. The x axis indicates the minimum area of a multigrid-point event, thus suggesting its spatial scale. The models tend to produce very heavy events covering a larger area than the observations. MIROC4h has approximately the same resolution as the observational dataset and has a similar pattern in Figure 5.

Further analysis focuses on very heavy events occurring on at least 15 equivalent 0.5° grid boxes on the same day. We denote these as widespread very heavy events. For at least the higher-resolution models, these events are more likely to be the outcome of resolved behavior.

Table 5 shows the distribution of widespread very heavy events by winter months. There does not seem to be a dominant month for widespread very heavy events. This contrasts with the NARCCAP RCMs, driven by the National Centers for Environmental Prediction–Department of Energy (NCEP–DOE) reanalysis (Kanamitsu et al. 2002), for which five of the six had maximum frequency in December (Kawazoe and Gutowski 2013), in agreement with observations. Here only nine of the 21 models have the highest frequency of very heavy events occurring in December. The speculation for the NARCCAP models was that warmer Gulf of Mexico sea surface temperatures (SSTs) in December promote higher humidity over the Gulf and thus more atmospheric moisture for transport in the upper Mississippi region (Kunkel et al. 2002; Kawazoe and Gutowski 2013). Such a climatological control does not appear to operate here. We also examined monthly changes in large-scale baroclinicity, using temperature differences between the Gulf of Mexico and the upper Mississippi region, and found no systematic relationship with the occurrence of our very heavy events. We do find, however, that for each model, the average Gulf of Mexico SST during our widespread very heavy events is warmer than the model's climatological SST for each DJF month, usually by more than 1.5°C (not shown). Thus, warmer Gulf temperatures do promote very heavy events in these GCMs, but not for a particular month.

Figure 6 shows composite precipitation during widespread very heavy events. Composite fields are from models that provided all supporting environmental fields for this analysis, that is, models used for Figures 2 and 4. Models and observations show similar locations of very heavy precipitation, centered near the southeastern corner of our analysis region. Our analysis region in

winter is warmest to the south. The warmer air can have more precipitable water, so the composite very heavy precipitation occurs where there will generally be more moisture in the atmosphere. Also, the southern end of the analysis region is closest to the primary source of the region's precipitable water, the Gulf of Mexico. This behavior is consistent with NARCCAP RCM analysis in Kawazoe and Gutowski (2013). Precipitation intensity by the CMIP5 GCMs agrees well with the NARCCAP RCMs in Kawazoe and Gutowski (2013), though the events in the CMIP5 GCMs typically cover a broader area and thus show a smoother composite.

4. Supporting Environmental Conditions

Figures 7–10 show composite fields produced by averaging over the widespread event days from each data source. Again, the anomaly fields for a given source come from subtracting the 20-yr DJF average from the composite. The NARR provided the observational results, with the days to composite determined from analysis of the UW precipitation. Composite fields are from models that provided all supporting environmental fields for this analysis. Inspection of individual events shows that the composites for each field are representative of the behavior of individual events.

a. 500-hPa geopotential heights

As suggested by Figure 7, a key ingredient for very heavy precipitation in the upper Mississippi region is the transport of warm, moist air from the Gulf of Mexico. Composite 500-hPa heights show very heavy events occurring when a deep trough develops around the southern Rockies, promoting a more pronounced southerly flow into the region when compared with the seasonal climatology. The presence of lower heights to the west and higher heights to the east of the analysis region highlighted in Kawazoe and Gutowski (2013) is also evident in the composite

plots shown in Figure 7. The magnitudes of the largest anomalies were roughly 5 times greater than the 2–5-day variability in 500-hPa heights for the same locations (not shown). Resolution does not seem to affect the depth or location of the trough.

b. 10-m horizontal wind

Figure 8 shows the composite 10-m winds for widespread very heavy events. As with 500-hPa heights, the composites are representative of the behavior of individual events. As discussed earlier, the winds indicate the direction of moisture transport and also the location of surface pressure centers, although these winds are not perfectly synonymous with the moisture flux direction and convergence, as discussed earlier.

During the widespread very heavy events, winds turn counterclockwise to the west of the area of very heavy precipitation. The behavior corresponds to a surface low in the vicinity of Oklahoma accompanying the 500-hPa trough. This was seen in Kawazoe and Gutowski (2013) and Wendland et al. (1983), who focused on higher than average precipitation during the 1982/83 winter. In addition, the behavior shows low-level convergence. Because relatively strong winds blow from the Gulf of Mexico, the momentum convergence likely coincides with the moisture convergence, especially in the vicinity of the very heavy precipitation. Momentum convergence of 10-m winds at the 99th percentile during widespread very heavy events is shown in Table 6. There is no evident correlation between precipitation intensities and momentum convergence, nor are these values substantially different from corresponding quantities for all days in the analysis period (not shown). Table 6 also does not show momentum convergence varying with resolution.

Winds in the Gulf of Mexico highlight the importance of surface high pressure to the east of the analysis region. Strong winds in the composites tend to start as southwesterly flow around

the southern tip of Florida. Over the Gulf, the winds turn clockwise toward the northern coast. This pattern provides substantial fetch for moistening air before it enters the southern U.S. Similar results were found in Brubaker et al. (2001), which emphasized the presence of anticyclonic flow around the Bermuda high, promoting moisture transport not only from the Gulf of Mexico, but also from the Caribbean and tropical Atlantic. Figure 8 does show flow possibly originating south of the Gulf. Although Brubaker et al. (2001) focused on the warm half of the year, Figure 8 highlights the importance of the moisture fetch during the winter season when, climatologically, Gulf of Mexico moisture does not often penetrate our upper Mississippi region and existing terrestrial moisture supply within the region is low (Brubaker et al. 2001; Kunkel and Liang 2005). The BCC-CSM1.1, MIROC-ESM-CHEM, and BNU-ESM show lower-intensity winds in the Gulf of Mexico compared to the models. This may explain the lower-intensity precipitation events at higher percentiles, since it lowers the moisture from the Gulf of Mexico. NARCCAP RCMs from Kawazoe and Gutowski (2013) show stronger 10-m winds in the Gulf than CMIP5 GCMs.

c. ***2-m air temperature and specific humidity***

We also analyzed 2-m air temperature and specific humidity from most of the models and the NARR. Figures 9 and 10 show these two fields as composite anomalies. Regions of very heavy precipitation tend to occur in regions of positive temperature and specific humidity anomalies. Like the 500-hPa height anomalies, the maximum temperature and humidity anomalies are roughly 5 times greater than their corresponding 2–5-day variability in the same locations (not shown). Thus, by this measure, all three anomaly fields examined have large, comparable departures from typical daily variability.

The composite temperatures (not shown) in areas of very heavy precipitation are above 275 K, which increases the likelihood that the precipitation type during these events is rain, not snow. Comparisons with Kawazoe and Gutowski (2013) show warm temperature anomalies are stronger for most NARCCAP RCMs than for the CMIP5 GCMs. The BCC-CSM1.1, MIROC-ESM-CHEM, and BNU-ESM mentioned in the 10-m wind analysis also show weaker specific humidity anomalies compared to most of the other models. This supports the results in Table 4, which shows these models having weaker very heavy events, and the lower moisture fetch in these models discussed above. Comparisons with Kawazoe and Gutowski (2013) show specific humidity anomalies agree well between NARCCAP RCMs and CMIP5 GCMs. Finally, Table 6 shows 99th percentile temperature and specific humidity gradients during widespread very heavy events. Temperature gradients show a slight decrease in values as model resolution becomes coarser, while specific humidity does not. As with momentum convergence, there is no evidence of correlation between temperature and specific humidity gradient with respect to precipitation intensities, nor are these values substantially different from corresponding quantities for all days in the analysis period (not shown). This suggests that the variety of modeling differences such as cloud microphysics and boundary layer parameterizations may have a larger impact than model resolutions.

5. Conclusion

Twenty-one GCMs from the CMIP5 project were compared with observational data (University of Washington precipitation and the North American Regional Reanalysis) to determine the ability of models to reproduce very heavy daily precipitation events during winter (December–February) between 1980 and 1999 in an upper Mississippi region. Our very heavy

daily precipitation was the top 0.5% of all daily values exceeding 0.25 mm day^{-1}. Widespread very heavy precipitation was defined as very heavy daily precipitation occurring on at least 15 equivalent 0.5° grid boxes simultaneously. For these events, we analyzed daily 500-hPa heights, 2-m air temperature and specific humidity, and 10-m surface winds from a subset of 13 models that archived all these variables to diagnose the environment favorable for the production of very heavy precipitation.

The models, for the most part, tend to produce too much precipitation compared to observations. Also, the models tend to produce fewer precipitation days than observed, which differs from NARCCAP RCM results from Kawazoe and Gutowski (2013). The frequency of days with precipitation above 2.5 mm day^{-1} agrees well between models and observations, indicating that the GCMs produce too few light precipitation, or drizzle, events, again in contrast with results from the NARCCAP RCMs. The CMIP5 models and observations are in good agreement for frequency versus intensity of precipitation up to about 20 mm day^{-1} compared to observations. Above this value, most models produce a higher frequency of events than observed, but fail to produce the very intense events seen in observations. The finer-resolution models tend to show more intense precipitation at the 99.5th percentile, with MPI-ESM-LR having the largest value. With the exception of CanESM2, the coarsest-resolution GCMs have lower precipitation intensities at the 99.5th percentile than observations, which may indicate that coarser-resolution GCMs are unable to capture small-scale events that produce very heavy events.

The models do not have a dominant winter month when very heavy precipitation events occur. In the NARCCAP RCMs analyzed by Kawazoe and Gutowski (2013), December showed the highest frequency of very heavy events, likely due to warmer SSTs in the Gulf of Mexico in

December. Such a climatological control did not appear in this analysis. However, warmer SSTs were seen during widespread very heavy events, supporting the assumption that warmer SSTs do allow more moisture to enter the atmosphere for transport into the central United States.

For environmental features, the observations and models show similar characteristics. Composite 500-hPa heights show a predominant southwesterly flow into the upper Mississippi region, caused by a deep trough or cutoff low near the Rockies. This allows increased moisture transport into the central United States from the Gulf of Mexico, which aids the development of very heavy precipitation. The 500-hPa heights in CMIP5 GCMs are similar in location and depth of the trough compared to the NARRCAP RCMs studied in Kawazoe and Gutowski (2013). Anomaly plots show that areas experiencing very heavy precipitation tend to occur in areas of positive anomalies of surface air temperatures, which provide an environment capable of holding more moisture compared to climatology. Areas experiencing very heavy precipitation also tend to occur in areas of positive moisture anomalies, showing that the warmer air does indeed have greater moisture. Temperature anomalies tend to be stronger in the NARCCAP RCMs analyzed by Kawazoe and Gutowski (2013) than in the CMIP5 GCMs, while specific humidity anomalies are similar between NARCCAP RCMs and CMIP5 GCMs. Surface wind analysis suggests a strong transport of Gulf of Mexico moisture into the upper Mississippi region. Features of a surface low exist slightly to the west of the area of very heavy precipitation. Low-level momentum convergence of 10-m winds near very heavy events is also present, indicating moisture convergence. Very heavy events tend to occur near the southern portion of the analysis region, centered over central Missouri. This is likely due to the warmer air in the southern part of the analysis region and transport of moisture into the part of the domain that is closest to the moisture source, the Gulf of Mexico. Aside from CanESM2, the coarsest models show slower

10-m winds in the Gulf compared to both higher-resolution GCMs and the NARCCAP RCMs analyzed by Kawazoe and Gutowski (2013). This is consistent with their smaller specific humidity anomalies and 99.5th percentile precipitation, possibly indicating that these models do not have the adequate transport of moisture into the region.

Resolution in itself could not account for differences in precipitation values or composite fields between models. However, these models appear to be capable of producing very heavy precipitation in the analysis region with the correct physical behavior compared to observations. Further diagnosis would be possible if other variables were available for all CMIP5 models studied here. These would include vertically integrated moisture transport, vertical velocity, and horizontal winds at multiple atmospheric levels. However, based on the fields we could analyze, the capability of both the NARCCAP RCMs and CMIP5 GCMs should support using them to assess changes in very heavy precipitation under future climate scenarios.

Acknowledgements

This work was supported by National Science Foundation Grants AGS-1125971 and BCS-1114978. Daily gridded observed precipitation data were obtained from the Surface Water Modeling group at the University of Washington. We acknowledge the World Climate Research Programme's Working Group on Coupled Modelling, which is responsible for CMIP, and we thank the climate modeling groups (listed in Table 1 of this paper) for producing and making available their model output. For CMIP the U.S. Department of Energy's Program for Climate Model Diagnosis and Intercomparison provided coordinating support and led development of software infrastructure in partnership with the Global Organization for Earth System Science Portals. We thank the reviewers for their helpful comments.

References

Brubaker, K.L., P.A. Dirmeyer, A. Sudradjat, B.S. Levy, F. Bernal, 2001: A 36-yr Climatological Description of the Evaporative Sources of Warm-Season Precipitation in the Mississippi River Basin. *J. Hydrometeor.*, **2**, 537-557.

Daly, C., R.P. Neilson, and D.L. Phillips, 1994: A statistical-topographic model for mapping climatological precipitation over mountainous terrain. *J. Appl. Meteor.*, **33,** 140-158.

Groisman, P.Y, R.W. Knight, D.R. Easterling, T.R. Karl, G.C. Hegerl, and V.N. Razuvaev, 2005: Trends in Intense Precipitation in the Climate Record. *J. Climate,* **18**, 1326–1350.

Gutowski,W.J., S.S. Willis., J. C. Patton, B.R.J. Schwedler, R.W. Arritt, and E.S. Takle, 2008: Changes in extreme, cold-season synoptic precipitation events under global warming. *Geophys. Res. Lett.,* **35**, L20710, doi:10.1029/2008GL035516.

Gutowski,W.J., R.W. Arritt, S. Kawazoe, D.M. Flory, E.S. Takle, S. Biner, D. Caya, R.G. Jones, R. Laprise, L.R. Leung, L.O. Mearns, W. Moufouma-Okia, A.M.B. Nunes, Y. Qian, J.O. Roads, L.C. Sloan, and M.A. Snyder, 2010: Regional Extreme Monthly Precipitation Simulated by NARCCAP RCMs. *J. Hydrometeor.*, **11(6)**,1373-1379

Kanamitsu, M., W. Ebisuzaki, J. Woollen, S.K. Yang, J.J. Hnilo, M. Fiorino, and G.L. Potter, 2002: NCEP/DOE AMIP-II reanalysis (R-2). *Bull. Amer. Meteor. Soc*., **83**, 1631-1643.

Kawazoe, S., W.J. Gutowski, 2013: Regional, Very Heavy Daily Precipitation in NARCCAP Simulations. *J. Hydrometeor.*, in press.

Kunkel, K.E., K. Andsager, X-Z. Liang, R.W. Arritt, E.S. Takle, W.J. Gutowski, and Z. Pan, 2002: Observations and Regional Climate Model Simulations of Heavy Precipitation Events and Seasonal Anomalies: A Comparison. *J. Hydrometeor.*, **3**, 322-334.

Kunkel, K.E., and X-Z Liang, 2005: GCM Simulations of the Climate in the Central United States. *J. Climate,* **18**, 1016-1031.

Maurer, E.P., A.W. Wood, J.C. Adam, D.P. Lettenmaier, and B. Nijssen, 2002: A long-term hydrological based dataset of land surface fluxes and states for the conterminous United States. *J. Climate,* **15,** 3237-3251.

Mesinger, F., and Coauthors, 2006: North American Regional Reanalysis. *Bull. Amer. Meteor. Soc.,* **87,** 343-360.

Schumacher, R.S., and R.H. Johnson, 2005: Organization and Environmental Properties of Extreme-Rain-Producing Mesoscale Convective Systems. *Mon. Wea. Rev.*, **133**, 961-976.

Schumacher, R.S., and R.H. Johnson, 2006: Characteristics of U.S. Extreme Rain Events during 1999–2003. *Wea. Forecasting*, **21**, 69-85.

Shepard, D.S., 1984: Computer Mapping: The SYMAP interpolation algorithm. *Spatial Statistics and Models,* G.L Gaile and C.J. Willmott, Eds., D.Reidel, 133-145.

Taylor, K.E., R.J. Stouffer, G.A. Meehl, 2012: An Overview of CMIP5 and the experiment design. *Bull. Amer. Meteor. Soc.,* **93**, 485-498, doi: 10.1175/BAMS-D-11-00094.1.

Wendland, W.M., L.D. Bark, D.R. Clark, R.B. Curry, J.W. Enz, K.G. Hubbard, V. Jones, 5 E.L. Kuehnast, W. Lytle, J. Newman, F.V. Nurnberger, and P. Waite, 1983: Review of the Unusual Winter of 1982-83 in the Upper Midwest. *Bull. Amer. Meteor. Soc*., **64**, 7 1346-1356.

Widmann, M., and C.S. Bretherton, 2000: Validation of Mesoscale Precipitation in the NCEP Reanalysis Using a New Gridcell Dataset for the Northwestern United States. *J. Climate.*, **13,** 1936-1950.

Table 1. CMIP5 GCMs analyzed in this paper.

Model	Model expansion	Modeling center/country
MIROC4h	Model for Interdisciplinary Research on Climate, version 4 (high resolution)	Atmosphere and Ocean Research Institute (The University of Tokyo), National Institute for Environmental Studies, and Japan Agency for Marine-Earth Science and Technology, Japan
CCSM4	Community Climate System Model, version 4	National Center for Atmospheric Research, USA
MRI-CGCM3	Meteorological Research Institute Coupled Atmosphere–Ocean General Circulation Model, version 3	Meteorological Research Institute, Japan
MIROC5	Model for Interdisciplinary Research on Climate, version 5	Atmosphere and Ocean Research Institute (The University of Tokyo), National Institute for Environmental Studies, and Japan Agency for Marine-Earth Science and Technology, Japan
CNRM-CM5	Centre National de Recherches Météorologiques Coupled Global Climate Model, version 5	Centre National de Recherches Météorologiques/Centre Europeen de Recherche et Formation Avancees en Calcul Scientifique, France
HadGEM2-CC	Hadley Centre Global Environmental Model, version 2 (Carbon Cycle)	Met Office Hadley Centre, UK
HadGEM2-ES	Hadley Centre Global Environmental Model, version 2 (Earth System)	Met Office Hadley Centre, UK
INM-CM4	Institute of Numerical Mathematics Coupled Model, version 4	Institute for Numerical Mathematics, Russia
IPSL-CM5A-MR	L'Institut Pierre-Simon Laplace Coupled Model, version 5, coupled with NEMO, mid resolution	Institute for Numerical Mathematics, France
MPI-ESM-LR	Max Planck Institute Earth System Model, low resolution	Low-Resolution Earth System Model of MPI, Germany
CSIRO-Mk3.6.0	Commonwealth Scientific and Industrial Research Organisation Mark, version 3.6.0	Max Planck Institute for Meteorology, Australia
NorESM1-M	Norwegian Earth System Model, version 1 (medium resolution)	Norwegian Climate Centre, Norway
FGOALS-s2	Flexible Global Ocean–Atmosphere–Land System Model gridpoint, second spectral version	LASG, Institute of Atmospheric Physics, Chinese Academy of Sciences, China
GFDL CM3	Geophysical Fluid Dynamics Laboratory Climate Model, version 3	NOAA Geophysical Fluid Dynamics Laboratory, USA
GFDL-ESM2M	Geophysical Fluid Dynamics Laboratory Earth System Model with MOM4 ocean component (ESM2M)	NOAA Geophysical Fluid Dynamics Laboratory, USA

Table 1 continued.

IPSL-CM5A-LR	L'Institut Pierre-Simon Laplace Coupled Model, version 5, coupled with NEMO, low resolution	Institut Pierre-Simon Laplace, France
BCC-CSM1.1	Beijing Climate Center, Climate System Model, version 1.1	Beijing Climate Center, China Meteorological Administration, China
CanESM2	Second Generation Canadian Earth System Model	Canadian Centre for Climate Modelling and Analysis, Canada
MIROC-ESM-CHEM	Model for Interdisciplinary Research on Climate, Earth System Model, Chemistry Coupled	Japan Agency for Marine-Earth Science and Technology, Atmosphere and Ocean Research Institute (The University of Tokyo), and National Institute for Environmental Studies, Japan
BNU-ESM	Beijing Normal University Earth System Model	College of Global Change and Earth System Science, Beijing Normal University, China
HadCM3	Hadley Centre Coupled Model, version 3	Met Office Hadley Centre, UK

Table 2. Approximate resolution and nominal area for a model's grid box in the upper Mississippi domain in terms of a 0.5° x 0.5° grid box. (Note: UW/NARR resolution is for precipitation. All other fields use NARR's 0.3° x 0.3° resolution).

Source	Resolution	Nominal area	Source	Resolution	Nominal area
UW/NARR	0.5° x 0.5°		CSIRO-Mk3-6	1.87° x 1.88°	$(14.0°)^2$
MIROC4h	0.56° x 0.56°	$(1.25°)^2$	NorESM1-M	1.9° x 2.5°	$(19.0°)^2$
CCSM4	0.94° x 1.25°	$(4.7°)^2$	FGOALS-s2	1.65° x 2.81°	$(18.55°)^2$
MRI-CGCM3	1.12° x 1.25°	$(5.6°)^2$	GFDL-CM3	2.0° x 2.5°	$(20.0°)^2$
MIROC5	1.4° x 1.4°	$(7.8°)^2$	GFDL-ESM2M	2.02° x 2.5°	$(20.0°)^2$
CNRM-CM5	1.4° x 1.4°	$(7.8°)^2$	IPSL-CM5A-LR	1.9° x 3.75°	$(28.5°)^2$
HadGEM2-CC	1.25° x 1.88°	$(9.0°)^2$	BCC-CSM1-1	2.8° x 2.8°	$(31.0°)^2$
HadGEM2-ES	1.25° x 1.88°	$(9.0°)^2$	CanESM2	2.8° x 2.8°	$(31.0°)^2$
INM-CM4	1.5° x 2.0°	$(12.0°)^2$	MIROC-ESM-CHEM	2.79° x 2.81°	$(31.36°)^2$
IPSL-CM5A-MR	1.27° x 2.5°	$(12.7°)^2$	BNU-ESM	2.79° x 2.81°	$(31.36°)^2$
MPI-ESM-LR	1.85° x 1.88°	$(13.88°)^2$	HadCM3	2.5° x 3.75°	$(37.5°)^2$

Table 3. Properties of CMIP models and UW: overall average precipitation rate and percentage of days reporting precipitation (parentheses: the percentage of days with precipitation exceeding 2.5 mm day^{-1}).

Source	Precipitation Rate (mm day^{-1})	Days with Precipitation (%)	Source	Precipitation Rate (mm day^{-1})	Days with Precipitation (%)
UW	1.00	53.7 (10.9)	CSIRO-Mk3-6	1.27	46.1 (11.6)
MIROC4h	1.27	46.9 (11.6)	NorESM1-M	0.93	37.6 (9.5)
CCSM4	1.27	39.3 (12.2)	FGOALS-s2	1.41	39.5 (13.9)
MRI-CGCM3	1.51	37.6 (14.8)	GFDL-CM3	1.60	54.4 (15.7)
MIROC5	1.39	41.3 (14.0)	GFDL-ESM2M	1.56	46.2 (14.8)
CNRM-CM5	1.09	28.9 (10.3)	IPSL-CM5A-LR	1.34	49.2 (13.0)
HadGEM2-CC	1.18	45.5 (11.1)	BCC-CSM1-1	1.43	59.5 (15.1)
HadGEM2-ES	1.20	46.2 (11.4)	CanESM2	1.41	26.5 (11.8)
INM-CM4	1.59	46.0 (15.2)	MIROC-ESM-CHEM	0.94	34.4 (10.2)
IPSL-CM5A-MR	1.53	50.9 (14.2)	BNU-ESM	1.49	62.8 (14.9)
MPI-ESM-LR	1.80	36.8 (16.0)	HadCM3	1.67	48.4 (17.2)

Table 4. Precipitation intensity for models and observations at the 95, 99, and 99.5th percentiles for all non-zero precipitation.

Source	95% (mm day^{-1})	99% (mm day^{-1})	99.5% (mm day^{-1})	Source	95% (mm day^{-1})	99% (mm day^{-1})	99.5% (mm day^{-1})
UW	11.19	22.84	28.71	CSIRO-Mk3-6	13.36	25.35	30.69
MIROC4h	11.27	24.48	30.48	NorESM1-M	9.37	19.49	24.81
CCSM4	12.98	27.34	33.53	FGOALS-s2	14.26	26.25	32.47
MRI-CGCM3	15.92	29.10	35.12	GFDL-CM3	12.09	23.74	29.62
MIROC5	13.26	25.75	31.39	GFDL-ESM2M	14.03	28.07	34.05
CNRM-CM5	15.31	31.15	38.00	IPSL-CM5A-LR	10.37	23.91	30.86
HadGEM2-CC	10.30	22.20	27.30	BCC-CSM1-1	9.21	18.19	23.17
HadGEM2-ES	9.85	23.58	30.33	CanESM2	22.28	39.49	47.44
INM-CM4	14.50	26.49	32.07	MIROC-ESM-CHEM	9.86	19.79	24.25
IPSL-CM5A-MR	11.64	27.91	36.45	BNU-ESM	9.36	18.79	22.45
MPI-ESM-LR	19.54	35.95	42.70	HadCM3	13.52	23.32	27.91

Table 5. Percentage of widespread very heavy events by month for observations and for each model. Highest values during the season are in bold. GCM average is: December: 37.7%, January: 27.8%, Feburary: 34.5%.

Source	December	January	February	Source	December	January	February
UW	**53.5%**	21.4%	25%	CSIRO-Mk3-6	32.5%	**42.5%**	25.0%
MIROC4h	30.6%	22.2%	**47.2%**	NorESM1-M	27.5%	27.5%	**45.0%**
CCSM4	**57.1%**	14.3%	28.6%	FGOALS-s2	32.7%	32.7%	**34.6%**
MRI-CGCM3	30.3%	30.3%	**39.4%**	GFDL-CM3	**41.5%**	18.5%	40.0%
MIROC5	**40.9%**	27.3%	31.8%	GFDL-ESM2M	27.5%	**37.3%**	35.3%
CNRM-CM5	**39.5%**	31.6%	28.9%	IPSL-CM5A-LR	31.8%	**36.4%**	31.8%
HadGEM2-CC	27.8%	27.8%	**44.4%**	BCC-CSM1-1	30.8%	25.6%	**43.6%**
HadGEM2-ES	**51.9%**	19.2%	28.8%	CanESM2	**56.7%**	16.7%	26.7%
INM-CM4	**37.1%**	28.6%	34.3%	MIROC-ESM-CHEM	33.3%	**37.0%**	29.6%
IPSL-CM5A-MR	**52.0%**	24.0%	24.0%	BNU-ESM	**43.2%**	25.0%	31.8%
MPI-ESM-LR	28.2%	**46.2%**	25.6%	HadCM3	38.1%	14.3%	**47.6%**

Table 6. Ninety-nine percent values of surface air temperature and specific humidity gradients and horizontal 10-m wind convergence on very heavy event days for observations and for each model.

Source	Temp (10^{-5} K m^{-1})	Spec. Hum (10^{-8} kg kg^{-1} m^{-1})	Wind Conv (10^{-5} m s^{-1} m^{-1})	Source	Temp (10^{-5} K m^{-1})	Spec. Hum (10^{-8} kg kg^{-1} m^{-1})	Wind Conv (10^{-5} m s^{-1} m^{-1})
NARR	6.67	3.56	3.34	CSIRO-Mk3-6	4.47	1.95	1.86
MIROC4h	6.00	2.02	2.61	NorESM1-M	7.00	2.56	X
CCSM4	6.67	X	X	FGOALS-s2	7.74	2.26	1.86
MRI-CGCM3	5.81	2.44	1.25	GFDL-CM3	4.84	1.62	1.00
MIROC5	5.25	2.11	2.00	GFDL-ESM2M	5.19	1.87	1.15
CNRM-CM5	6.00	1.66	1.58	IPSL-CM5A-LR	5.73	2.00	1.14
HadGEM2-CC	6.00	2.25	1.34	BCC-CSM1-1	7.00	2.05	1.11
HadGEM2-ES	6.72	2.96	1.37	CanESM2	5.35	2.19	2.56
INM-CM4	7.00	2.57	1.17	MIROC-ESM-CHEM	3.62	1.42	1.83
IPSL-CM5A-MR	5.38	2.04	1.27	BNU-ESM	4.74	1.63	1.28
MPI-ESM-LR	5.87	X	1.60	HadCM3	4.58	1.95	X

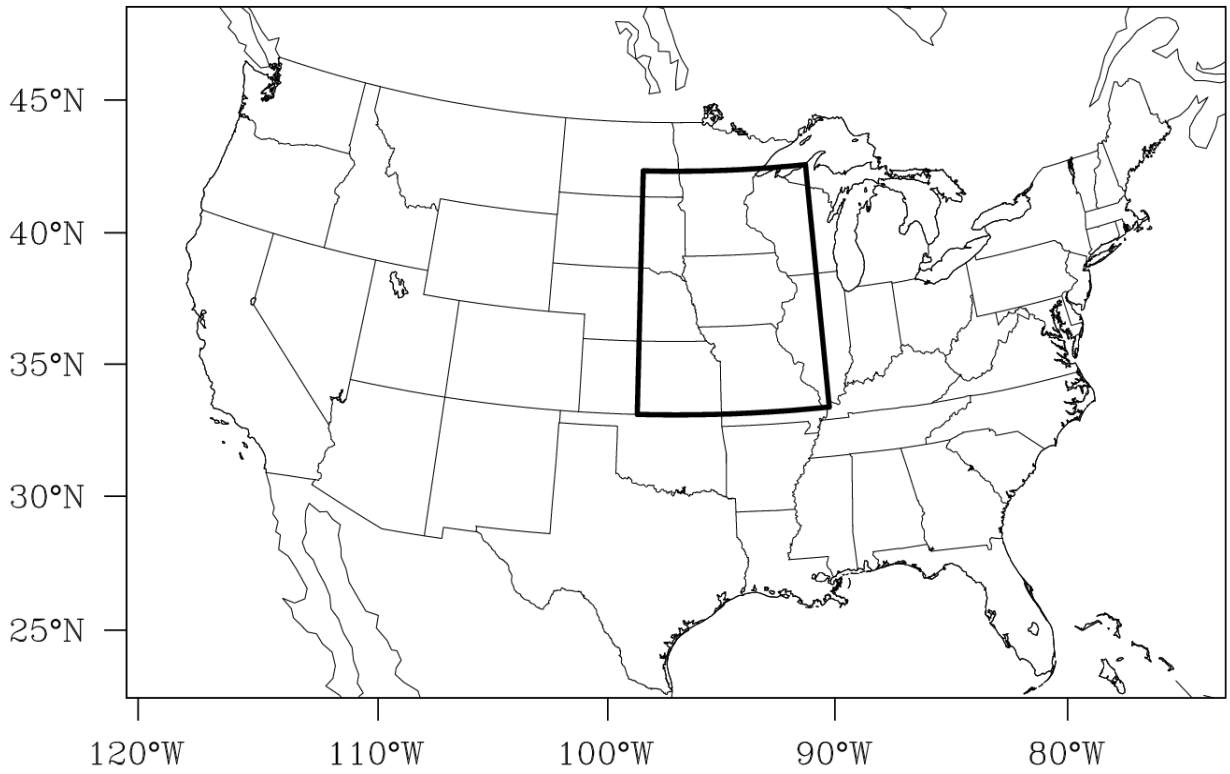

Figure 1. Region covered by each CMIP5 model, UW, and NARR. The upper Mississippi analysis region is in the boxed area.

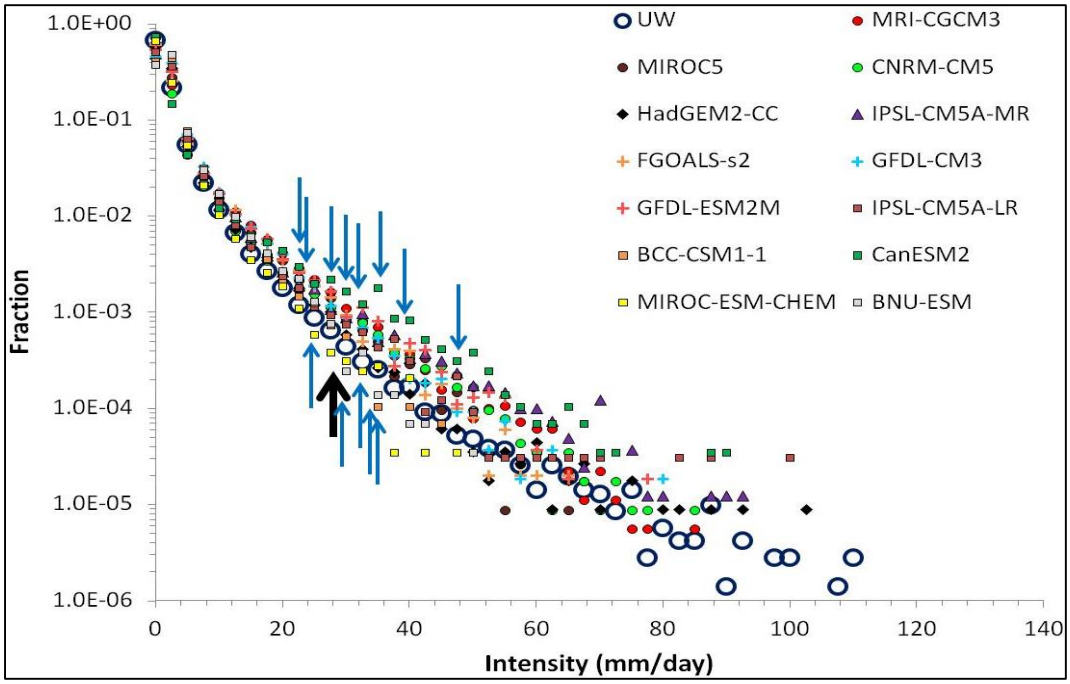

Figure 2. Normalized frequency of precipitation as a function of daily intensity for 1980-1999 in models and observations that provided all analyzed supporting fields. Arrows mark the 99.5th percentile: black: UW, blue: GCMs.

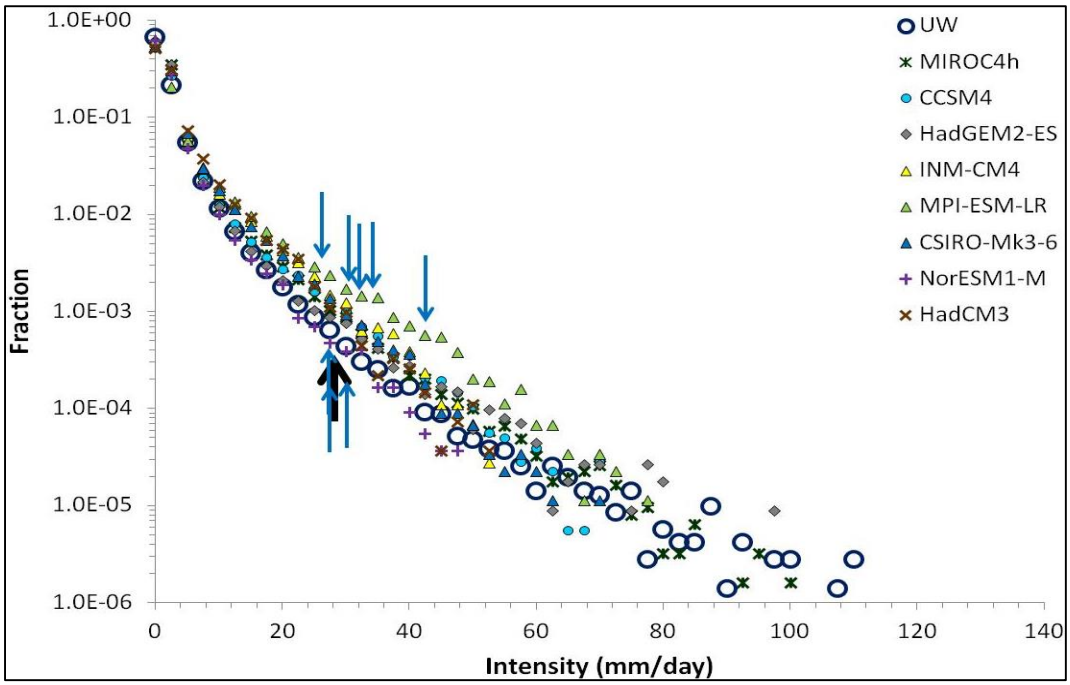

Figure 3. Normalized frequency of precipitation as a function of daily intensity for 1980-1999 for observations and for additional models that did not provide all analyzed supporting fields. Arrows mark the 99.5th percentile: black: UW, blue: GCMs.

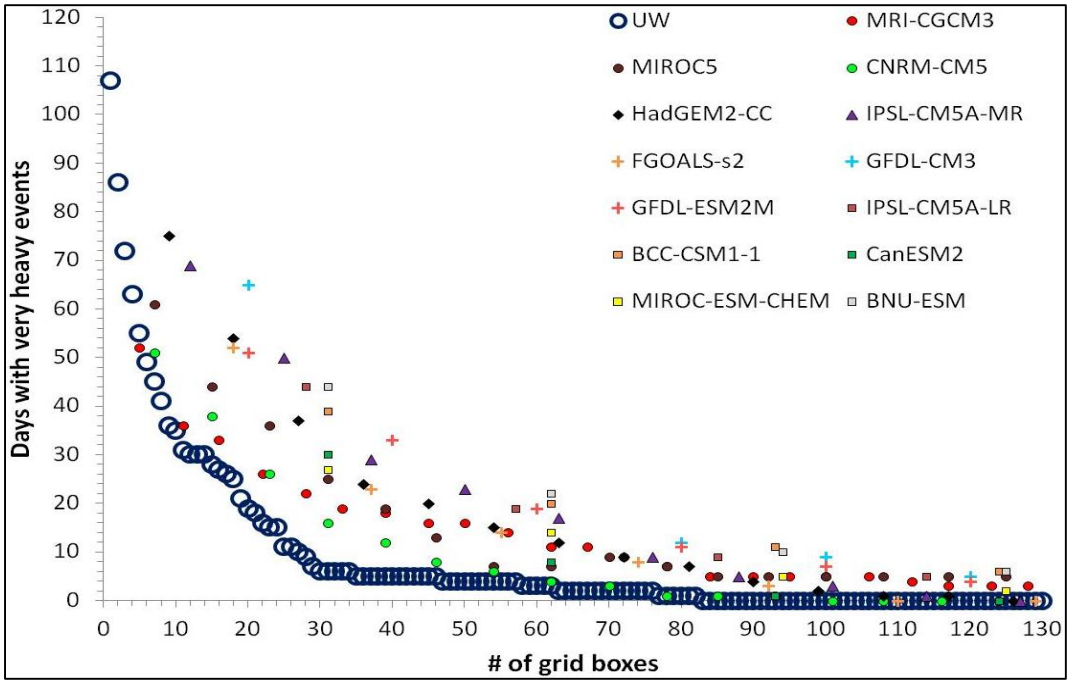

Figure 4. Days with simultaneous very heavy events on "N" grid points for models and observations that provided all analyzed supporting fields.

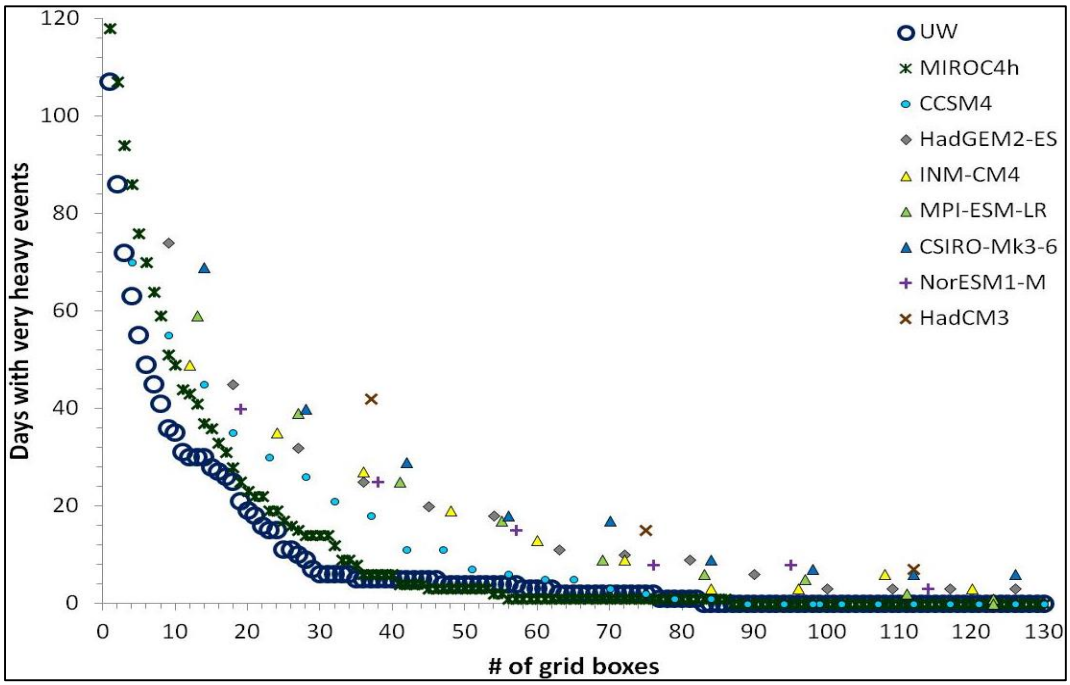

Figure 5. Days with simultaneous very heavy events on "N" grid points for additional models and observations that did not provide all analyzed supporting fields.

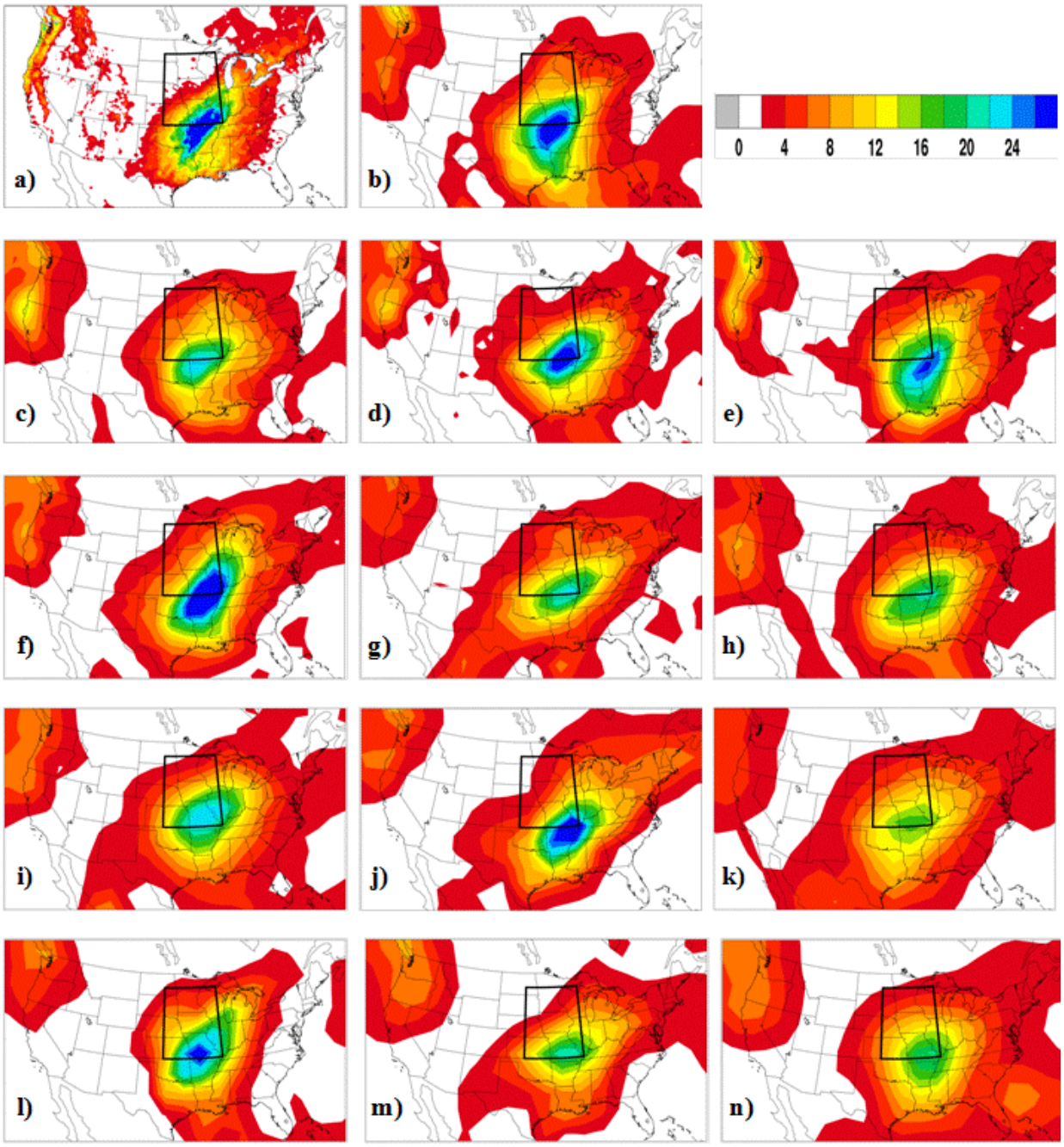

Figure 6. Composite daily precipitation during widespread very heavy events: (a) UW, (b) MRI-CGCM3, (c) MIROC5, (d) CNRM-CM5, (e) HadGEM2-CC, (f) IPSL-CM5A-MR, (g) FGOALS-s2, (h) GFDL-CM3, (i) GFDL-ESM2M, (j) IPSL-CM5A-LR, (k) BCC-CSM1-1, (l) CanESM2, (m) MIROC-ESM-CHEM, (n) BNU-ESM. Contour scale for all plots is in the upper right, in mm day^{-1}.

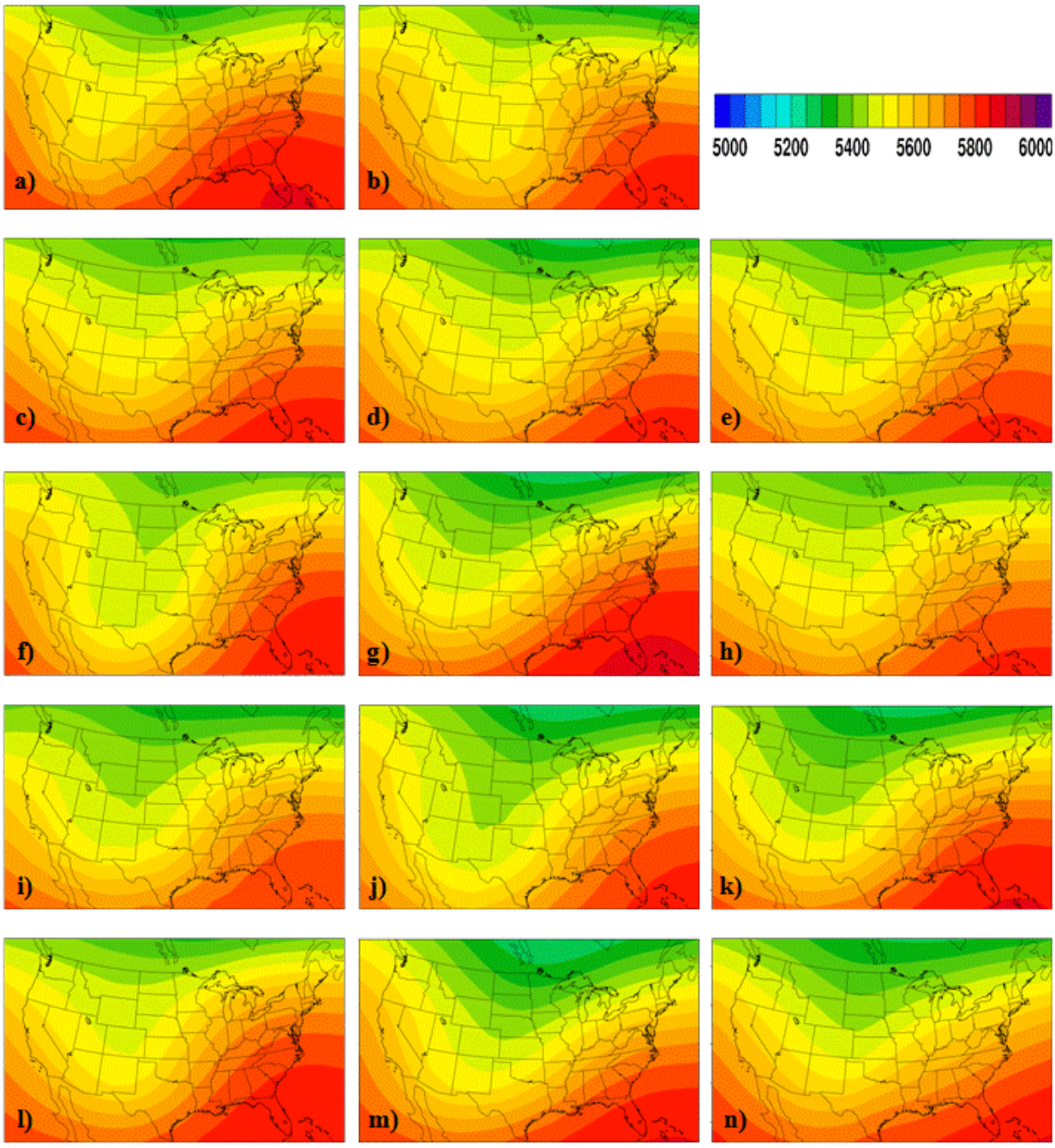

Figure 7. Composite 500-hPa heights during widespread very heavy events: (a) NARR, (b) MRI-CGCM3, (c) MIROC5, (d) CNRM-CM5, (e) HadGEM2-CC, (f) IPSL-CM5A-MR, (g) FGOALS-s2, (h) GFDL-CM3, (i) GFDL-ESM2M, (j) IPSL-CM5A-LR, (k) BCC-CSM1-1, (l) CanESM2, (m) MIROC-ESM-CHEM, (n) BNU-ESM. Contour scale for all plots is in the upper right, in meters.

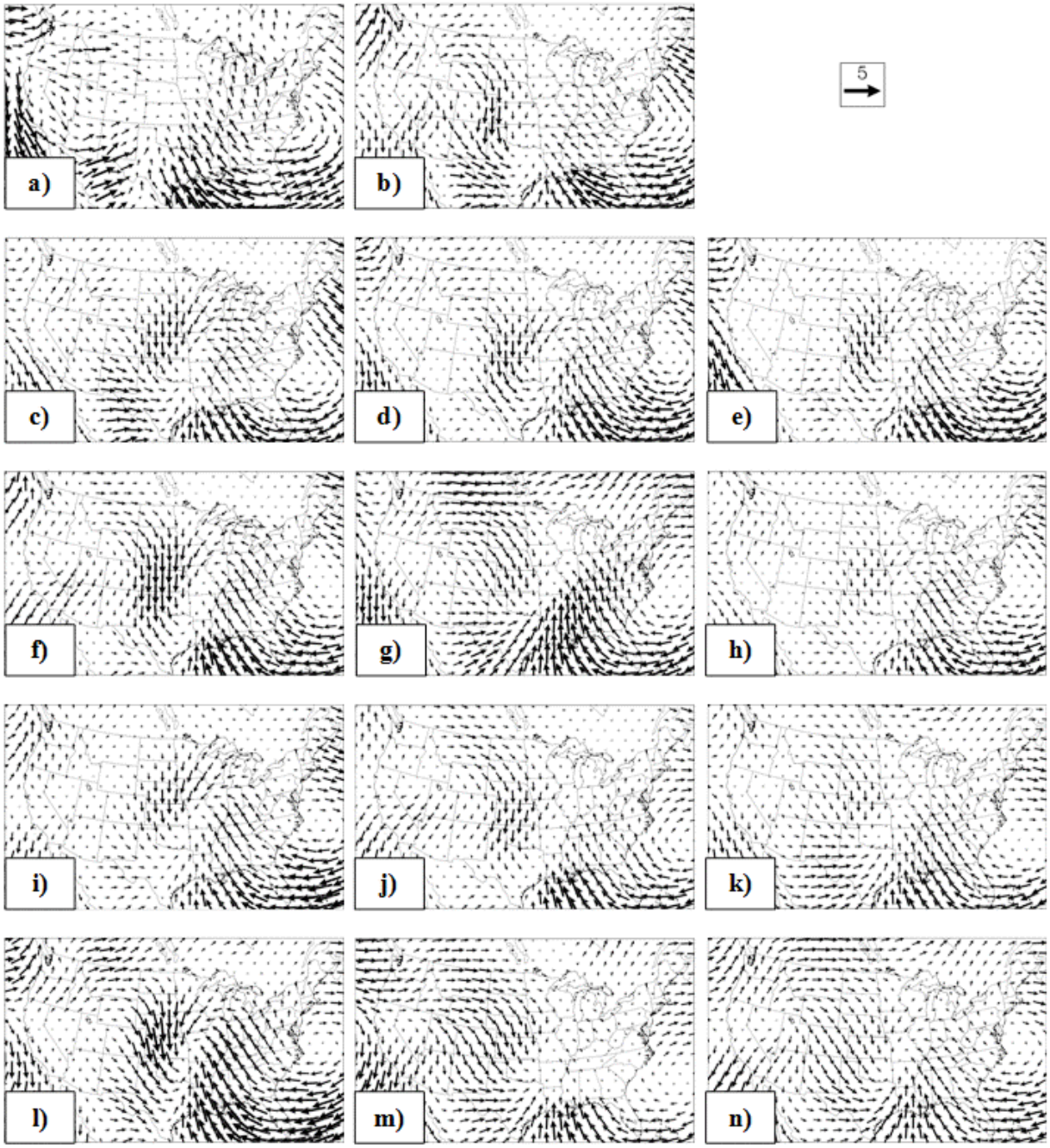

Figure 8. Composite 10-m horizontal winds during widespread very heavy events: (a) NARR, (b) MRI-CGCM3, (c) MIROC5, (d) CNRM-CM5, (e) HadGEM2-CC, (f) IPSL-CM5A-MR, (g) FGOALS-s2, (h) GFDL-CM3, (i) GFDL-ESM2M, (j) IPSL-CM5A-LR, (k) BCC-CSM1-1, (l) CanESM2, (m) MIROC-ESM-CHEM, (n) BNU-ESM. Wind vector for all plots is in the upper right, in m s^{-1}.

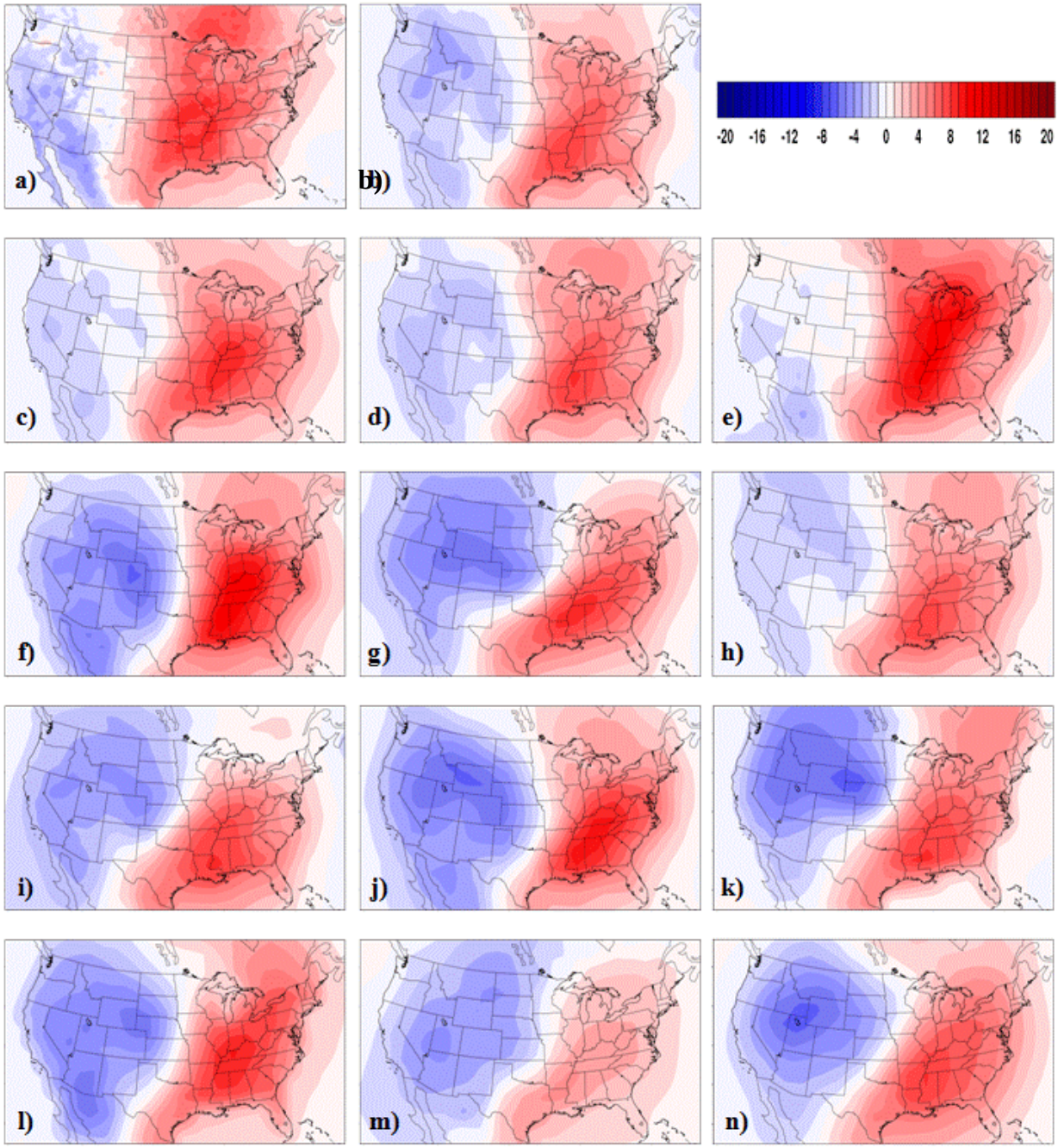

Figure 9. Composite 2-m temperature anomalies during widespread very heavy events: (a) NARR, (b) MRI-CGCM3, (c) MIROC5, (d) CNRM-CM5, (e) HadGEM2-CC, (f) IPSL-CM5A-MR, (g) FGOALS-s2, (h) GFDL-CM3, (i) GFDL-ESM2M, (j) IPSL-CM5A-LR, (k) BCC-CSM1-1, (l) CanESM2, (m) MIROC-ESM-CHEM, (n) BNU-ESM. Contour scale for all plots is in the upper right, in Kelvin.

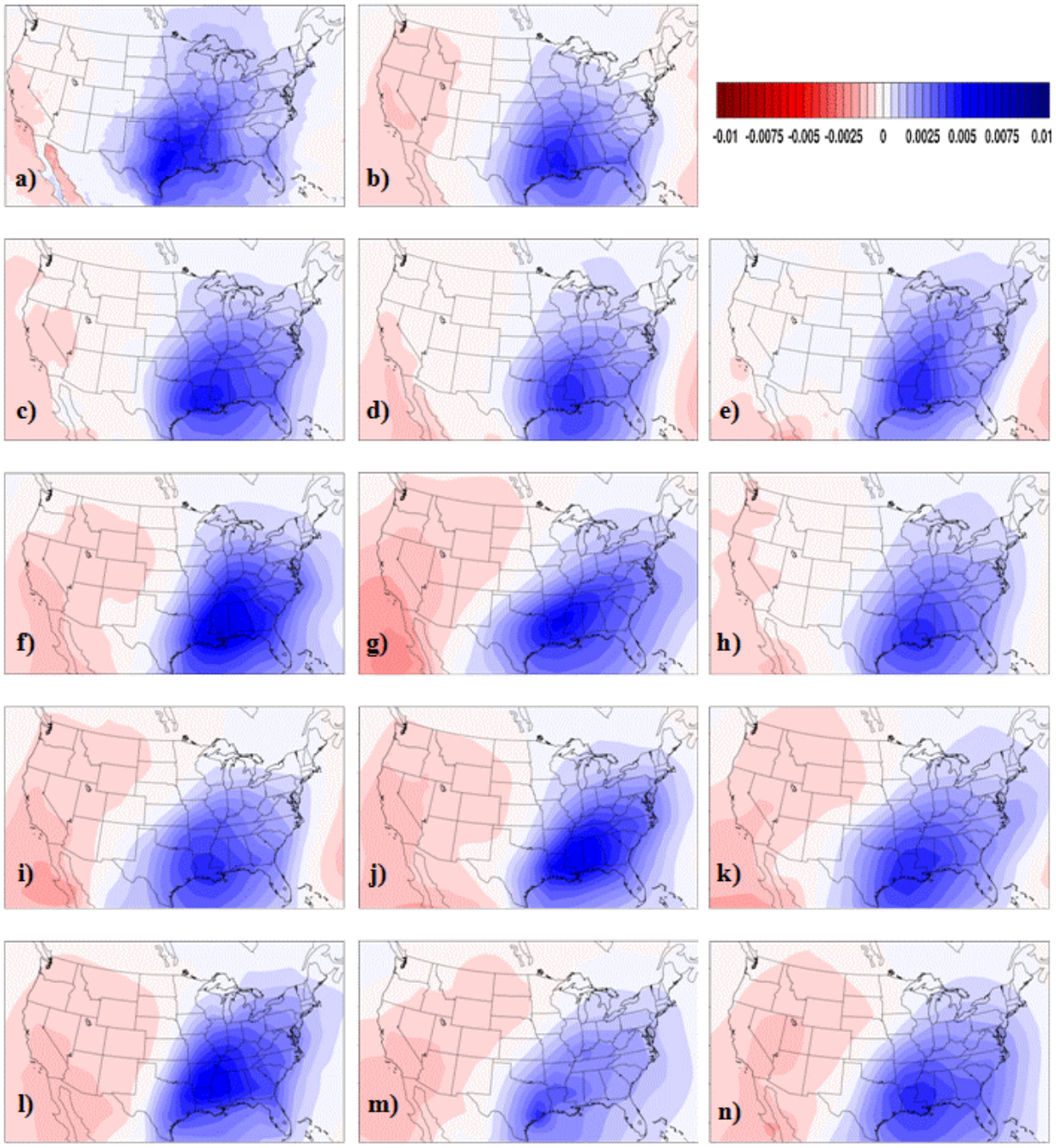

Figure 10. Composite 2-m specific humidity anomalies during widespread very heavy events: (a) NARR, (b) MRI-CGCM3, (c) MIROC5, (d) CNRM-CM5, (e) HadGEM2-CC, (f) IPSL-CM5A-MR, (g) FGOALS-s2, (h) GFDL-CM3, (i) GFDL-ESM2M, (j) IPSL-CM5A-LR, (k) BCC-CSM1-1, (l) CanESM2, (m) MIROC-ESM-CHEM, (n) BNU-ESM. Contour scale for all plots is in the upper right, in kg kg^{-1}.

CHAPTER 3

EVALUATION OF REGIONAL, VERY HEAVY PRECIPITATION EVENTS DURING THE SUMMER SEASON USING NARCCAP SIMULATIONS: CONTEMPORARY CLIMATE SIMULATIONS

To be submitted to the Journal of Climate

Sho Kawazoe and William J. Gutowski Jr.

Abstract

Regional climate models (RCMs) from the North American Regional Climate Change Assessment Program (NARCCAP) are compared with the Climate Prediction Center (CPC) gridded dataset and the North American Regional Reanalysis (NARR) to examine if RCMs are able to reproduce very heavy precipitation characteristics under similar physical conditions seen in observations. The analysis focuses on the contemporary climate (1982-1999) in upper Mississippi region during the summer (June-August) months and utilizes NARCCAP RCMs forced with a reanalysis and atmosphere-ocean global climate models (AOGCMs).

The NARCCAP models generally reproduce well the precipitation frequency-vs.-intensity spectrum seen in observations up to around 25 mm day^{-1}, before producing overly strong precipitation at high-intensity thresholds. CRCM simulations produce lower precipitation amounts than the rest of the models and observations past the 25 mm day^{-1} threshold. Further analysis focuses on precipitation events exceeding the 99.5^{th} percentile that occur simultaneously at several points in the region, yielding so-called "widespread events". With the exception of the CRCM and EPC2 simulations, models and observations produce precipitation peaks around

0300UTC-0900UTC, though at models produce slightly weaker intensities compared to observations, on average. Precipitation still falls too frequently throughout the day, especially between 1500UTC and 2100UTC, compared to observations. Composite precipitation shows intensity and location differences between the models. Examination of additional fields shows that NARCCAP models produce credible simulations of very heavy precipitation and their supporting environments when compared to observations. However, biases seen between individual models and observations are noted and highlighted in this study.

1. Introduction

Recent catastrophic flooding events, highlighted by the Midwest floods of 1993 (Kunkel et al. 1994) and 2008 (Dirmeyer and Kinter 2010; Coleman and Budikova 2010) have resulted in massive social-economic damages. Many flooding events vary in spatial and temporal characteristics, as some may be caused by single extreme events falling on saturated surfaces from previous seasons, while others may be caused by a series of storms that by themselves may not be classified as extreme events (Senevirantne et al. 2012). In addition to the variability of precipitation characteristics, the frequency of heavy precipitation events has increased since the middle of the last century, even in locations where mean precipitation shows minimal changes (Groisman et al. 2005; Karl et al 2008). Policy makers, stakeholders, and the general public are wary of such events becoming increasingly common and require reliable forecasts in order to determine if adaptive responses are needed in order to mitigate the societal impact they may have.

Climate model simulations are an integral tool in understanding how such events develop, and how they will change in the future. With ongoing improvements in climate model

performance, they are more capable of replicating real world events, and we are able to gain higher confidence in their ability to simulate future changes to very heavy events (Palmer and Räisänen 2002; Emori and Brown 2005; Meehl et al. 2005). This confidence can aid in understanding how we can best adapt to precipitation changes at multiple spatiotemporal scales.

This paper will follow the framework of two of our most recent publications, which focused on very heavy precipitation events during the winter season in the upper Mississippi region. Kawazoe and Gutowski (2013a) used regional climate models (RCMs) from the North American Regional Climate Change Assessment Program (NARCCAP), while Kawazoe and Gutowski (2013b) used 21 global climate models (GCMs) from the Coupled Model Intercomparison Project – Phase 5 (CMIP5; Taylor et al. 2012). We now shift our focus to the summer season, where local and regional scale convective forcing play a larger role in producing very heavy events compared to the winter, where it is largely governed by synoptic-scale dynamics (Maddox et al. 1979; Schumacher and Johnson 2006).

Current GCMs (~100-300km grid spacing), despite their considerable improvements, do not resolve important regional scale characteristics that require the use of parameterizations (Duffy et al. 2003). As a result, higher resolution models that implement regional scale features of land, atmosphere, and ocean fields are therefore needed (Fowler et al. 2005, Frei et al. 2006; Gutowski et al. 2010; Bukovsky and Karoly 2011). One project using such models is the North American Regional Climate Change Assessment Program (NARCCAP; Mearns et al. 2009,2012), a set of dynamically downscaled simulations nested within atmosphere and ocean GCMs (AOGCMs). Dynamically downscaling GCMs by nesting RCMs has shown promise, as it adds realistic spatiotemporal details to GCMs, which is especially important when mesoscale forcing dominates the development of convective summer storms (Leung et al. 2004;

Christensen et al. 2007; Mahoney et al. 2013). We will use climate simulation from NARCCAP during the summer months (June-July-August) in the upper Mississippi region.

The goals of this study are to assess the ability of the ensemble of NARCCAP models to reproduce very heavy daily precipitation in observations, and to provide a baseline for understanding how very heavy daily precipitation and its causal processes change under enhanced greenhouse warming scenarios. Multi-model ensembles are commonly used to identify and reduce characteristic bias and uncertainties associated with how a particular climate model represents the climate system (Hagedorn et al. 2005; Meehl et al. 2007; Mailhot et al. 2011). If an ensemble analysis produces similar precipitation characteristics to those seen in observations, and under similar physical conditions, greater confidence can be put into the collective ability climate models have in the assessment of the changing risk (Murphy et al. 2004; Gutowski et al. 2008). This is in line with our study objective, which is to offer better potential for assessing the capability of climate models to produce very heavy precipitation events.

This paper is structured as follows: section 2 gives an overview of datasets and analysis methods implemented. Results for both precipitation and there supporting environmental conditions are presented in section 3. The conclusions will follow in section 4.

2. Data and Methods

a. Observations

For this study, we use the same gridded observational datasets of daily precipitation from Kawazoe and Gutowski (2013a):

- Climate Prediction Center (CPC) Unified Gauge-Based Analysis of Daily Precipitation (Higgins et al. 2000). 0.25° x 0.25° horizontal resolution. Data available from 1948-2006.
- University of Washington's (UW) gridded precipitation (Maurer et al. 2002). 0.125° x 0.125° horizontal resolution. Data available from 1950-1999.

We use the CPC data as the basis for identifying days when very heavy precipitation occurs. The additional observed dataset (UW) is to acknowledge the uncertainty that may exist in different gridding products when identifying these days. For all other fields, we use the North American Regional Reanalysis (NARR; Mesinger et al. 2006). The fields we use are 2-m specific humidity, the convective available potential energy (CAPE), vertically integrated moisture flux convergence (hereafter VI-MFC) and vertically integrated moisture transport (hereafter VI-MT). These fields represent key environmental conditions during very heavy precipitation development. The NARR is also used for diurnal cycle analysis, as the gridded datasets do not provide output in hourly intervals.

b. Simulations

Climate model output comes from two main phases in NARCCAP. Phase I (Mearns et al. 2012) includes six regional climate models (RCMs) driven by the National Center for Environmental Prediction (NCEP) and U.S. Department of Energy (DOE) Reanalysis II for their boundary conditions:

- Canadian Regional Climate Model version 4 (CRCM).
- Experimental Climate Prediction Center Regional Spectral Model (ECP2).
- Hadley Centre Regional Model version 3 (HRM3).
- Fifth-generation Pennsylvania State University-National Center for Atmospheric Sciences (NCAR) Mesoscale Model (MM5I).
- International Centre for Theoretical Physics Regional Climate Model version 3 (RCM3).
- NCAR Weather Research and Forecasting Model (WRFG).

For the ECP2, we only analyze the precipitation characteristics, as the vertical coordinate for this dataset available to the public had not been interpolated to standard pressure levels. All models used approximately 0.5° horizontal resolution to simulate a 25-year period from 1980-2004.

Phase II used the same six RCMs to downscale four global climate models (GCMs) from World Climate Research Program's (WCRP's) Coupled Model Intercomparison Project- Phase 3 (CMIP3):

- NCAR-Community Climate Model version 3 (ccsm3). 1.4º x 1.4º horizontal resolution.
- Canadian Climate Centre Third Generation Coupled General Climate Model (cgcm3). 1.9º x 1.9º horizontal resolution.
- Geophysical Fluid Dynamic Laboratory (gfdl) Atmosphere-Ocean general circulation model (AOGCM) CM2.1. 2.0º x 2.5º horizontal resolution.
- Hadley Centre Hadley Climate Model version 3 (hadcm3). 2.5º x 3.75º horizontal resolution.

Of the 24 nesting combinations possible, 12 pairings were completed as part of NARCCAP. Contemporary climate spans a 29-year timeframe from 1971-1999, and results are recorded at 3-hourly intervals. A full list of model combinations available from NARCCAP, which is also those used for this study, are shown in Table 1. Because of their importance to precipitation in models during the summer season, the convective parameterization used in each RCM is listed in Table 2. Further details of each model appear in both the NARCCAP website (http://narccap.ucar.edu), and Mearns et al. (2009, 2012).

c. Methods

This study utilizes the same domain (upper Mississippi region), and years studied (1982-1999) in Kawazoe and Gutowski (2013a,b). We define our "day" as 1200UTC – 1200UTC (0600 - 0600 local standard time in the upper Mississippi region) so precipitation from nocturnal storms commonly seen during the summer is accumulated throughout a storm's duration (e.g., Anderson et al. 2003). The CPC observational data set is already in daily increments that match our defined "day", while the UW observational dataset defines a "day" as 0600UTC – 0600UTC (0000 – 0000 local standard time in the upper Mississippi region) a factor that may affect some of our results. We interpolated both the CPC and UW output to a 0.5° grid to give the datasets the same nominal resolution as the RCMs, as recommended by Chen and Knutson (2007). Analysis examining conditions other than precipitation during very heavy events focused on instantaneous fields at 2100UTC (1500 local standard time in the upper Mississippi region), which provided information on the state of the atmosphere during the day of a very heavy event, prior to the time of maximum frequency of convective storms (Wallace 1975).

We defined a "precipitation event" as precipitation above 0.25 mm day^{-1}, as was the case in Kawazoe and Gutowski (2013b). Very heavy precipitation was defined as any event above the

99.5th percentile. We then found widespread events by searching for very heavy events occurring on multiple grid points on the same day. For our analysis, we designated simultaneous very heavy events on 10 or more grid points as widespread events. We selected this threshold in order to have sufficient numbers of events to analyze while requiring enough spatial distribution that resolved synoptic and mesoscale dynamics could be a governing factor. This threshold is lower than our previous studies (Kawazoe and Gutowski 2013a,b), as summer storms usually concentrate over a smaller area than do winter storms. We examined several atmospheric fields (2-m specific humidity, CAPE, VI-MFC, and VI-MT) to understand conditions conducive to very heavy events. These fields gave insight into the preferred conditions for very heavy precipitation events and became the basis for assessing simulated versus observed processes yielding very heavy precipitation. For some of the fields, we examined anomalies. These anomalies were composites of fields on the days of widespread very heavy events minus the 17-year time average during the summer season.

3. Results

a. Precipitation statistics

Table 3 shows the average precipitation rate and frequency of daily precipitation events in the upper Mississippi region, for models and observations. The numbers in parentheses are the percentage of days with precipitation above 2.5 mm day^{-1}. Among the simulations,14 of the 17 produce lower precipitation compared to CPC, with the RCM3 simulations producing the most, and WRFG simulations producing the least. Average precipitation rates tend to vary more with RCM choice than the lateral driving source. Among the simulations, 9 of the 17 show fewer days of precipitation than CPC, 6 of which are either the MM5I or WRFG simulations. For

precipitation exceeding 2.5 mm day^{-1}, models typically produce frequencies in the range of 16-32%, which is approximately ±6% of the CPC frequency. The differences between CPC and UW results may come from how each gridded dataset defines a "day". Because UW reports precipitation from 0600UTC – 0600UTC, nocturnal storms may not be accumulated in their entirety during a single UW "day", and may spill over to the next day. This could account for a slightly lower average precipitation and higher frequency of days with precipitation in UW compared to CPC. The difference may also come from the differences in the gridding schemes.

Table 4 shows precipitation for each model and for observations at the 95th, 99th, and 99.5th percentiles. At the respective percentiles, 8, 12, and 13 of the 17 models produce higher precipitation rates compared to the CPC. Similar to Table 2, consistency at each percentile seems to be determined more by the downscaling RCM rather than the boundary conditions. At the 95th, 99th, and 99.5th percentile, there is a 38%, 32%, and 32% difference, respectively, between the lowest precipitation intensity (CRCMccsm) and the highest precipitation intensity (RCM3ncep). The CRCM simulations consistently show the lowest precipitation rates at each percentile, while the RCM3 simulations tend to produce the highest precipitation. The CRCM and ECP2 are spectrally nudged models. Spectral nudging, as the term implies, "nudges" large-scale characteristics (e.g., geopotential height, U and V wind components, and temperature) within the RCM domain towards the driving reanalysis or GCM simulation (Waldron et al. 1996; von Storch et al. 2000). The potential value of spectral nudging has been well documented (Miguez-Macho et al. 2004; Alexandru et al. 2009; Mearns et al 2012; Glisan et al. 2013). For the CRCM, our results show an evident lowering of precipitation at high-intensity thresholds. This was also seen Alexandru et al (2009), where a reduction of precipitation extremes appeared when the spectral nudging became stronger, and overly adjusted the large-scale characteristics within the

RCM domain back towards the driving GCM simulation. It is unclear if this in itself explains our results, particularly because the EPC2 simulations do not show similar precipitation characteristics. Our results may also be due to the tendency for CRCM to underestimate precipitation maxima, which is well documented in previous studies (e.g., Mailhot et al. 2007), or how the parameterization scheme (Table 2) used by the CRCM initiates convection with respect to the rest of the NARCCAP models. The CRCM differences are important to keep in mind, as it consistently deviates from the rest of the models in our study.

Figure 2 (NCEP) and Figure 3 (GCM) show a histogram of normalized frequency versus intensity in the upper Mississippi region using 2.5 mm day^{-1} bins. Figure 2 contains simulations that used NCEP as the lateral boundary source, and Figure 3 contains simulations driven by GCMs. Models generally reproduce well the precipitation frequency-vs.-intensity spectrum seen in observations up to around 25 mm day^{-1}. Beyond this threshold, the ECP2 and MM5I simulations closely resemble the CPC distribution throughout the entire intensity spectrum, while the rest of the models (other than CRCM) show more high intensity events. The CRCM produces precipitation amounts that are lower than the rest of the models and observations. CMIP5 models used in Chen and Knutson (2007) were compared with the CPCs' native 0.25º x 0.25º resolution and with CPC precipitation interpolated to the same resolution as each model. Native CPC resolution showed almost all models underestimating observations, while interpolation to a model's grid showed most models either agreeing or overestimating high-intensity precipitation, which is consistent with our findings.

Figure 4 (NCEP) and 5 (GCM) show the number of very heavy events occurring simultaneously over a given number of grid points. This simultaneity plot represents the spatial scale of very heavy precipitation events (x-axis), and the frequency of days in which they occur

(y-axis). Compared to our winter analysis in Kawazoe and Gutowski (2013a), a much steeper drop with increasing number of event grid points occurs at lower spatial scales, suggesting that very heavy events during the summer months' result from systems with smaller spatial scale than in winter. As mentioned earlier, summer very heavy events often result from MCSs as opposed to winter, synoptic-scale storms dominate, usually resulting in more spatially distributed precipitation. The CRCM, and the ECP2 to a lesser extent, have a larger spatial scale for their very heavy events, suggesting that spectral nudging increases the spatial scale of simulated very heavy events.

b. Widespread very heavy precipitation

Table 5 shows the distribution of widespread very heavy events by summer months. Both the CPC and UW show July having the highest frequency of widespread events. Among the simulations, 13 of the 17 model combinations show June to have the highest frequency of widespread very heavy events, though large inter-model differences are seen on the actual percentages. This difference may be from the strength and timing of the North American monsoon, as its onset can strengthen and enhance the monsoon high in our study domain, creating subsidence and suppressing low-level jet (LLJ) related rainfall around the central US (Higgins et al. 1997; Wang and Chen 2009).

Area-averaged precipitation's diurnal cycle during widespread very heavy precipitation events appears in Figure 6. Again, results are more dictated by the individual RCMs than the driving boundary conditions. CRCM simulations show good agreement with each other throughout the day, but they deviate greatly from observed behavior, as their timing of the peak is 6-9 hours earlier, and approximately 40% of the peak intensity seen in observations. This is the lowest peak intensity among all the models. The ECP2 simulations also deviate from

observations, with the ECP2gfdl resembling occurs in the CRCM simulations in terms of peak intensity and timing, while only a slight change in precipitation occurs (~0.3 mm) throughout the day. With the exception of the MM5Iccsm (which resembles CRCM simulations and the ECP2gfdl), the rest of the RCMs show peak precipitation near the 0300-0900UTC hours peak seen in observations, with model peak intensities slightly lower that observations on average. Climate models, particularly during the warm season in and around our analysis domain tend to have precipitation that occurs too frequently, too light, and too early, compared to observations (Randall et al. 1991, Liang et al. 2004, Lee et al. 2007), often as a result of the models' convective parameterization schemes (Liang et al. 2006, Bukovsky and Karoly 2011). Although precipitation still tends to be lighter at its peak and more frequent throughout the day, it does not peak too early, with some exceptions mentioned earlier. For the GCM driven HRM3 and RCM3 simulations, we also note a secondary peak occurs around 1800UTC.

Figures 7 (NCEP) and 8 (GCM) shows composite daily precipitation during widespread very heavy events. Observational composites show a local maximum around the center of our domain, similar to some of the models, while others may show multiple precipitation maxima within the domain. Precipitation intensities are clearly lower in the CRCM models, which was seen in our precipitation intensities in Table 4, and throughout the precipitation intensity spectrum in Figures 2 and 3. This, as well as our simultaneity plots Figures 4 and 5, suggests that the CRCM does not produce the intense, convective storms seen in the rest of the models and observations. As for the rest of the models, there seems to be a high amount of variability in the precipitation characteristics. Other than the CRCM simulations and perhaps the slight southern bias of precipitation in the WRFG simulations, no clear similarities are seen regardless of the

RCM or driving boundary source. These results seem typical of summer, very heavy precipitation events when storms are often highly localized in space and time (Gershunov 1998).

c. Supporting environmental conditions

Figures 9 – 16 show composite fields produced by averaging over the widespread event days from each data source. The NARR provided the observational results, with the days to composite determined from the CPC widespread event days.

Figures 9 (NCEP) and 10 (GCM) show composite 2-m specific humidity during widespread very heavy events. Both models and observations show positive specific humidity anomaly in our region, and the location with strongest positive specific humidity anomaly coincides fairly well with locations of precipitation maxima. However, the greatest specific humidity anomaly seen in our region does not imply the strongest precipitation intensities. In addition to the strong positive anomalies within our domain, there is a corresponding dry anomaly in the southwestern US for both models and observations. This negative anomaly may be due to the pre-onset of the North American monsoon. As discussed earlier, lack of a North American monsoon provides an environment that favors the development of very heavy precipitation events around our study domain. A deeper look into the connection between the North American monsoon and precipitation in our analysis domain is needed before a more robust statement can be made, however, and is outside the scope of this paper.

Figures 11 (NCEP) and 12 (GCM) show VI-MFC (contours) and VI-MT (vectors) composites during widespread very heavy events. For VI-MT, there is strong moisture transport from the Caribbean and the Gulf of Mexico, with a northwestward moisture flow near central Texas turning northeastward toward our study region for all models and observations. VI-MT anomalies (not shown) show enhanced moisture transport into our study region compared to

climatology for all models and observations. This is seen in a wide range of studies, as heavy rain events are often caused by the added contribution of remote moisture from the Gulf/Caribbean (Bell and Janowiak 1995; Trenbreth and Guillemot 1996; Brubaker et al. 2001; Moore et al. 2012) in addition to terrestrial moisture (Dirmeyer and Brubaker 1999; Dirmeyer and Kinter 2010). For most models, highest VI-MT vectors are located at locations similar to where composite precipitations are the greatest, though the strength of the VI-MT does not seem to imply higher precipitation values. Strong VI-MFC, especially near the base of the storm, implies upward motion and convective initiation (Banacos and Schultz 2005). During widespread very heavy precipitation events, VI-MFC tends to be more positive (convergence), and aside from the RCM3ncep, shows spatial patterns similar to the composite precipitation figures. VI-MFC anomalies (not shown) show positive convergence anomalies at or near the area where precipitation is seen in the composites for all models and observations. This was also seen in Min and Schubert (1997) in the Central Plains, and Holman and Vavrus (2012) in Wisconsin, where heavy rain locations occurred in areas of high VI-MFC.

Figures 15 (NCEP) and 16 (GCM) show composite CAPE anomalies during widespread very heavy precipitation events. CAPE for the RCM3 ensemble was also computed, but it produces extremely low CAPE values (maximum values ~300 J kg^{-1}, while the rest of the models and observations produce maxima 4 to 5 times larger). The reason for this is unclear at present, and requires a deeper look into the vertical structure characteristics of this model. CAPE represents the amount of buoyant energy available in an air parcel and is related to the maximum vertical velocity within an updraft. High CAPE values will therefore represent enhanced convective potential. Both models and observations show higher CAPE values during widespread very heavy events compared to climatology, with their maxima predominantly

located to the southwest portion of our domain, which usually corresponds to higher VI-MT and higher near surface temperatures (not shown). The location of CAPE maxima is usually southwest of the precipitation maxima for both models and observations, and higher CAPE values do not always imply higher precipitation composites. Both could be an artifact the time in which we extract instantaneous CAPE values, a possible disconnect between the diurnal cycle of maximum CAPE and maximum precipitation (Lee et al. 2007), or the removal of CAPE by cumulus parameterization (e.g. Arakawa and Schubert 1974; Emanuel et al. 1994; Kain 2004). Liang et al. (2004) mention that the timing of convection may not be predicted by CAPE, but when and how convection is triggered based on particular parameterization schemes.

4. Conclusion

Six different RCMs, driven by four GCMs and NCEP reanalysis from the NARCCAP project were compared with observational data from the Climate Prediction Center (CPC), University of Washington (UW), and the North American Regional Reanalysis (NARR) to assess the capability of climate models to produce very heavy precipitation. Our study region is the upper Mississippi region, examining the years 1982-1999 during the summer months (June-August). Widespread very heavy precipitation was defined as the top 0.5% of all precipitation of above 0.25 mm day^{-1} occurring on at least 10 grid points simultaneously. During these events, composites were created for 2-m specific humidity, vertically integrated moisture flux convergence (VI-MFC), vertically integrated moisture transport (VI-MT), and convective available potential energy (CAPE).

Most simulations show lower average precipitation compared to observations and approximately half the simulations show fewer days of precipitation. In contrast, for precipitation

at the 95th, 99th, and 99.5th percentile, most simulations produce higher precipitation rates than observed at each threshold. The CRCM simulations all show the lightest precipitation at each percentile. The CRCM also has a larger spatial scale for their very heavy events. Models and observations are in good agreement for frequency-vs.-intensity up to about 25 mm day^{-1}. Above this value, the CRCM produces precipitation frequencies that are lower than the rest of the models and observations. For the rest of the models, the ECP2 and MM5I simulation reproduce well the frequency-vs.-intensity seen in observations throughout the entire spectrum, while the rest produce higher intensity precipitation compared to observations.

Models tend to produce their most frequent widespread very heavy events in June, perhaps because of the pre-onset environment of the North American monsoon, when the monsoon high does not act to suppress LLJ-related rainfall over the Great Plains. Aside from the CRCM and ECP2, whose precipitation tends to peak 6-9 hours earlier than observations, the models do well in producing the observed timing of peak precipitation, which occurs between 0300UTC-0900UTC. Simulated precipitation peaks tend to occur at slightly lower intensities than observed on average. As with earlier models, these models still tend to precipitate too much and too frequently throughout the day, especially between 1500UTC and 2100UTC. Precipitation composites show differences in spatial and intensity characteristics between models and observations. Unlike the winter, where synoptic scale forcing dictates widespread very heavy precipitation, more complex local and regional scale forcing, in addition to the large-scale forcing, appears to play a role during the summer, yielding a spread of precipitation spatial distribution and statistical characteristics. The 2-m specific humidity shows high moisture content in the region in both models and observations during the widespread events, with corresponding lower moisture to the southwest, perhaps due to the pre-onset environment of the

North American monsoon. The location of positive VI-MFC during the widespread events agrees fairly well with the location of precipitation, and both models and observations show VI-MT from the Gulf of Mexico. Positive CAPE anomalies in the composites dominate the areas where precipitation is present as well.

In summary, though there are differences in precipitation characteristics, NARCCAP models as an ensemble appear capable of producing very heavy precipitation events in the analysis region for the correct physical behavior seen in observations. Although differences between models and observations and between models need consideration, results here should support the use of the NARCCAP models to evaluate changes in future climates.

Acknowledgements

This work was supported by National Science Foundation Grants AGS-1243106 and BCS-1114978. Daily gridded observed precipitation data were obtained from the Surface Water Modeling group at the University of Washington. CPC US Unified Precipitation data and NCEP Reanalysis data was provided by the NOAA/OAR/ESRL PSD, Boulder, Colorado, USA, from their website at http://www.esrl.noaa.gov/psd/. We thank the North American Regional Climate Change Assessment Program (NARCCAP) for providing the data used in this paper. NARCCAP is funded by the National Science Foundation (NSF), the U.S. Department of Energy (DoE), the National Oceanic and Atmospheric Administration (NOAA), and the U.S. Environmental Protection Agency Office of Research and Development (EPA). We also thank Melissa Bukovsky for providing us the CAPE data that is not yet available to the public. This study would not be as effective without her assistance.

References

Alexandru, A., R. de Ella, R. Laprise, L. Separovic, and S. Biner, 2009: Sensitivity study of regional climate model simulations to large-scale nudging parameters. *Mon. Wea. Rev.*, **137**, 1666–1686, doi:10.1175/2008MWR2620.1.

Anderson, C. J., and Coauthors, 2003: Hydrological processes in regional climate model simulations of the central United States flood of June–July 1993. *J. Hydrometeor.*, **4**, 584–598, doi:10.1175/1525-7541(2003)004<0584:HPIRCM>2.0.CO;2

Arakawa, A., and W. H. Schubert, 1974: Interaction of a cumulus cloud ensemble with the large-scale environment, Part I. *J. Atmos. Sci.*, **31**, 674–701, doi:10.1175/1520-0469(1974)031<0674:IOACCE>2.0.CO;2.

Banacos, P., and D. Schultz, 2005: The use of moisture flux convergence in forecasting convection initiation: Historical and operational perspectives. *Wea. Forecasting*, **20**, 351–366, doi:10.1175/WAF858.1.

Bell, G. D., and J. E. Janowiak, 1995: Atmospheric circulation associated with the Midwest floods of 1993. *Bull. Amer. Meteor. Soc.*, **76,** 681–696, doi:10.1175/1520-0477(1995)076<0681:ACAWTM>2.0.CO;2

Bechtold, P., E. Bazile, F. Guichard, P. Mascart, and E. Richard, 2001: A mass-flux convection scheme for regional and global models. *Quart. J. Roy. Meteor. Soc.*, **127**, 869–886, doi:10.1002/qj.49712757309.

Brubaker, K.L., P.A. Dirmeyer, A. Sudradjat, B.S. Levy, F. Bernal, 2001: A 36-yr Climatological Description of the Evaporative Sources of Warm-Season Precipitation in the Mississippi River Basin. *J. Hydrometeor.*, **2**, 537-557, doi:10.1175/15257541(2001)002<0537:AYCDOT>2.0.CO;2.

Bukovsky, M. S., and D. J. Karoly, 2011: A regional modeling study of climate change impacts on warm-season precipitation in the central United States. *J. Climate*, **24**, 1985–2002, doi:10.1175/2010JCLI3447.1.

Chen, C.-T., and T. Knutson, 2008: On the verification and comparison of extreme rainfall indices from climate models. *J. Climate*, **21**, 1605–1621, doi:10.1175/2007JCLI1494.1.

Christensen, J. H., T. R. Carter, M. Rummukainen, and G. Amanatidis, 2007: Evaluating the performance and utility of regional climate models: The PRUDENCE project. *Climatic Change*, **81**, 1–6, doi:10.1007/s10584-006-9211-6

Coleman, J.S.M., and D. Budikova, 2010: Atmospheric aspects of the 2008 Midwest floods: a repeat of 1993? *International Journal of Climatology*, **30**, 1645-1667, doi:10.1002/joc.2009.

Dirmeyer, P. A., and K. L. Brubaker, 1999: Contrasting evaporative moisture sources during the drought of 1988 and the flood of 1993. *J. Geophys. Res.*, **104**, 19 383–19 397, doi:10.1029/1999JD900222.

Dirmeyer, P. A., and J. L. Kinter, 2010: Floods over the U.S. Midwest: A regional water cycle perspective. *J. Hydrometeor.*, **11**, 1172–1181, doi:10.1175/2010JHM1196.1.

Duffy, P. B., B. Govindasamy, J. P. Iorio, J. Milovich, K. R. Sperber, K. E. Taylor, M. F. Wehner, and S. L.Thompson, 2003: High-resolution simulations of global climate, part 1: Present climate. *Climate Dyn.*, **21**, 371–390, doi:10.1007/s00382-003-0339-z.

Emanuel, K. A., J. D. Neelin, and C. S. Bretherton, 1994: On large-scale circulations in convecting atmospheres. *Quart. J. Roy. Meteor. Soc.*, **120**, 1111–1143, doi:10.1002/qj.49712051902.

Emori, S., A. Hasegawa, T. Suzuki, and K. Dairaku. 2005: Validation, parameterization dependence and future projection of daily precipitation simulated with a high-resolution atmospheric GCM. *Geophys. Res. Lett.*, **32**, L06708, doi:10.1029/2004GL022306.

Frei, C., R. Schooll, S. Fukutome, J. Schmidli, and P. L. Vidale, 2006: Future change of precipitation extremes in Europe: Intercomparison of scenarios from regional climate models. *J. Geophys. Res.*, **111**, D06105, doi:10.1029/2005JD005965.

Fritsch, J. M., and C. F. Chappell, 1980: Numerical prediction of convectively driven mesoscale pressure systems. Part I: Convective parameterization. *J. Atmos. Sci.*, **37**, 1722–1733, doi: 10.1175/1520-0469(1980)037<1722:NPOCDM>2.0.CO;2.

Fowler, H. J., M. Ekström, C. G. Kilsby, and P. D. Jones, 2005: New estimates of future changes in extreme rainfall across the UK using regional climate model integrations. 1. Assessment of control climate. *J. Hydrol.*, **300**, 212–233, doi:10.1016/j.jhydrol.2004.06.017

Gershunov, A., 1998: ENSO influence on intraseasonal extreme rainfall and temperature frequencies in the contiguous United States: Implications for long-range predictability. *J. Climate*, **11**, 3192–3203, doi:10.1175/1520-0442(1998)011<3192:EIOIER>2.0.CO;2.

Glisan, J. M., W. J. Gutowski, J. J. Cassano, and M. E. Higgins, 2013: Effects of spectral nudging in WRF on Arctic temperature and precipitation simulations. *J. Climate*, **26**, 3985–3999, doi:10.1175/JCLI-D-12-00318.1.

Gregory, D., and P. R. Rowntree, 1990: A mass-flux convection scheme with representation of cloud ensemble characteristics and stability dependent closure. *Mon. Wea. Rev.*, **118**, 1483–1506, doi:10.1175/1520-0493(1990)118<1483:AMFCSW>2.0.CO;2.

Gregory, D., and S. Allen, 1991: The effect of convective scale downdrafts upon NWP and climate simulations. Preprints, *Ninth Conf. on Numerical Weather Prediction,* Denver, CO, Amer. Meteor. Soc.,122–123.

Gregory, D., R. Kershaw, and P. M. Inness, 1997: Parametrization of momentum transport by convection. II: Tests in single-column and general circulation models. *Quart. J. Roy. Meteor. Soc.*, **123**,1153–1183, doi:10.1002/qj.49712354103.

Grell, G. A., J. Dudhia, and D. R. Stauffer, 1993: A description of the fifth-generation Penn State/NCAR Mesoscale Model (MM5). NCAR Tech. Note NCAR/TN-398+STR, 107 pp.

Grell, G. A., and D. Devenyi, 2002: A generalized approach to parameterizing convection combining ensemble and data assimilation techniques. *Geophys. Res. Lett.*, **29** (14), doi:10.1029/2002GL015311.

Groisman, P.Y, R.W. Knight, D.R. Easterling, T.R. Karl, G.C. Hegerl, and V.N. Razuvaev, 2005: Trends in Intense Precipitation in the Climate Record. *J. Climate*, **18**, 1326–1350, doi:10.1175/JCLI3339.1

Gutowski, W. J., S.S. Willis., J. C. Patton, B.R.J. Schwedler, R.W. Arritt, and E.S. Takle, 2008: Changes in extreme, cold-season synoptic precipitation events under global warming. *Geophys. Res. Lett.,* **35**, L20710, doi:10.1029/2008GL035516.

Gutowski, W. J., and Coauthors, 2010: Regional extreme monthly precipitation simulated by NARCCAP RCMs. *J. Hydrometeor.,* **11**, 1373–1379, doi:10.1175/2010JHM1297.1.

Hagedorn R, F.J. Doblas-Reyes, and T.N. Palmer, 2005: The rationale behind the success of multi-model ensembles in seasonal forecasting. *Tellus* **57A,** 219-233, doi:10.1111/j.1600-0870.2005.00103.x.

Higgins, R. W., Y. Yao, and X. L. Wang, 1997: Influence of the North American monsoon system on the U.S. summer precipitation regime. *J. Climate,* **10**, 2600–2622, doi:10.1175/1520-0442(1997)010<2600:IOTNAM>2.0.CO;2.

Higgins, R. W., W. Shi, E. Yarosh, and R. Joyce, 2000: Improved United States precipitation quality control system and analysis. *NCEP/Climate Prediction Center Atlas, No. 7.*

Holman, K. D., and S. J. Vavrus, 2012: Understanding simulated extreme precipitation events in Madison, Wisconsin, and the role of moisture flux convergence during the late twentieth and twenty-first centuries. *J. Hydrometeor.*, **13**, 877–894, doi:10.1175/JHM-D-11-052.1.

Kain, J. S., and J. M. Fritsch, 1990: A one-dimensional entraining/detraining plume model and its application in convective parameterization. *J. Atmos. Sci.,* **47**, 2784–2802, doi: 10.1175/1520-0469(1990)047<2784:AODEPM>2.0.CO;2.

Kain, J. S., 2004: The Kain–Fritsch convective parameterization: An update. *J. Appl. Meteor.*, **43**,170–181, doi:10.1175/1520-0450(2004)043<0170:TKCPAU>2.0.CO;2.

Karl, T. R., G. A. Meehl, C. D. Miller, S. J. Hassol, A. M. Waple, and W. L. Murray, Eds., 2008: Weather and climate extremes in a changing climate: Regions of focus: North America, Hawaii, Caribbean, and U.S. Pacific Islands. U.S. Climate Change Science Program Rep., 162 pp.

Kawazoe, S., and W.J. Gutowski. 2013a: Regional, Very Heavy Daily Precipitation in NARCCAP Simulations. *J. Hydrometeor*., **14**, 1212-1227, doi:10.1175/JHM-D-12-068.1.

Kawazoe, S., and W.J. Gutowski. 2013b: Regional, Very Heavy Daily Precipitation in CMIP5 Simulations *J. Hydrometeor*., **14**, 1228-1242, doi:10.1175/JHM-D-12-0112.1.

Kunkel, K.E., S.A. Changnon, and J.R. Angel, 1994: Climatic aspects of the 1993 Upper Mississippi River Basin flood. *Bull. Amer. Meteor. Soc.*, **75,** 811-822, doi:10.1175/1520-0477(1994)075<0811:CAOTUM>2.0.CO;2.

Lee, M.-I., S. D. Schubert, M. J. Suarez, I. M. Held, N.-C. Lau, J. J.Ploshay, A. Kumar, H.-K. Kim, and J. E. Schemm. 2007: An analysis of the warm season diurnal cycle over the continental United States and northern Mexico in general circulation models. *J. Hydrometeorol*., **8**, 344-366, doi:10.1175/JHM581.1.

Leung, L. R., Y. Qian, X. Bian, W. M. Washington, J. Han, and J. O. Roads, 2004: Mid-century ensemble regional climate change scenarios for the western United States. *Climatic Change*, **62**, 75–113, doi:10.1023/B:CLIM.0000013692.50640.55

Liang, X.-Z., L. Li, A. Dai, and K.E. Kunkel, 2004: Regional climate model simulation of summer precipitation diurnal cycle over the United States. *Geophys. Res. Lett*., **31**, L24208, doi:10.1029/2004GL021054.

Liang, X. Z., J. Pan, J. Zhu, K. E. Kunkel, J. X. L. Wang, and A.Dai, 2006: Regional climate model downscaling of the U.S. summer climate and future change. *J. Geophys. Res.*, **111**, D10108, doi:10.1029/2005JD006685.

Maddox, R. A., C. F. Chappell, and L. R. Hoxit, 1979: Synoptic and meso-α scale aspects of flash flood events. *Bull. Amer. Meteor. Soc.*, **60**, 115–123, doi:10.1175/1520-0477-60.2.115.

Mailhot, A., S. Duchesne, D. Caya, and G. Talbot, 2007: Assessment of future change in intensity–duration–frequency (IDF) curves for Southern Quebec using the Canadian Regional Climate Model (CRCM). *J. Hydrol.*, **347,** (1–2). 197–210, doi:10.1016/j.jhydrol.2007.09.019.

Mailhot, A., I. Beauregard, G. Talbot, D. Caya, and S. Biner, 2011: Future changes in intense precipitation over Canada assessed from multi-model NARCCAP ensemble simulations, *Int. J. Climatol*., **32**, 1151-1163, doi:10.1002/joc.2343.

Mahoney, K., M. Alexander, J. D. Scott, and J. Barsugli, 2013: High-resolution downscaled simulations of warm-season extreme precipitation events in the Colorado Front Range under past and future climates. *J. Climate*, **26**, 8671–8689, doi:10.1175/JCLI-D-12-00744.1.

Maurer, E.P., A.W. Wood, J.C. Adam, D.P. Lettenmaier, and B. Nijssen, 2002: A long-term hydrological based dataset of land surface fluxes and states for the conterminous United States. *J. Climate,* **15,** 3237-3251, doi:10.1175/1520-0442(2002)015<3237:ALTHBD>2.0.CO;2.

Miguez-Macho, G., G. L. Stenchikov, and A. Robock, 2004: Spectral nudging to eliminate the effects of domain position and geometry in regional climate model simulations. *J. Geophys. Res.*, **109**, D13104, doi:10.1029/2003JD004495.

Min, W., and S. Schubert, 1997: The climate signal in regional moisture fluxes: A comparison of three global data assimilation products. *J. Climate*, **10**, 2623–2642, doi:10.1175/1520-0442(1997)010<2623:TCSIRM>2.0.CO;2.

Mearns, L. O., W. J. Gutowski, R. Jones, L.-Y. Leung, S. McGinnis, A. M. B. Nunes, and Y. Qian, 2009: A regional climate change assessment program for North America. *Eos, Trans. Amer.Geophys. Union*, **90,** 311, doi:10.1029/2009EO360002.

Mearns, L.O., and Coauthors, 2012: The North American Regional Climate Change Assessment Program: Overview of Phase I results. *Bull. Amer. Meteor. Soc.*, **93**, 1337–1362, doi:10.1175/BAMS-D-11-00223.1.

Meehl, G.A., J.M. Arblaster, and C. Tebaldi, 2005: Understanding future patterns of increased precipitation intensity in climate model simulations. *Geophys. Res. Lett*., **32,** L18719, doi:10.1029/2005GL023680.

Meehl G.A., C. Covey, T. Delworth, M. Latif, B. McAvaney, J.F.B. Mitchell, R.J. Stouffer, and K.E. Taylor, 2007: The WCRP CMIP3 Multimodel Dataset: A new era in climate change research. *Bull. Amer. Meteor. Soc.*, **88,** 1383-1394, doi:10.1175/BAMS-88-9-1383.

Mesinger, F., and Coauthors, 2006: North American Regional Reanalysis. *Bull. Amer. Meteor. Soc.*, **87,** 343-360, doi:10.1175/BAMS-87-3-343

Moore, G. J., P. J. Neiman, F. M. Ralph, and F. Barthold, 2012: Physical processes associated with heavy flooding rainfall in Nashville, Tennessee, and vicinity during 1–2 May 2010: The role of an atmospheric river and mesoscale convective systems. *Mon. Wea. Rev.*, **140**, 358–378, doi:10.1175/MWR-D-11-00126.1.

Murphy, J. M., D. M. H. Sexton, D. N. Barnett, G. S. Jones, M. J. Webb, M. Collins, and D.A. Stainforth, 2004: Quantification of modelling uncertainties in a large ensemble of climate change simulations. *Nature*, **429**, 768-772, doi:10.1038/nature02771.

Palmer, T.N., and J. Räisänen, 2002: Quantifying the risk of extreme seasonal precipitation events in a changing climate. *Nature,* **415,** 512-514, doi:10.1038/415512a.

Pan, H.-L., and W.-S. Wu, 1995: Implementing a mass flux convective parameterization package for the NMC medium-range forecast model. NMC Office Note 409, 40 pp.

Randall, D. A., Harsvardhan, and D. A. Dazlich, 1991: Diurnal variability of the hydrologic cycle in a general circulation model. *J. Atmos. Sci.*, **48**, 40–62, doi:10.1175/1520-0469(1991)048<0040:DVOTHC>2.0.CO;2.

Seneviratne, S.I., and Coauthors 2012: Changes in climate extremes and their impacts on the natural physical environment. In: *Managing the Risks of Extreme Events and Disasters to Advance Climate Change Adaptation* Field, C.B., Eds., A Special Report of Working Groups I and II of the Intergovernmental Panel on Climate Change (IPCC). Cambridge University Press, Cambridge, UK, and New York, NY, USA, pp. 109-230.

Schumacher, R. S., and R. H. Johnson, 2006: Characteristics of U.S. Extreme Rain Events during 1999–2003. *Wea. Forecasting*, **21**, 69–85, doi:10.1175/WAF900.1

Shepard, D.S., 1984: Computer Mapping: The SYMAP interpolation algorithm. *Spatial Statistics and Models,* G.L Gaile and C.J. Willmott, Eds., Theory and Decision Library, Vol. 40, D. Reidel, 133–145.

Taylor, K. E., R. J. Stouffer, and G. A. Meehl, 2012: An overview of CMIP5 and the experiment design. *Bull. Amer. Meteor. Soc*., **93**, 485–498, doi:10.1175/BAMS-D-11-00094.1.

Trenberth, K. E., and C. J. Guillemot, 1996: Physical processes involved in the 1988 drought and 1993 floods in North America. *J. Climate*, **9**, 1288–1298, doi:10.1175/1520-0442(1996)009<1288:PPIITD>2.0.CO;2

Waldron, K. M., J. Peagle, and J. D. Horel, 1996: Sensitivity of a spectrally filtered and nudged limited-area model to outer model options. Mon. Wea. Rev., 124, 529–547, doi : 10.1175/1520-0493(1996)124<0529:SOASFA>2.0.CO;2.

Wallace, J. M., 1975: Diurnal variations in precipitation and thunderstorm frequency over the conterminous United States. *Mon. Wea. Rev.*, **103**, 406–419, doi:10.1175/1520-0493(1975)103<0406:DVIPAT>2.0.CO;2.

Wang, S., and T. Chen, 2009: The late-spring maximum of rainfall over the U.S. central plains and the role of the low-level jet. *J. Climate*, **22**, 4696–4709, doi:10.1175/2009JCLI2719.1.

von Storch, H., H. Langenberg, and F. Feser, 2000: A spectral nudging technique for dynamical downscaling purposes. *Mon. Wea. Rev.*, **128**, 3664–3673, doi:10.1175/1520-0493(2000)128<3664:ASNTFD>2.0.CO;2.

Table 1. NARCCAP RCM and GCM simulations. “X” designate combinations available and used for both precipitation and their supporting environments, “O” represents combinations available but only used for precipitation, and “n” denotes combinations available, but is not used in this study.

	Phase I	Phase II			
Model	ncep	ccsm	cgcm3	gfdl	hadcm3
CRCM	X	X	X		
ECP2	O			O	n
HRM3	X			X	X
MM5I	X	X			X
RCM3	X		X	X	
WRFG	X	X	X		

Table 2. Convective parameterization scheme used in each NARCCAP RCM.

	Convective parameterization scheme
CRCM	Bechtold–Kain–Fritsch (Bechtold et al. 2001; Kain and Frisch 1990)
ECP2	Simplified Arakawa–Schubert (Pan and Wu 1995)
HRM3	Mass flux with downdraft and momentum transport (Gregory and Rowntree 1990; Gregory and Allen 1991; Gregory et al. 1997)
MM5I	Kain–Fritsch 2 (Kain 2004)
RCM3	Grell with Fritsch–Chappell closure (Grell 1993; Fritsch and Chappell 1980)
WRFG	Grell–Devenyi (Grell and Devenyi 2002)

Table 3. Properties of NARCCAP models, CPC, and UW: overall average precipitation rate, and percentage of days reporting precipitation (the percentage of days exceeding 2.5 mm precipitation is in parentheses).

	Average Precipitation Rate (mm day^{-1})	Days with precipitation (%)
CPC	3.35	47.0 (26.7)
UW	3.28	56.4 (31.2)
CRCMccsm	1.97	53.4 (23.4)
CRCMcgcm3	2.65	57.0 (27.7)
CRCMncep	2.75	53.0 (28.8)
ECP2gfdl	3.95	48.9 (30.0)
ECP2ncep	2.64	29.1 (19.7)
HRM3gfdl	3.04	52.2 (26.3)
HRM3hadcm3	3.27	48.7 (25.6)
HRM3ncep	2.28	41.7 (17.6)
MM5Iccsm	2.74	38.1 (24.1)
MM5Ihadcm3	3.10	35.4 (23.4)
MM5Incep	2.52	32.4 (20.8)
RCM3cgcm3	4.26	49.3 (30.1)
RCM3gfdl	4.07	54.2 (32.2)
RCM3ncep	3.11	35.7 (20.7)
WRFGccsm	1.68	34.7 (13.5)
WRFGcgcm3	2.13	38.4 (15.9)
WRFGncep	2.23	35.5 (16.2)

Table 4. Precipitation intensity (in mm day^{-1}) for models and observations at the 95^{th}, 99^{th}, and 99.5^{th} percentiles for all precipitation events.

Source	95^{th}	99^{th}	99.5^{th}
CPC	26.52	47.05	56.41
UW	20.24	34.77	41.37
CRCMccsm	12.39	23.20	28.57
CRCMcgcm3	16.71	29.76	35.58
CRCMncep	17.46	30.45	36.71
ECP2gfdl	28.21	47.38	56.43
ECP2ncep	30.54	51.33	61.82
HRM3gfdl	21.58	43.70	57.58
HRM3hadcm3	25.34	54.09	70.34
HRM3ncep	22.37	47.73	63.52
MM5Iccsm	24.48	44.43	55.28
MM5Ihadcm3	30.31	56.45	69.85
MM5Incep	26.53	48.35	59.89
RCM3cgcm3	33.00	61.64	75.09
RCM3gfdl	28.16	53.32	66.19
RCM3ncep	34.20	70.93	89.42
WRFGccsm	21.00	47.40	59.17
WRFGcgcm3	24.53	50.78	62.46
WRFGncep	27.22	59.15	74.45

Table 5. Percentage of widespread very heavy events by month for observations and for each model. Month with highest frequncy of very heavy preciptaiton events per source is bolded.

Source	June	July	August
CPC	31.8%	**38.6%**	29.5%
UW	28.8%	**44.1%**	27.1%
CRCMccsm	**91.4%**	7.1%	1.4%
CRCMcgcm3	**51.7%**	24.1%	24.1%
CRCMncep	**57.8%**	36.1%	6.0%
ECP2gfdl	**47.7%**	23.1%	29.2%
ECP2ncep	**51.3%**	28.2%	20.5%
HRM3gfdl	35.6%	21.9%	**42.5%**
HRM3hadcm3	**36.9%**	35.4%	27.7%
HRM3ncep	**59.3%**	25.9%	14.8%
MM5Iccsm	**52.2%**	34.8%	13.0%
MM5Ihadcm3	35.0%	**47.5%**	17.5%
MM5Incep	**47.2%**	30.6%	22.2%
RCM3cgcm3	**49.0%**	27.5%	23.5%
RCM3gfdl	29.1%	**36.4%**	34.5%
RCM3ncep	34.3%	**51.4%**	14.3%
WRFGccsm	**70.6%**	23.5%	5.9%
WRFGcgcm3	**64.5%**	16.1%	19.4%
WRFGncep	**44.8%**	41.4%	13.8%

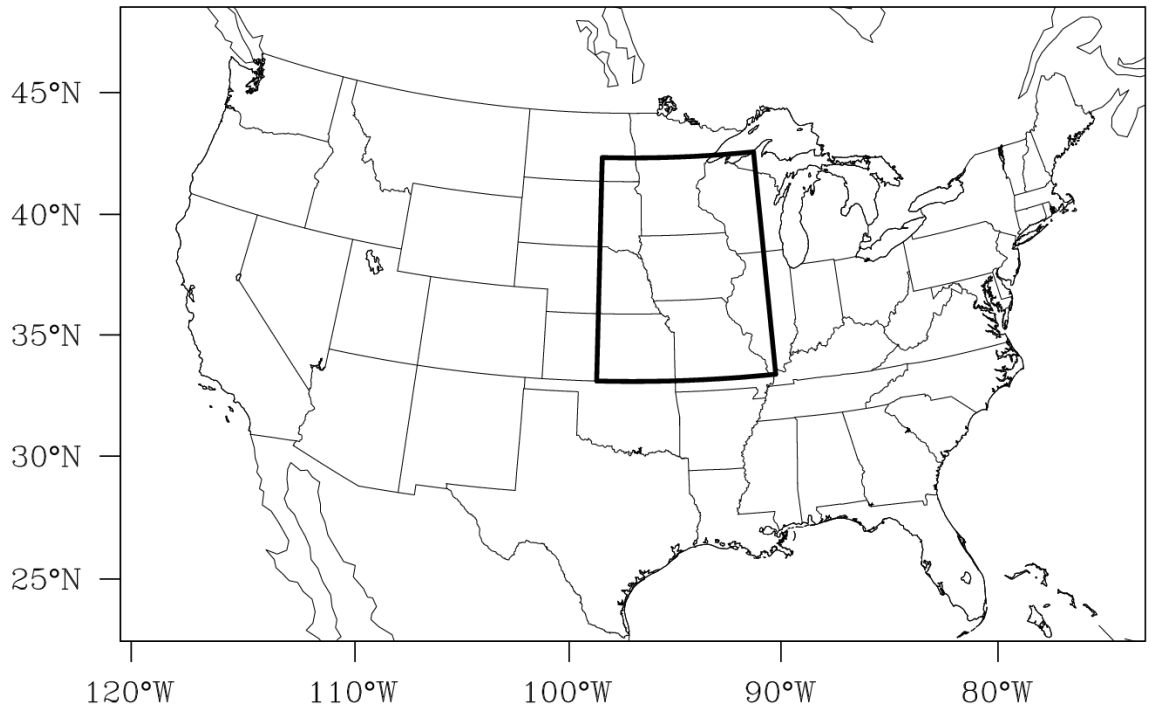

Figure 1. Region covered by each NARCCAP models and the NARR. Analyzed region is highlighted: Upper Mississippi region.

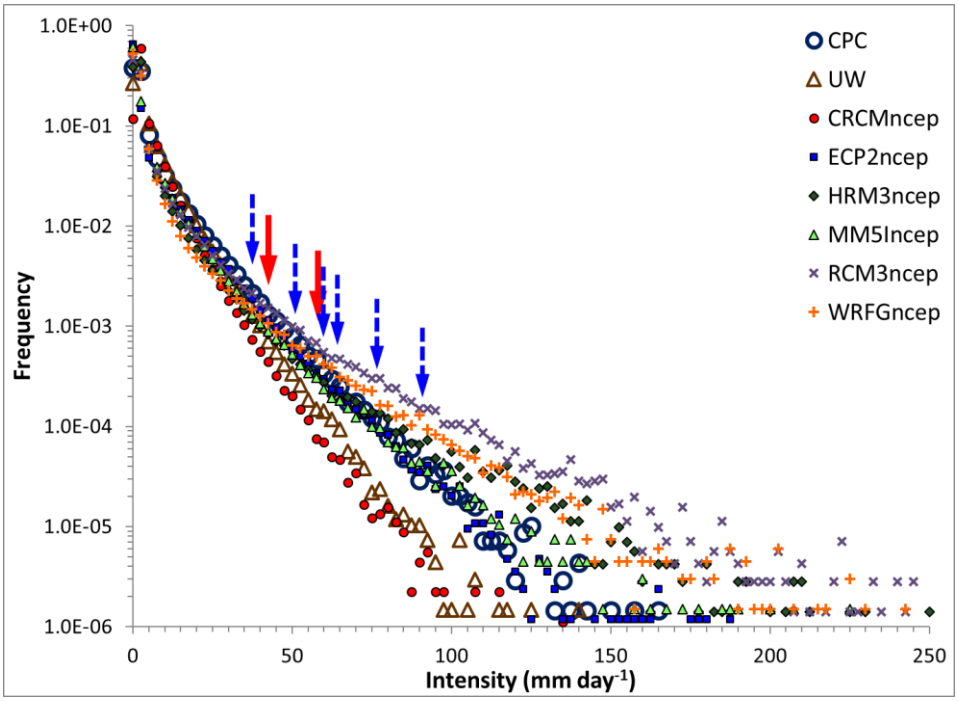

Figure 2. Normalized frequency of precipitation as a function of daily intensity for 1982-1999 in NARCCAP NCEP-driven runs and observation. Arrows mark the 99.5th percentile: red: CPC and UW, blue: RCMs.

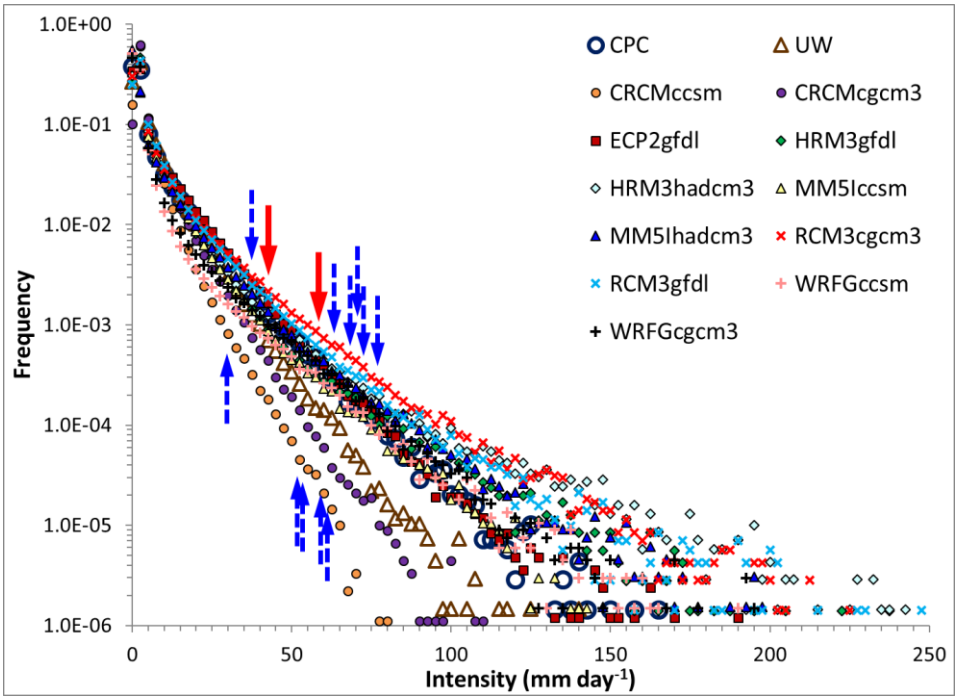

Figure 3. Same as Figure 2, but with NARCCAP GCM-driven runs and observations.

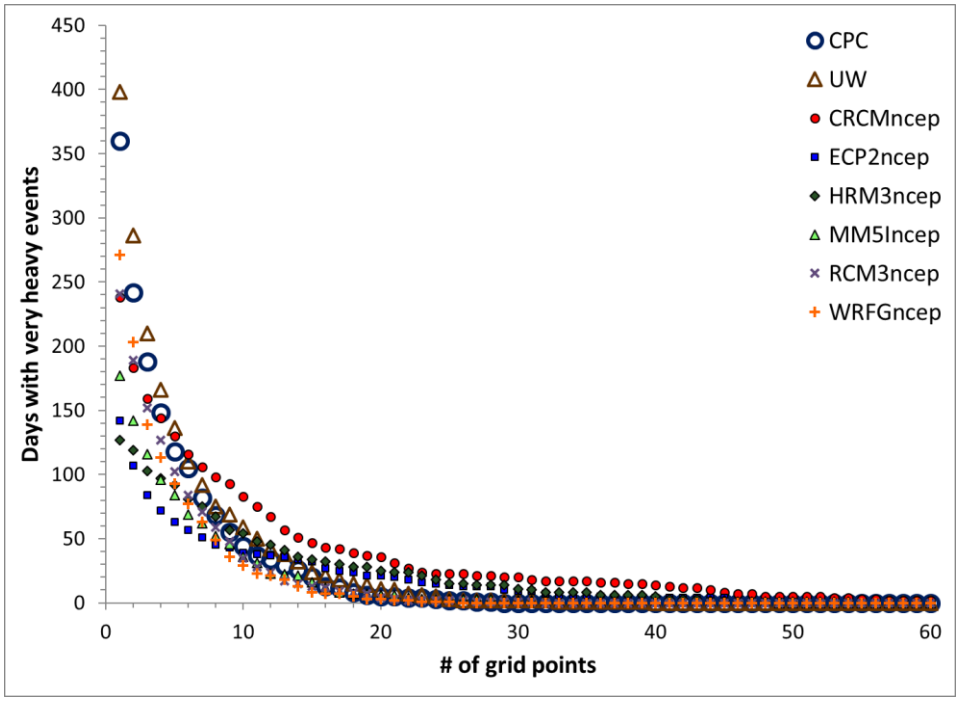

Figure 4. Days with simultaneous very heavy events on "N" grid points for NARCCAP NCEP-driven runs and observations.

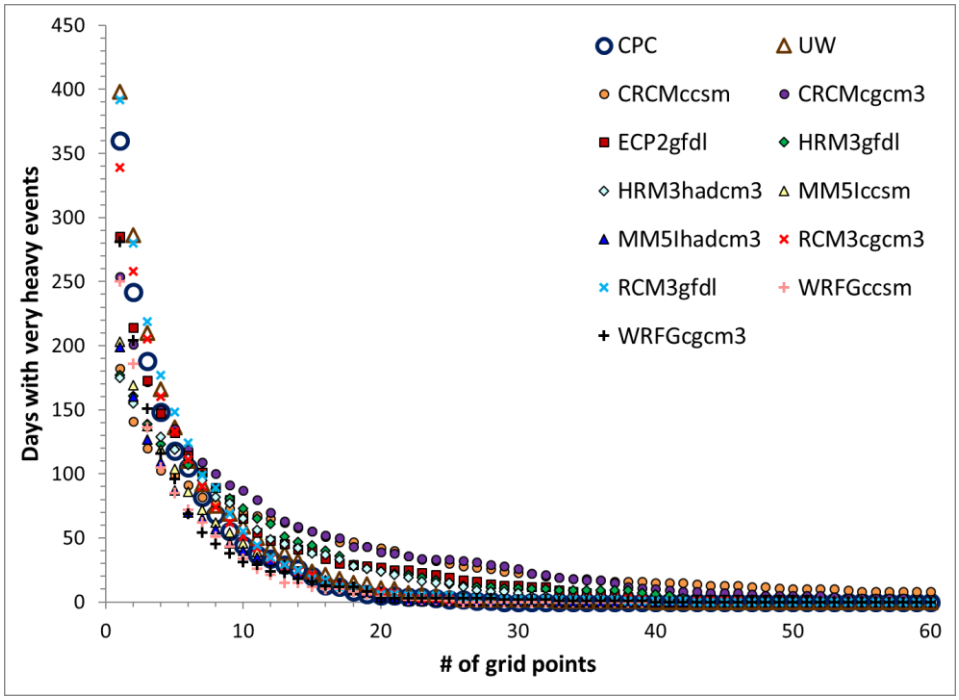

Figure 5. Same as Figure 4, but with NARCCAP GCM-driven runs and observations.

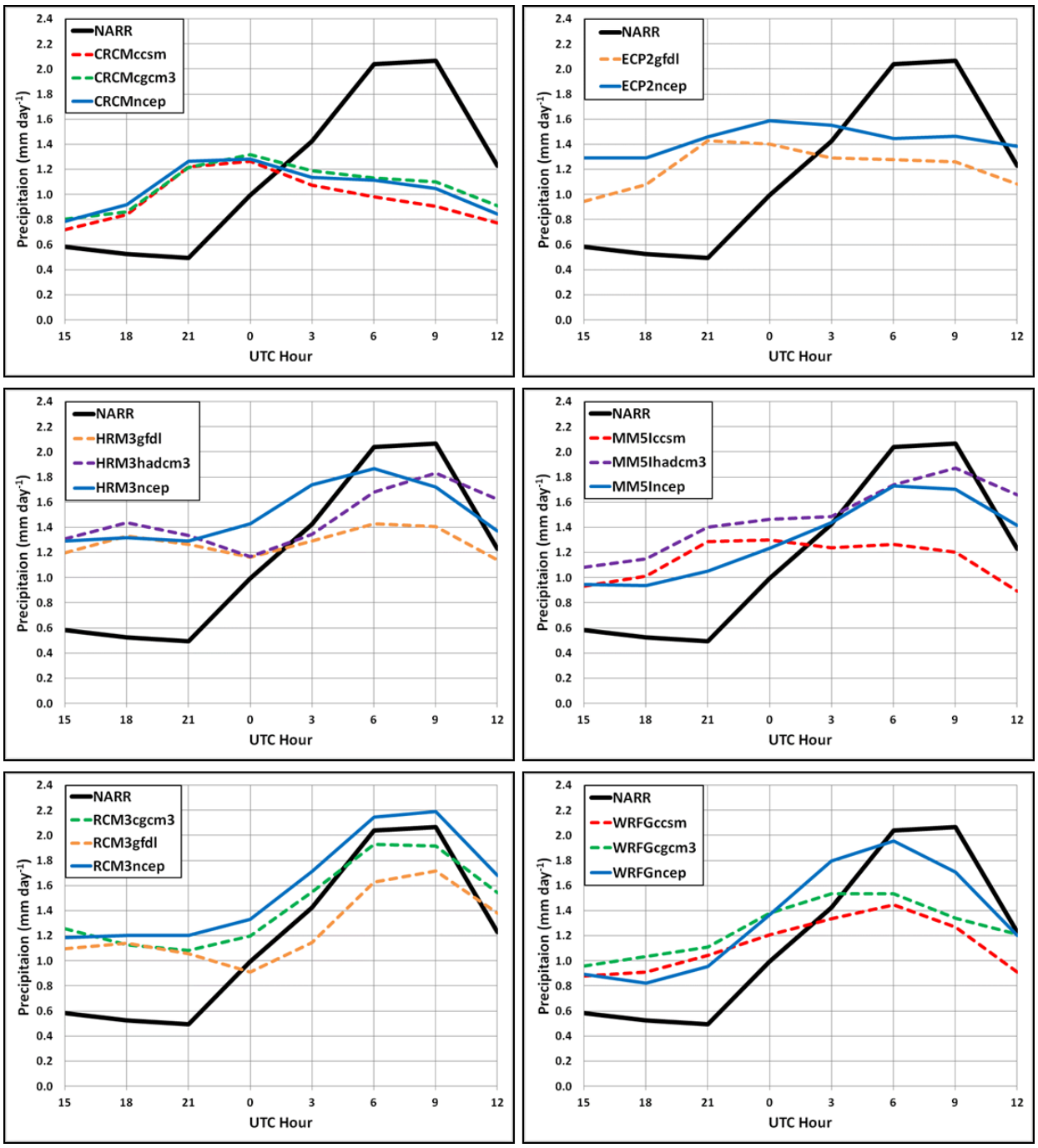

Figure 6. Diurnal cycle composites of area-averaged, widespread very heavy precipitation events each model and NARR observations. NARR: black solid line. RCM-GCM: dashed lines. RCM-NCEP: Solid blue lines. Time indicated on x-axis represents the end of each 3-hour interval.

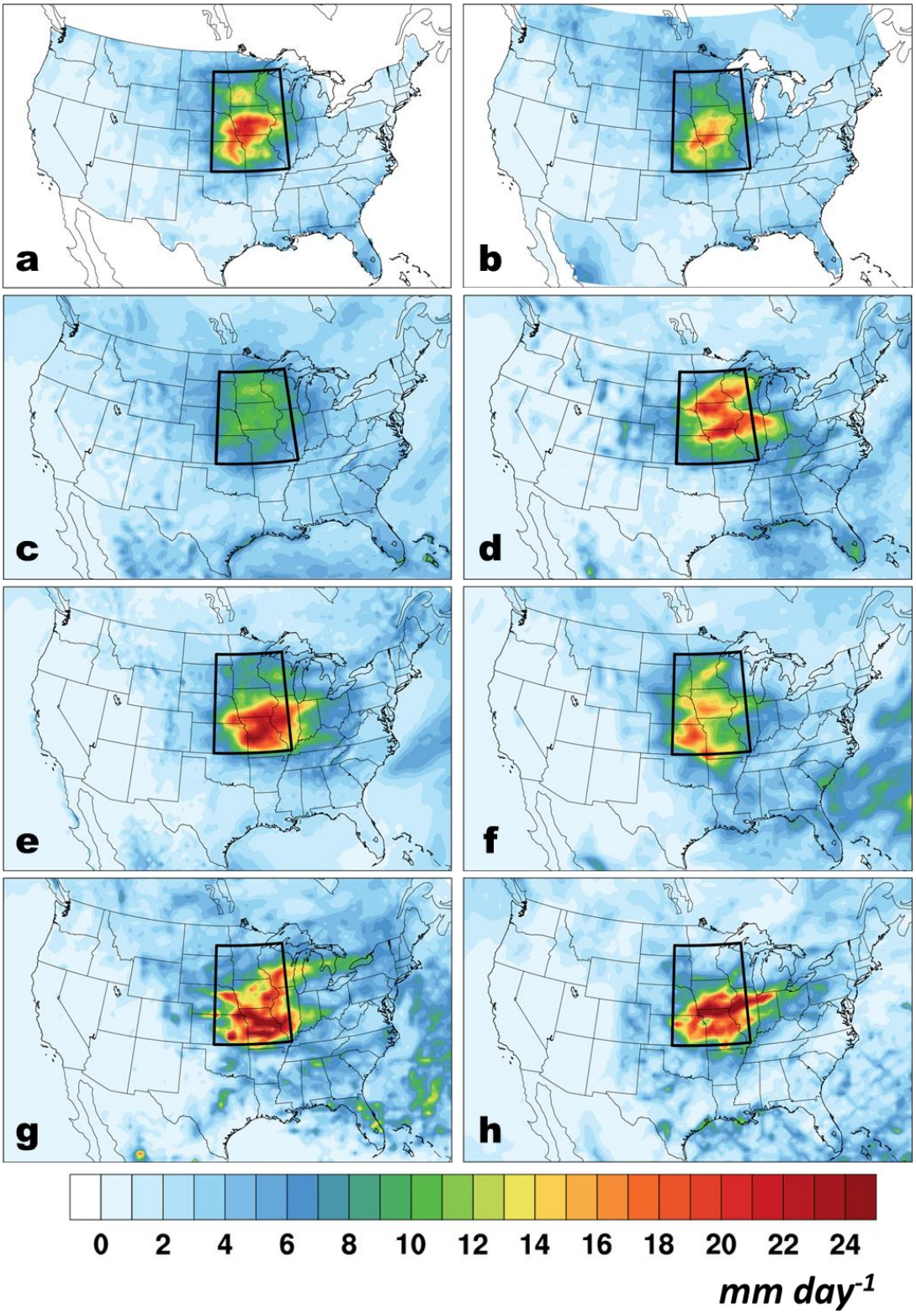

Figure 7. Composite daily precipitation during widespread very heavy events for observations and NCEP driven runs: (a) CPC, (b) UW, (c) CRCM, (d) ECP2, (e) HRM3, (f) MM5I, (g) RCM3, (h) WRFG. Contour scale for all plots is on the bottom, in mm day^{-1}.

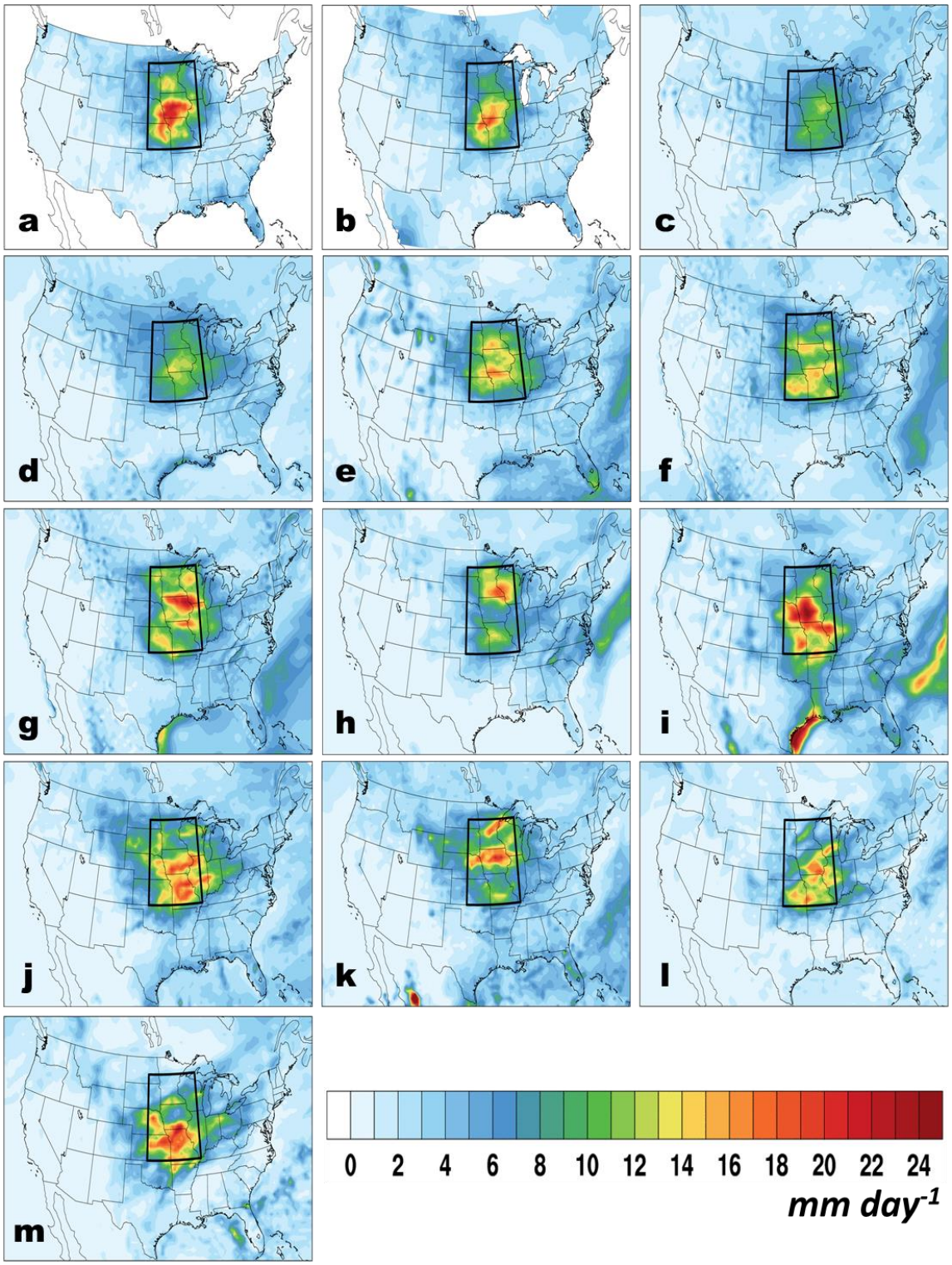

Figure 8. Same as Figure 7, but for observations and GCM driven runs: (a) CPC, (b) UW, (c) CRCMccsm, (d) CRCMcgcm3, (e) ECP2gfdl, (f) HRM3gfdl, (g) HRM3hadcm3, (h) MM5Iccsm, (i) MM5Ihadcm3, (j) RCM3cgcm3, (k) RCM3gfdl, (l) WRFGccsm, (m) WRFGcgcm3.

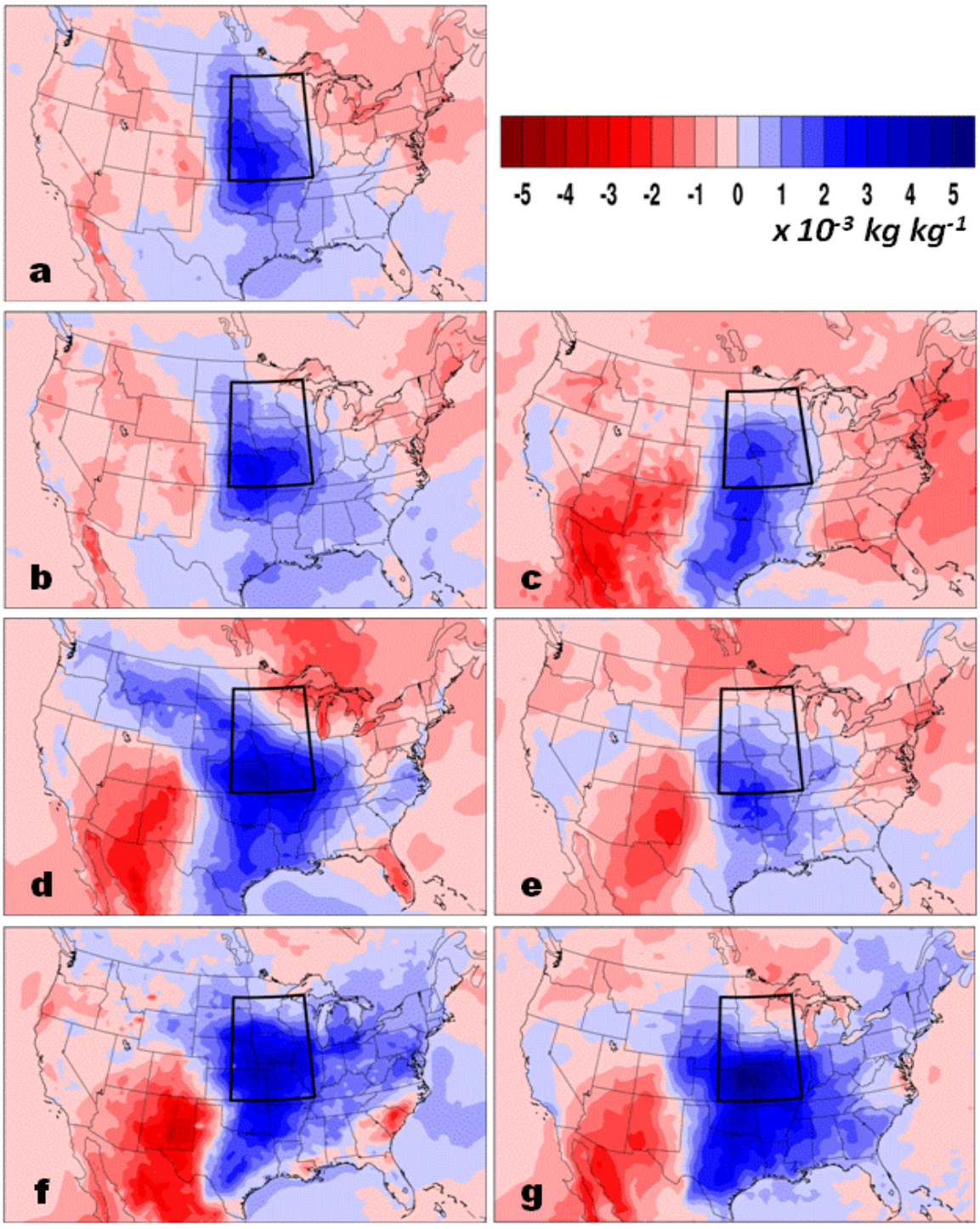

Figure 9. Composite 2-m specific humidity anomalies during widespread very heavy events for observations and NCEP driven runs: (a) NARR (CPC days) (b) NARR (UW days), (c) CRCM, (d) HRM3, (e) MM5I, (f) RCM3, (g) WRFG. Contour scale for all plots is in the upper right, in 10^{-3} kg kg^{-1}.

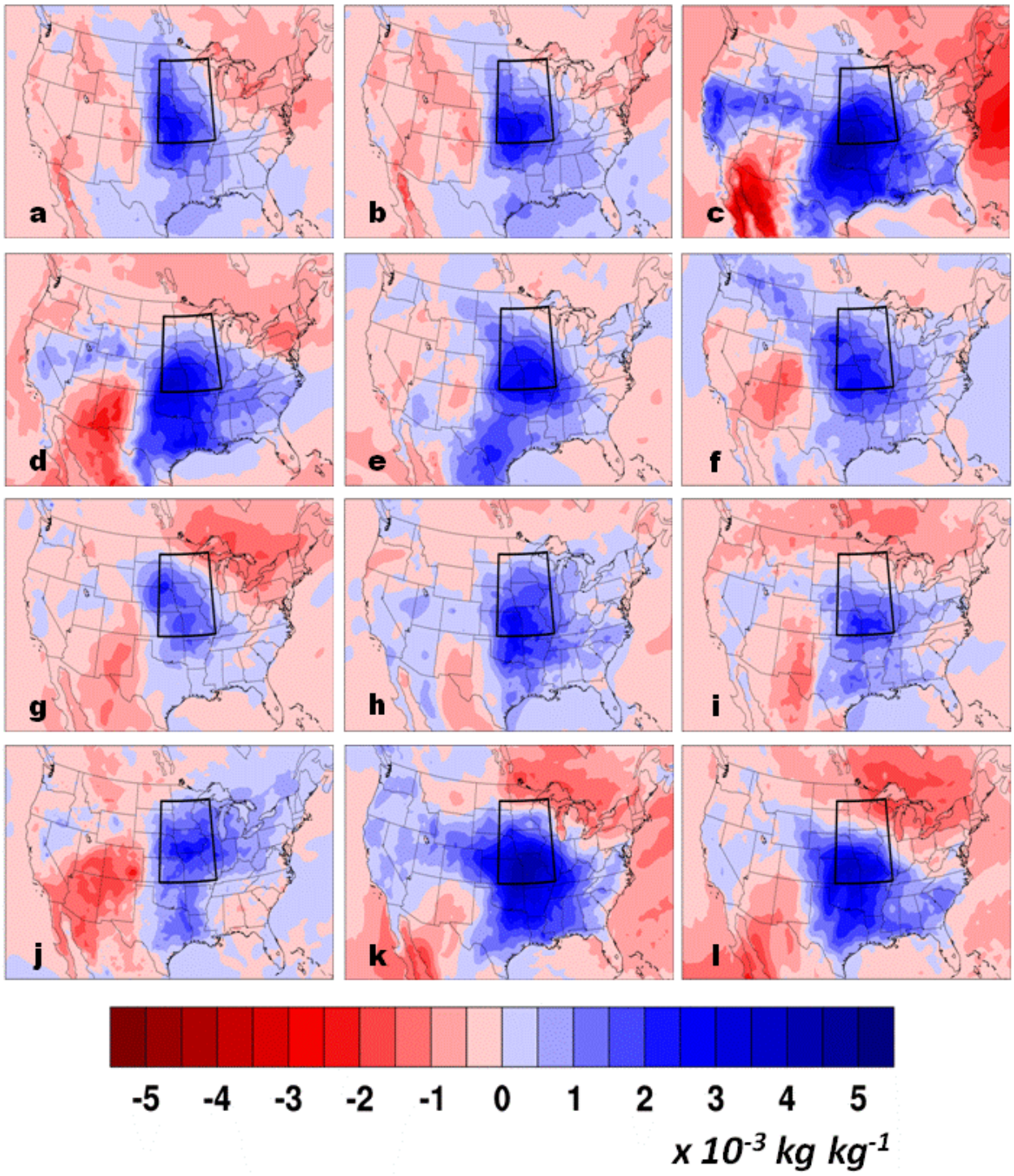

Figure 10. Same as Figure 9, but for observations and GCM driven runs: (a) NARR (CPC days) (b) NARR (UW days), (c) CRCMccsm, (d) CRCMcgcm3, (e) HRM3gfdl, (f) HRM3hadcm3, (g) MM5Iccsm, (h) MM5Ihadcm3, (i) RCM3cgcm3, (j) RCM3gfdl, (k) WRFGccsm, (l) WRFGcgcm3.

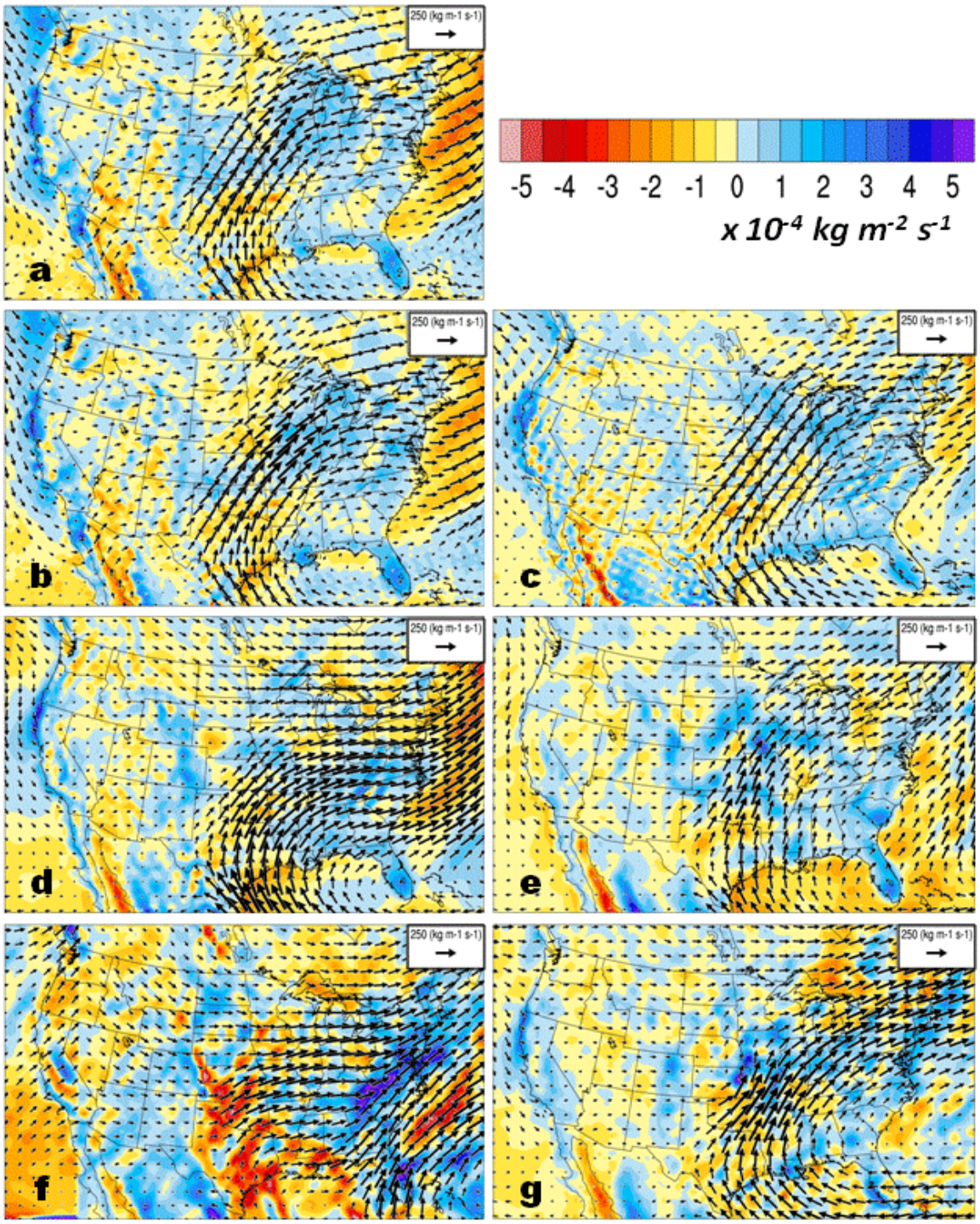

Figure 11. Vertically integrated moisture flux convergence (VI-MFC) and integrated moisture transport (VI-MT) composites during widespread very heavy events for observations and NCEP driven runs: (a) NARR (CPC days) (b) NARR (UW days), (c) CRCM, (d) HRM3, (e) MM5I, (f) RCM3, (g) WRFG. Vector scale and units are at the top right of each plot, representing 250 kg m^{-1} s^{-1}. Contour scale for VI-MFC is in the upper right, in 10^{-4} kg m^{-2} s^{-1}. Positive values indicate convergence, and negative values indicate divergence.

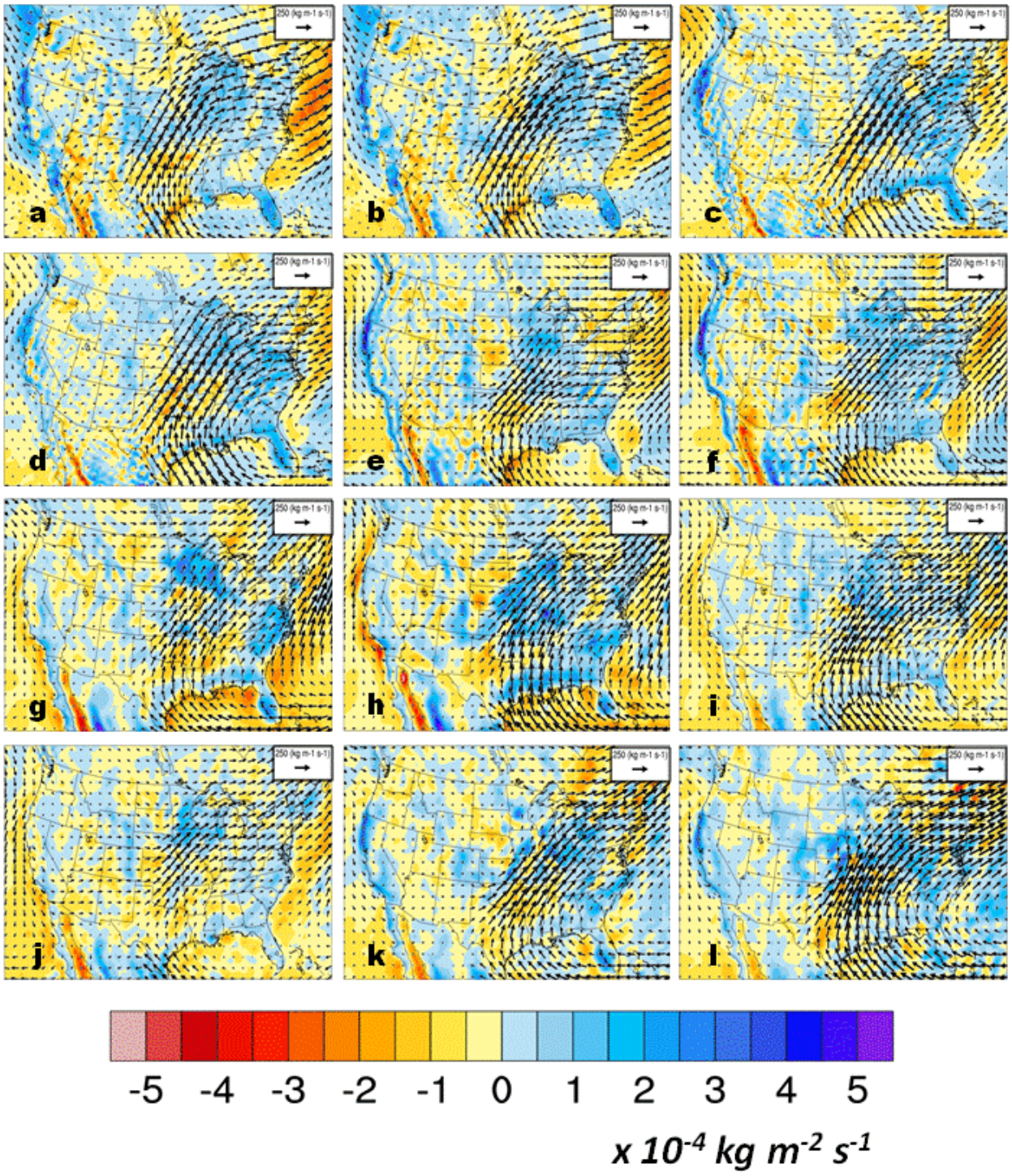

Figure 12. Same as Figure 13, but for observations and GCM driven runs: (a) NARR (CPC days) (b) NARR (UW days), (c) CRCMccsm, (d) CRCMcgcm3, (e) HRM3gfdl, (f) HRM3hadcm3, (g) MM5Iccsm, (h) MM5Ihadcm3, (i) RCM3cgcm3, (j) RCM3gfdl, (k) WRFGccsm, (l) WRFGcgcm3.

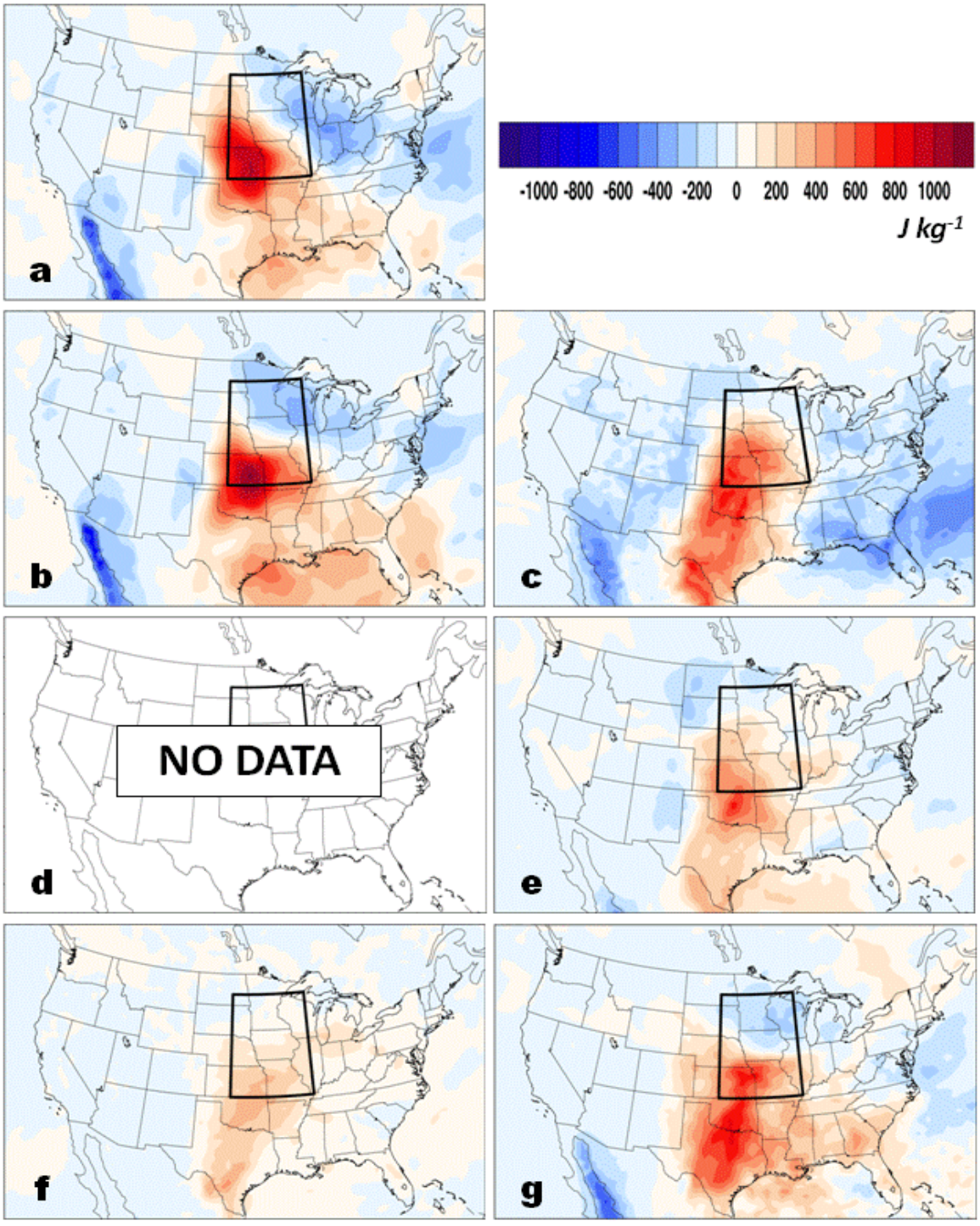

Figure 13. Composite CAPE anomalies during widespread very heavy events for observations and NCEP driven runs: (a) NARR (CPC days) (b) NARR (UW days), (c) CRCM, (d) HRM3, (e) MM5I, (f) RCM3, (g) WRFG. HRM3ncep was not available at time of analysis. Contour scale for all plots is in the upper right, in J kg^{-1}.

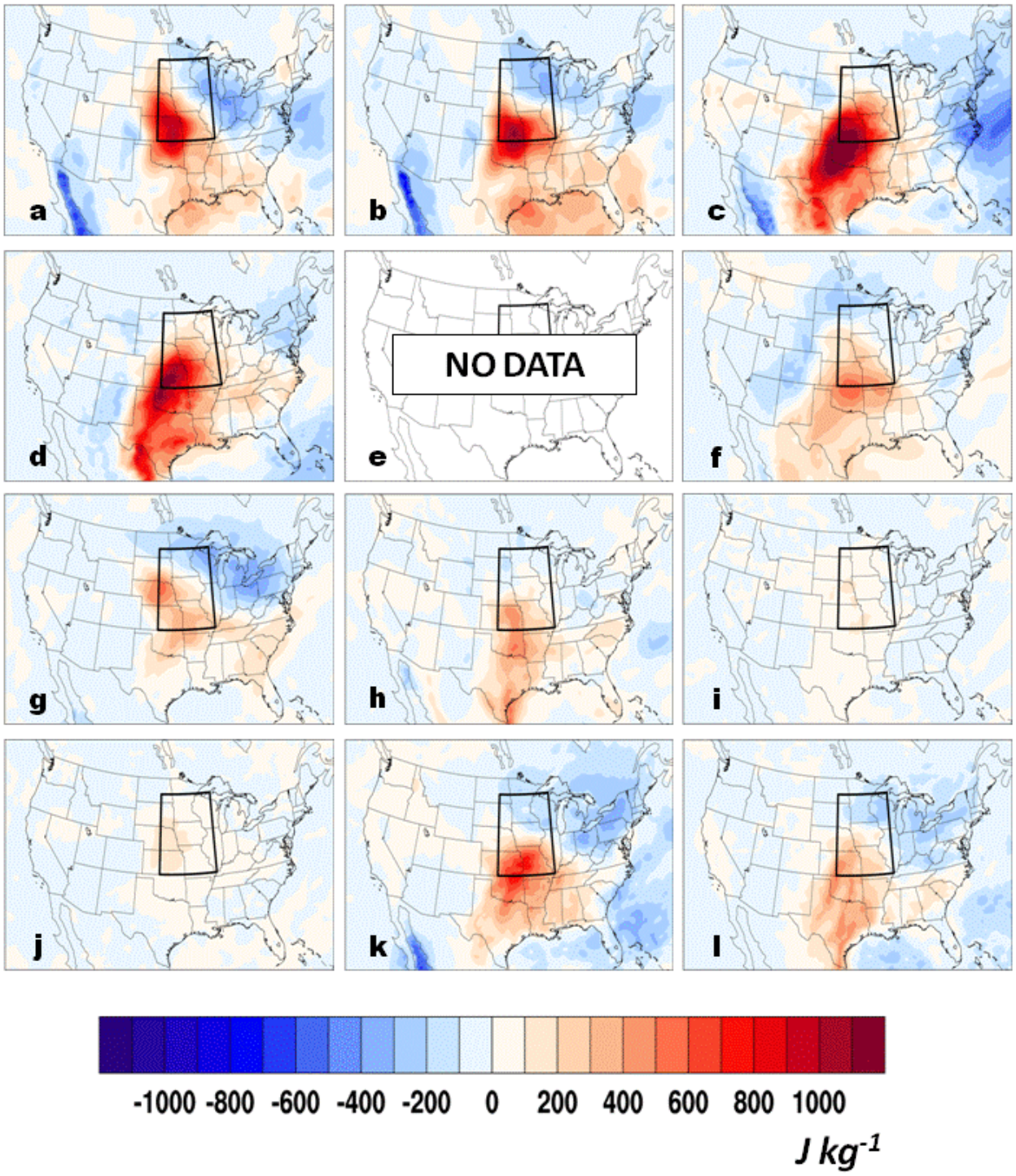

Figure 14. Same as Figure 13, but for observations and GCM driven runs: (a) NARR (CPC days) (b) NARR (UW days), (c) CRCMccsm, (d) CRCMcgcm3, (e) HRM3gfdl, (f) HRM3hadcm3, (g) MM5Iccsm, (h) MM5Ihadcm3, (i) RCM3cgcm3, (j) RCM3gfdl, (k) WRFGccsm, (l) WRFGcgcm3. HRM3gfdl was not available at time of analysis.

CHAPTER 4

EVALUATION OF REGIONAL, VERY HEAVY PRECIPITATION EVENTS DURING THE SUMMER SEASON USING NARCCAP SIMULATIONS: CLIMATE CHANGE ANALYSIS

To be submitted to the Journal of Climate

Sho Kawazoe and William J. Gutowski Jr.

Abstract

This study presents climate change results using regional climate models (RCMs) from the North American Regional Climate Change Assessment Program (NARCCAP). NARCCAP models are driven by four global climate models (GCMs) from World Climate Research Program's (WCRP's) Coupled Model Intercomparison Project- Phase 3 (CMIP3). Changes in very heavy daily precipitation and supporting processes between contemporary and future-scenario simulations in the upper Mississippi region during the summer (June-August) months are examined. Among the simulations, 8 of 11 shows negative change in average precipitation. For 8 of the 11 simulations, an increase in precipitation is projected for the future-scenario climate at the 95^{th}, 99^{th}, and 99.5^{th} percentiles. Over the entire precipitation-vs.-intensity spectrum, the NARCCAP ensemble show decreased contribution of light to moderate precipitation intensities to total precipitation in the scenario climate and increases at higher intensities. Further analysis focuses on precipitation events exceeding the 99.5^{th} percentile that occur simultaneously at several points in the region, yielding so-called "widespread events". Changes in composite precipitation show large differences between models. For widespread

events, environmental parameters such as 2-m specific humidity, vertically integrated moisture flux convergence (VI-MFC), vertically integrated moisture transport (VI-MT), and convective available potential energy (CAPE) are examined, to compare atmospheric states and processes leading to such events. Results show that for most simulations, areas of precipitation increase tend to occur in areas where projected increases in specific humidity, VI-MFC, VI-MT, and CAPE are seen. Similarities seen within the NARCCAP ensemble seems to be more in line with the RCMs, and less with the driving GCMs.

1. Introduction

There is strong evidence from both observations and climate simulations that the frequency and intensity of precipitation extremes have increased and will continue to increase into the future. This is supported by a wide range of publications (e.g., Zwiers and Kharin 1998; Meehl 2000, Alexander et al. 2006; Karl et al. 2008), including the Intergovernmental Panel on Climate Change (IPCC) Fifth Assessment Report (AR5), which states that more frequent and/or intense heavy rainfall events around much of the mid-latitude regions are “very likely” (Collins et al. 2013), as a result of projected increases in global temperatures and atmospheric water content through the Clausius-Claperyron relation (Allen and Ingram 2002; Held and Soden 2006; Min et al. 2011). This could lead to heightened flooding, which often results in massive social-economic impacts through agricultural loss, erosion, and property damage. Stakeholders and policy makers have become much more sensitive to this issue, as heavy rainfall events have increased in intensity and frequency over the last half century (Karl and Knight 1998; Groisman et al. 2005; DeGaetano 2009). As a result, they are requesting robust estimates to potential future

changes in heavy precipitation events to determine if near-term mitigations strategies and/or long-term adaptive policies need to be considered.

Mesoscale convective systems (MCSs) are the dominant contributor to heavy rain events in the central US (Houze 2004; Schumacher and Johnson 2006). This factor provides a number of modeling challenges that have been well documented over the years. First, coarse resolution models, particularly GCMs, do not capture the complex regional topography and forcing mechanisms that are vital to convective storm development (Wehner et al. 2010). Secondly, an inadequate observational record, both spatially and temporally, produces uncertainty when attempting to verify model simulations (Kiktev et al. 2007; Diffenbaugh et al. 2013). This is especially the case when dealing with precipitation at the highest intensities, which requires data at daily to sub-daily timescales (Frich et al. 2002). Given these systemic challenges, it is vital to (i) utilize higher resolution climate simulations that better resolve orographic and mesoscale forcing is utilized (Dulière et al. 2011; Bukovsky et al. 2013) and (ii) evaluate models first in the contemporary climate in order to ensure that the physical mechanisms that produce very heavy precipitation events are consistent with observations.

This study builds upon Chapter 3, which utilized regional climate model (RCM) simulations from the North American Regional Climate Change Assessment Program (NARCCAP; Mearns et al. 2009, 2012) to assess their ability to replicate summertime, very heavy precipitation events under the same physical conditions seen in observations. NARCCAP provides a series of regional climate model (RCM) simulations with 50-km resolution in an attempt to overcome the aforementioned resolution problem by dynamically downscaling a set of coarse resolution atmosphere-ocean general circulation models (AOGCMs). We will use the multi-model ensemble from NARCCAP to provide a comprehensive picture of the uncertainties

that are present in climate models (Hagedorn et al. 2005; Kawazoe and Gutowski 2013a,b). These uncertainties arise from the choices that are made to the structural design of each NARCCAP model in order to represent a highly complex climate system. All models have some bias with respect to observations and respond differently to the future-scenario considered. Therefore, using an ensemble of models that are each structurally different may provide collectively more consistent and reliable future projections (Frei et al. 2006; Tebaldi et al. 2006).

The aim of NARCCAP is to "produce high resolution climate change simulations in order to investigate uncertainties in regional scale projections of future climate and generate climate change scenarios for use in impacts research" (http://narccap.ucar.edu). Guided the aim of NARCCAP, we will in order to address the following questions. First, do the intensity and frequency of very heavy precipitation events change in the future scenario climate? Second, if changes occur, are there also changes in relevant environmental mechanisms that produce these changes in very heavy precipitation events?

This paper is structured as follows: section 2 gives an overview of datasets and analysis methods. Results for both precipitation and their supporting environmental conditions appear in section 3. The conclusions follow in section 4.

2. Data and Methods

a. Simulations

The climate simulations come from NARCCAP Phase II (Mearns et al. 2012). Phase II includes six RCMs paired with four separate GCMs for dynamical downscaling. Table 1 provides information on each RCM and GCM; Table 2 provides RCM-GCM combinations that

were available during our study. The ECP2 was used for precipitation analysis only, as three-dimensional variables were not available during the time of this study.

All models used approximately 0.5° horizontal resolution to simulate a 29-year period spanning from 1971-1999 in the contemporary climate, and 2041-2069 in the scenario climate. Scenario simulations used the A2 emission scenario from the IPCC Special Report on Emissions Scenarios (SRES; Nakićenović et al. 2000). This emission scenario, often referred as "business as usual", represents a very heterogeneous world with continuously increasing global population, regionally oriented economic growth, and a slow and fragmented technological advance, therefore representing one of the more aggressive emission scenarios. Further details of each model appear on the NARCCAP web site (http://narccap.ucar.edu), and in Mearns et al. (2009, 2012).

b. Methods

We use the years 1982-1999 from the contemporary (past) climate, and 2052-2069 from scenario (future) climate to investigate the impacts of climate change. The contemporary climate uses the same 17-year span from Chapter 3, as they were the years available for both the reanalysis and GCM driven RCM runs. Other than the study timeframe, we follow the same analysis methods as Chapter 3. As in Chapter 3, we study precipitation and their supporting environmental conditions in the upper Mississippi region (Figure 1) during the summer season (June-July-August). A precipitation "day" is defined as 1200UTC – 1200UTC (0600 – 0600 local standard time in the upper Mississippi region), and a precipitation "event" as all events exceeding 0.25 mm day^{-1}.

Widespread very heavy precipitation is defined as events exceeding the 99.5^{th} percentile that occur simultaneously on 10 or more grid points. We use 2-m specific humidity, convective

available potential energy (CAPE), vertically integrated moisture flux convergence (VI-MFC) and vertically integrated moisture transport (VI-MT) to examine environmental fields that promote the development of storms with widespread very heavy precipitation, and are the same fields examined in Chapter 3. These fields come from instantaneous data at 2100UTC (1500 local standard time in the upper Mississippi region), because this is prior to the time of maximum frequency of convective storms in observations (Wallace 1975; Chapter 3). For additional details on the methods, please refer to Kawazoe and Gutowski (2013a,b) and Chapter 3.

3. Results

a. Precipitation projections

Table 3 shows the scenario minus contemporary difference in average precipitation and at the 95th, 99th, and 99.5th thresholds. For average precipitation, 8 of 11 simulations show decreases in the scenario simulations, while 3 of 11 show increases, 2 of which are from the MM5I simulations. Average precipitation changes are in the range (-24.3%, +10.9%). The CRCMccsm and HRM3gfdl show the largest decrease in average precipitation compared to the rest of the models, while the MM5Iccsm and WRFGcgcm3 show the largest increases. Past modeling studies also show a slight decrease in average precipitation around our domain, though a small shift in our analysis region could result in a slight increase (Plummer et al. 2006; Chou and Lan 2012; Mearns et al. 2013). For the 95th, 99th, and 99.5th percentiles, with the exception of the CRCMccsm, HRM3gfdl, and HRM3hadcm3, the simulations show precipitation increases at each threshold. Precipitation rate changes are in the range (-12.7%, +26.7%). The CRCMccsm and HRM3gfdl, which showed the largest percent decrease in average precipitation, also shows the largest decreases at the 95th, 99th, and 99.5th percentile, while the opposite is true for the

MM5Iccsm and WRFGcgcm3, which shows the largest percent increases in average precipitation. With the exception of the WRFG simulations, greatest (lowest) percent increases (decreases) are seen at the 99.5th percentile.

Figure 2 shows histograms of normalized frequency-vs.-intensity in the upper Mississippi region using 2.5 mm day^{-1} bin width. Models show fairly good agreement up to around 20 mm day^{-1}. Beyond this threshold, CRCM simulations produce precipitation amounts that are lower compared to the rest of the models, while the HRM3, MM5I, and RCM3 simulations show more high-intensity precipitation. This characteristic is similar to what was seen in the contemporary analysis in Chapter 3, Figures 2 and 3. Also similar is that the distribution varies more from the choice of RCM than the choice of driving GCM. Comparing Figure 2 with Figure 3 in Chapter 3, for most models, there is a slight shift in the frequency-vs.-intensity distribution to favor higher precipitation intensities. This shift was also suggested in Table 3, especially at higher percentiles.

We use methods of Gutowski et al. (2007) to study changes in the distribution of precipitation intensities that contribute to total precipitation. Figure 3 shows the change in normalized precipitation for each model and for the ensemble. The ensemble is the average of the normalized precipitation change for each simulation. Aside from the CRCMccsm, ECP2gfdl, and HRM3gfdl, there is a decrease in the contribution of light to moderate precipitation to total precipitation, while higher precipitation intensities have an increased contribution, which is consistent with our results in Table 3 and Figure 2. This is represented in the model ensemble as well. This change in precipitation characteristics appears in other simulation studies (Gutowski et al. 2007; Sun et al. 2007; Boberg et al. 2009; Wuebbles et al. 2014; Villarini et al. 2013). The CRCMccsm, ECP2gfdl, and HRM3gfdl also show the greatest decrease in average precipitation in the future-scenario climate. This suggests that these simulations produce a drier future climate

perhaps as a result of weaker and/or less frequent convective storms that produce very heavy precipitation events.

Figure 4 shows the spatial distribution of scenario minus contemporary percent change of daily precipitation during widespread very heavy event days. In all models, there are areas of precipitation increases and decreases, and no clear spatial similarities between the models, typical of the complex local and regional forcing that characterize convective storm development. Both CRCM simulations show relatively small magnitude precipitation changes. The CRCMccsm and HRM3gfdl show larger areas of decreased precipitation compared to the other models, while areas of increased precipitation are lower in magnitude, consistent with results seen in Table 3.

b. Supporting environmental conditions

Figure 5 shows the climate change of composite 2-m specific humidity during widespread very heavy event days. Heaviest precipitation tends to occur in regions where specific humidity is projected to increase. There is fairly good correspondence between the magnitude of precipitation intensity compared to specific humidity changes, though the RCM3gfdl, which shows relatively little change in specific humidity, displays strong positive precipitation changes. The CRCMccsm shows the opposite feature, where our region experiences an overall decrease in widespread very heavy precipitation intensity, but one of the highest specific humidity increases. Other than those two simulations, our results are consistent with Held and Soden (2006), who highlight the importance of low-level specific humidity increases in future climates. However, while our analysis highlights the general importance of near-surface moisture, it ignores the vertical profile. Different moisture amounts at various vertical levels can

affect the lapse rate, alter lifting condensation level, and intensify updraft/downdrafts (James and Markowski 2010).

Figure 6 shows the climate change of composite VI-MFC and VI-MT during widespread very heavy events days. All models show an enhanced south/southwesterly VI-MT into our analysis domain, though the magnitude and location of peak transport change differs. This transport of moisture is vital in introducing moisture on top of local terrestrial sources (Dominguez and Kumar 2005; Dirmeyer and Kinter 2010; Lavers and Villarini 2013). VI-MFC change shows large spreads throughout the domain. The combination of peak VI-MT with areas of positive VI-MFC aligns roughly with the location of increased precipitation intensities in the scenario climate, perhaps more so than 2-m specific humidity changes in Figure 5. This was also seen in Holman and Vavrus (2012), where changes in precipitation correlated much better with MFC than changes in surface specific humidity. The CRCM simulations produce only small changes in the VI-MT and VI-MFC. The lack of change in both fields may be a reason why both CRCM simulations produce only small changes in precipitation during widespread very heavy event days. The CRCMccsm and HRM3gfdl showed negative precipitation change at the highest intensity spectrum (Table 3). Both models show small changes in VI-MT and VI-MFC, with the latter tending to be a negative change within the domain. This could help explain the precipitation decreases seen in both Table 3 and Figure 4.

Climate change in composite CAPE during widespread very heavy event days appears in Figure 7. Both RCM3 simulations and the HRM3gfdl were omitted for this study. RCM3 showed extremely low CAPE values (4~5 times lower than the other models), while the HRM3gfdl was not available at the time of this analysis (Melissa Bukovsky; personal correspondence). For all models, positive CAPE change corresponds very well with 2-m specific humidity change both in

location and magnitude. While positive CAPE anomalies in the contemporary climate concentrate mostly in the southern half of our analysis domain, the scenario climate displays increased CAPE values throughout the domain, suggesting a larger area will become more favorable for convective initiation. Increased CAPE values in the scenario climate agree with the consensus seen in previous literature (Sobel and Camargo 2011; Diffenbaugh et al. 2013; Gensini et al. 2014). However, there are other factors to consider when studying convective storm development, one of which is the vertical wind shear. Although the consensus is that high CAPE/high shear creates an environment favorable for strong convective development, several studies have shown that while convective storms are projected to increase in frequency and intensity, vertical wind shear is projected to decrease in intensity (Trapp et al. 2007, Vecchi and Soden 2007; Trapp et al. 2009; Brooks 2013). Their studies suggest that projected increases in CAPE will offset the projected decrease in vertical wind shear. A deeper look into the CAPE/shear interaction from NARCCAP simulations during widespread very heavy precipitation events is worth investigating in future studies.

4. Conclusion

Eleven RCM-GCM model combinations from NARCCAP were used to examine climate changes in precipitation and there supporting environmental fields during the summer months (June-August) in the upper Mississippi region. Climate change is the difference between contemporary climate (1982-1999) and future scenario (2052-2069). Widespread very heavy precipitation was defined as the top 0.5% of all precipitation of above 0.25 mm day^{-1} occurring on at least 10 grid points simultaneously. During these events, composites were created for 2-m

specific humidity, vertically integrated moisture flux convergence (VI-MFC), vertically integrated moisture transport (VI-MT), and convective available potential energy (CAPE).

Average precipitation change shows both positive and negative changes, but at the 95th, 99th, and 99.5th percentile, models other than the CRCMccsm, ECP2gfdl, and HRM3gfdl show increased precipitation. Figure 3 support these results, as high-intensity precipitation increases in frequency, and contributes more to total precipitation. On the other hand, light to moderate precipitation contribute less to total precipitation in the future-scenario climate. Precipitation changes vary in location, intensity, and sign of change. The CRCMccsm and HRM3gfdl show large areas of negative precipitation change, which corresponds to the precipitation characteristic seen through this study.

Examination of supporting environmental conditions reveals that 2-m specific humidity increases in the future climate. VI-MFC changes agree fairly well with the location of positive precipitation change, and stronger VI-MT from the Gulf of Mexico also occurs. Increases in CAPE also occur throughout the domain, showing increased convective potential. The combination of these fields suggests a future-scenario that is more favorable for the increased very heavy precipitation seen in the NARCCAP model ensemble.

Acknowledgements

This work was supported by National Science Foundation Grants AGS-1243106 and BCS-1114978. We thank the North American Regional Climate Change Assessment Program (NARCCAP) for providing the data used in this paper. NARCCAP is funded by the National Science Foundation (NSF), the U.S. Department of Energy (DoE), the National Oceanic and Atmospheric Administration (NOAA), and the U.S. Environmental Protection Agency Office of

Research and Development (EPA). We also thank Melissa Bukovsky for providing us the CAPE data that is not yet available to the public. This study would not be as effective without her assistance.

References

Alexander, L. V., and Coauthors, 2006: Global observed changes in daily climate extremes of temperature and precipitation.*J. Geophys. Res.,* **111,** D05109, doi:10.1029/2005JD006290.

Allen, M. R., and W. J. Ingram, 2002: Constraints on future changes in climate and the hydrological cycle. *Nature*, **419,** 224–232, doi:10.1038/nature01092

Bukovsky, M. S., D. J. Gochis, and L. O. Mearns, 2013: Towards assessing NARCCAP regional climate model credibility for the North American monsoon: Current climate simulations. *J. Climate*, **26**, 8802–8826, doi:10.1175/JCLI-D-12-00538.1.

Boberg, F., P. Berg, P. Thejll, W. J. Gutowski, and J. H. Christensen, 2009: Improved confidence in climate change projections of precipitation evaluated using daily statistics from the PRUDENCE ensemble. *Climate Dyn.,* **32**,1097–1106, doi:10.1007/s00382-008-0446-y.

Brooks, H. E., 2013: Severe thunderstorms and climate change. *Atmos. Res.*, **123**, 129–138, doi:10.1016/j.atmosres.2012.04.002.

Chou, C., and C.-W. Lan, 2012: Changes in the annual range of precipitation under global warming. *J. Climate*, **25**, 222–235, doi:10.1175/JCLI-D-11-00097.1.

Collins, M., R. Knutti, J. Arblaster, J.-L. Dufresne, T. Fichefet, P. Friedlingstein, X. Gao, W.J. Gutowski, T. Johns, G. Krinner, M. Shongwe, C. Tebaldi, A.J. Weaver and M. Wehner, 2013: Long-term Climate Change: Projections, Commitments and Irreversibility. In: *Climate Change 2013: The Physical Science Basis. Contribution of Working Group I to the Fifth Assessment Report of the Intergovernmental Panel on Climate Change* [Stocker, T.F., D. Qin, G.-K. Plattner, M. Tignor, S.K. Allen, J. Boschung, A. Nauels, Y. Xia, V. Bex and P.M. Midgley (eds.)]. Cambridge University Press, Cambridge, United Kingdom and New York, NY, USA, doi:10.1017/CBO9781107415324.024.

DeGaetano, A. T., 2009: Time-dependent changes in extreme-precipitation return-period amounts in the continental United States. *J. Appl. Meteor. Climatol.*, **48**, 2086–2099, doi:10.1175/2009JAMC2179.1.

Diffenbaugh, N. S., M. Scherer, and R. J. Trapp, 2013: Robust increases in severe thunderstorm environments in response to greenhouse forcing. Proc. Natl. Acad. Sci. USA, 110, 16 361–16 366, doi:10.1073/ pnas.1307758110.

Dirmeyer, P. A., and J. L. Kinter, 2010: Floods over the U.S. Midwest: A regional water cycle perspective. *J. Hydrometeor.*, **11**, 1172–1181, doi:10.1175/2010JHM1196.1.

Dominguez, F., and P. Kumar, 2005: Dominant modes of moisture flux anomalies over North America. *J. Hydrometeor.*, **6**, 194–209, doi:10.1175/JHM417.1.

Dulière, V., Y. Zhang, and E. P. Salathé Jr., 2011: Extreme precipitation and temperature over the U.S. Pacific Northwest: A comparison between observations, reanalysis data, and regional models. *J. Climate*, **24**, 1950–1964, doi:10.1175/2010JCLI3224.1.

Frei, C., R. Schooll, S. Fukutome, J. Schmidli, and P. L. Vidale, 2006: Future change of precipitation extremes in Europe: Intercomparison of scenarios from regional climate models. *J. Geophys. Res.*, **111**, D06105, doi:10.1029/2005JD005965.

Frich, P., L. V. Alexander, P. Della-Marta, B. Gleason, M. Haylock, A. M. G. Klein, and T. Peterson, 2002: Observed coherent changes in climatic extremes during the second half of the twentieth century. *Climate Res.*, **19,** 193–212, doi:10.3354/cr019193.

Gensini, V. A., C. Ramseyer, and T. L. Mote, 2014: Future convective environments using NARCCAP. *Int. J. Climatol.*, **34**, 1699–1705, doi:10.1002/joc.3769.

Groisman, P. Ya., R. W. Knight, D. R. Easterling, T. R. Karl, G. C. Hegerl, and V. N. Razuvaev, 2005: Trends in intense precipitation in the climate record. *J. Climate*, **18**, 1326–1350, doi:10.1175/JCLI3339.1.

Gutowski, W. J., E. S. Takle, K. A. Kozak, J. C. Patton, R. W. Arritt, and J. H. Christensen, 2007: A possible constraint on regional precipitation intensity changes under global warming. *J. Hydrometeor.*, **8**, 1382–1396, doi:10.1175/2007JHM817.1.

Hagedorn R, F.J. Doblas-Reyes, and T.N. Palmer, 2005: The rationale behind the success of multi-model ensembles in seasonal forecasting. *Tellus* **57A,** 219-233, doi:10.1111/j.1600-0870.2005.00103.x.

Held, I. M., and B. J. Soden, 2006: Robust responses of the hydrological cycle to global warming. *J. Climate*, **19**,5686–1560, doi:10.1175/JCLI3990.1.

Holman, K. D., and S. J. Vavrus, 2012: Understanding simulated extreme precipitation events in Madison, Wisconsin, and the role of moisture flux convergence during the late twentieth and twenty-first centuries. *J. Hydrometeor.*, **13**, 877–894, doi:10.1175/JHM-D-11-052.1.

Houze Jr., R. A., 2004: Mesoscale convective systems. *Rev. Geophys.*, **42,** RG4003. doi:10.1029/2004RG000150.

James, R. P., and P. M. Markowski, 2010: A numerical investigation of the effects of dry air aloft on deep convection. *Mon. Wea. Rev.*, **138**, 140–161, doi:10.1175/2009MWR3018.1.

Karl, T. R., G. A. Meehl, C. D. Miller, S. J. Hassol, A. M. Waple, and W. L. Murray, Eds., 2008: Weather and climate extremes in a changing climate: Regions of focus: North America, Hawaii, Caribbean, and U.S. Pacific Islands. U.S. Climate Change Science Program Rep., 162 pp.

Kawazoe, S., and W.J. Gutowski. 2013a: Regional, Very Heavy Daily Precipitation in NARCCAP Simulations. *J. Hydrometeor*., **14**, 1212-1227, doi:10.1175/JHM-D-12-068.1.

Kawazoe, S., and W.J. Gutowski. 2013b: Regional, Very Heavy Daily Precipitation in CMIP5 Simulations *J. Hydrometeor*., **14**, 1228-1242, doi:10.1175/JHM-D-12-0112.1.

Kiktev, D., J. Caesar, L. V. Alexander, H. Shiogama, and M. Collier, 2007: Comparison of observed and multimodeled trends in annual extremes of temperature and precipitation. Geophys. Res. Lett., 34, L10702, doi:10.1029/2007GL029539

Lavers, D. A., and G. Villarini, 2013: Atmospheric rivers and flooding over the central United States. *J. Climate*, **26**,7829–7836, doi:10.1175/JCLI-D-13-00212.1.

Meehl, G. A., F. Zwiers, J. Evans, T. Knutson, L. Mearns, and P. Whetton, 2000: Trends in extreme weather and climate events: Issues related to modeling extremes in projections of future climate change. *Bull. Amer. Meteor. Soc.*, **81**, 427–436, doi:10.1175/1520-0477(2000)081<0427:TIEWAC>2.3.CO;2.

Mearns, L. O., W. J. Gutowski, R. Jones, L.-Y. Leung, S. McGinnis, A. M. B. Nunes, and Y. Qian, 2009: A regional climate change assessment program for North America. *Eos, Trans. Amer.Geophys. Union*, **90,** 311, doi:10.1029/2009EO360002.

Mearns, L.O., and Coauthors, 2012: The North American Regional Climate Change Assessment Program: Overview of Phase I results. *Bull. Amer. Meteor. Soc.*, **93**, 1337–1362, doi:10.1175/BAMS-D-11-00223.1.

Mearns, L. O., and Coauthors, 2013: Climate change projections of the North American Regional Climate Change Assessment Program (NARCCAP). *Climatic Change*, **120**, 965–975, doi:10.1007/s10584-013-0831-3.

Min, S., X. Zhang, F. W. Zwiers, and G. C. Hegerl, 2011: Human contribution to more intense precipitation extremes. *Nature*, **470**, 378–381, doi:10.1038/nature09763.

Nakićenović, N., and Coauthors, 2000: *Special Report on Emissions Scenarios*. Cambridge University Press, 599 pp. [Available online at https://www.ipcc.ch/pdf/special-reports/emissions_scenarios.pdf.]

Plummer, D., D. Caya, A. Frigon, H. Côté, M. Giguère, D. Paquin, S. Biner, R. Harvey, and R. de Elia, 2006: Climate and climate change over North America as simulated by the Canadian RCM. *J. Climate*, **19**, 3112–3132, doi:10.1175/JCLI3769.1.

Schumacher, R. S., and R. H. Johnson, 2006: Characteristics of U.S. Extreme Rain Events during 1999–2003. *Wea. Forecasting*, **21**, 69–85, doi:10.1175/WAF900.1.

Sobel, A. H., and S. J. Camargo, 2011: Projected future seasonal changes in tropical summer climate. *J. Climate*, **24**,473–487, doi:10.1175/2010JCLI3748.1.

Sun, Y., S. Solomon, A. Dai, and R. W. Portman, 2007: How often will it rain? *J. Climate*, **20**, 4801–4818, doi:10.1175/JCLI4263.1.

Tebaldi, C., K. Hayhoe, J. M. Arblaster, and G. A. Meehl, 2006: Going to the extremes: An intercomparison of model-simulated historical and future changes in extreme events. *Climatic Change*, **79,** 185–211.

Trapp, R. J., N. S. Diffenbaugh, H. E. Brooks, M. E. Baldwin, E. D. Robinson, and J. S. Pal, 2007: Changes in severe thunderstorm environment frequency during the 21st century caused by anthropogenically enhanced global radiative forcing. *Proc. Natl. Acad. Sci. USA*, **104**, 19 719–19 723, doi:10.1073/pnas.0705494104.

Trapp, R. J., N. S. Diffenbaugh, and A. Gluhovsky, 2009: Transient response of severe thunderstorm forcing to elevated greenhouse gas concentrations. *Geophys. Res. Lett.*, **36**, L01703, doi:10.1029/2008GL036203.

Vecchi, G. A., and B. J. Soden, 2007: Increased tropical Atlantic wind shear in model projections of global warming.*Geophys. Res. Lett.*, **34**, L08702, doi:10.1029/2006GL028905

Villarini, G., E. Scoccimarro, and S. Gualdi, 2013: Projections of Heavy Rainfall Over the Central United States Based on CMIP5 Models. *Atmos. Sci. Lett.*,**14**, 200–205, doi:10.1111/1752-1688.12318.

Wallace, J. M., 1975: Diurnal variations in precipitation and thunderstorm frequency over the conterminous United States. *Mon. Wea. Rev.*, **103**, 406–419, doi:10.1175/1520-0493(1975)103<0406:DVIPAT>2.0.CO;2.

Wehner, M. F., R. Smith, P. Duffy, and G. Bala, 2010: The effect of horizontal resolution on simulation of very extreme US precipitation events in a global atmosphere model. *Climate Dyn.,* **32**, 241–247, doi:10.1007/s00382-009-0656-y.

Wuebbles, D. J., K. Kunkel, M. Wehner, and Z. Zobel, 2014: Severe weather in United States under a changing climate, *Eos Trans AGU*, **95**(18), 149–150, doi: 10.1002/2014EO180001.

Zwiers, F. W., and V. V. Kharin, 1998: Changes in the extremes of the climate simulated by CCC GCM2 under CO_2 doubling. *J. Climate*, **11**, 2200–2222, doi:10.1175/1520-0442(1998)011<2200:CITEOT>2.0.CO;2.

Table 1. RCMs and GCMs used in NARCCAP. All RCMs are at 0.5º x 0.5º horizontal resolution; GCM resolutions are listed.

Acronym	RCM
CRCM	Canadian Regional Climate Model version 4
ECP2	Experimental Climate Prediction Center Regional Spectral Model
HRM3	Hadley Centre Regional Model version 3
MM5I	Fifth-generation Pennsylvania State University-National Center for Atmospheric Sciences (NCAR) Mesoscale Model
RCM3	International Centre for Theoretical Physics Regional Climate Model version 3
WRFG	NCAR Weather Research and Forecasting Model
	GCM
ccsm	NCAR-Community Climate Model version 3 (1.4º x 1.4º)
cgcm3	Canadian Climate Centre Third Generation Coupled General Climate Model (1.9º x 1.9º)
gfdl	Geophysical Fluid Dynamic Laboratory Atmosphere-Ocean general circulation model (AOGCM; 2.0º x 2.5º)
hadcm3	Hadley Centre Hadley Climate Model version 3 (2.5º x 3.75º)

Table 2. NARCCAP RCM and GCM simulations. “X” designate combinations available and used for both precipitation and their supporting environments, “O” represents combinations available but only used for precipitation, and “n” denotes combinations available, but is not used in this study.

Model	ccsm	cgcm3	gfdl	hadcm3
CRCM	X	X		
ECP2			O	n
HRM3			X	X
MM5I	X			X
RCM3		X	X	
WRFG	X	X		

Table 3. Scenario-minus-contemporary difference in average precipitation (Avg; percent change and absolute change in mm day^{-1}), 95th, 99th, and 99.5th percentile (percent change absolute change in mm day^{-1}). Italics indicate lower values in scenario simulations. Model average is also shown.

	Avg (%)	Avg (mm day^{-1})	95th (%)	95th (mm day^{-1})	99th (%)	99th (mm day^{-1})	99.5th (%)	99.5th (mm day^{-1})
CRCMccsm	*-18.27*	*-0.36*	*-7.18*	*-0.89*	*-3.53*	*-0.82*	*-2.03*	*-0.58*
CRCMcgcm3	*-4.91*	*-0.13*	6.28	1.05	9.11	2.71	10.48	3.73
ECP2gfdl	*-10.60*	*-0.38*	0.14	0.04	0.63	0.30	0.61	0.34
HRM3gfdl	*-24.34*	*-0.74*	*-12.70*	*-2.74*	*-7.92*	*-3.46*	*-5.44*	*-3.13*
HRM3hadcm3	*-1.22*	*-0.04*	*-0.16*	*-0.04*	*-1.18*	*-0.64*	2.53	1.78
MM5Iccsm	10.95	0.30	18.59	4.55	25.64	11.39	26.74	14.78
MM5Ihadcm3	4.19	0.13	4.45	1.35	6.08	3.43	9.33	6.52
RCM3cgcm3	*-3.52*	*-0.15*	13.61	4.49	14.57	8.98	14.97	11.24
RCM3gfdl	*-0.74*	*-0.03*	10.30	2.90	12.23	6.52	14.41	9.54
WRFGccsm	*-2.38*	*-0.04*	15.62	3.28	14.28	6.77	12.86	7.61
WRFGcgcm3	10.33	0.22	20.46	5.02	19.14	9.72	17.29	10.80
AVERAGE	***-3.68***	***-0.11***	**6.31**	**1.72**	**8.10**	**4.08**	**9.14**	**5.63**

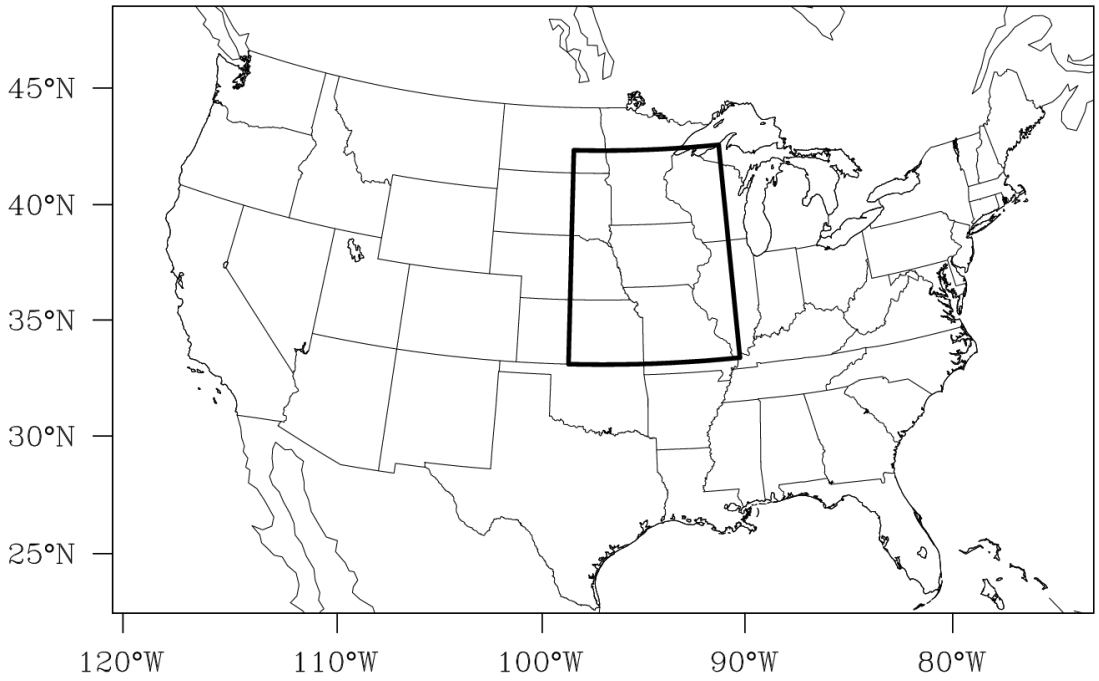

Figure 1. Region covered by each NARCCAP models. Analyzed region is highlighted: Upper Mississippi region.

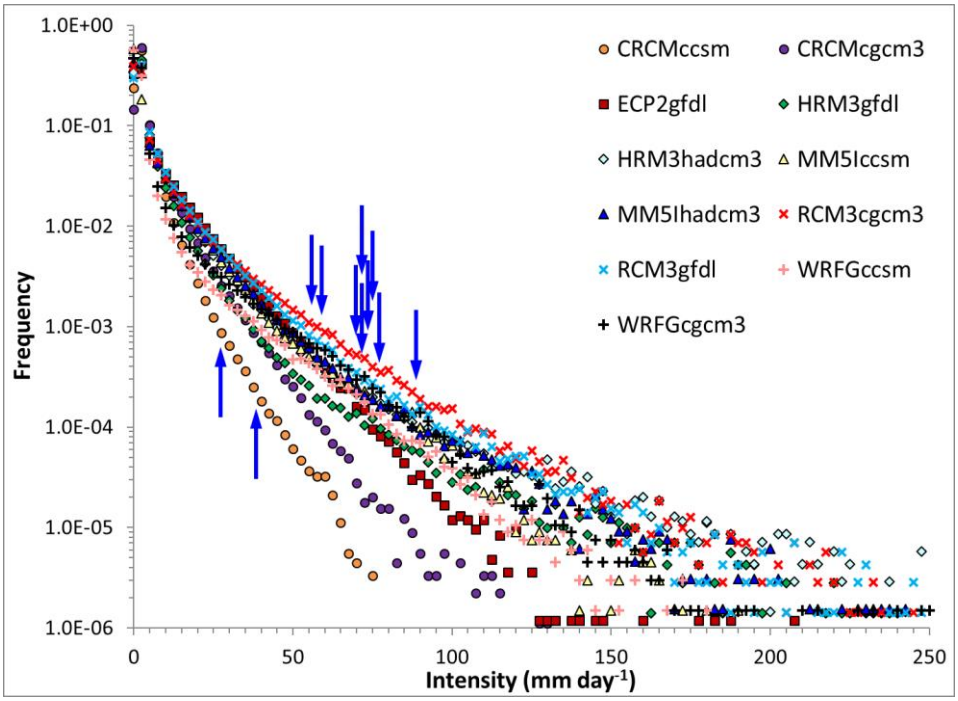

Figure 2. Normalized frequency of precipitation as a function of daily intensity for 2052-2069 in NARCCAP models. Arrows mark the 99.5th percentile.

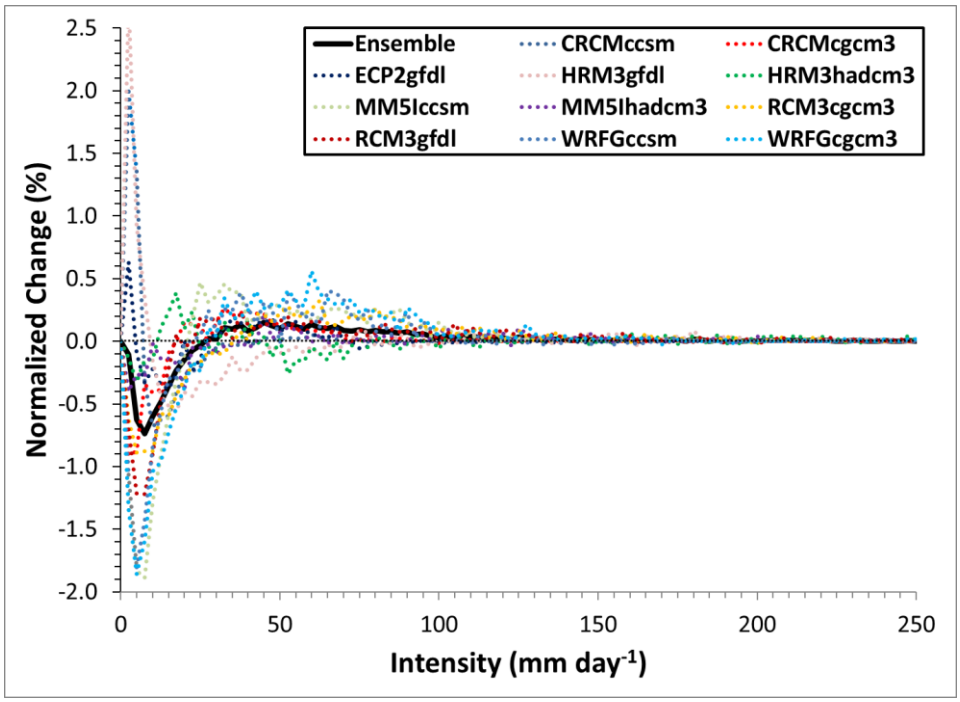

Figure 3. Normalized precipitation change (scenario-minus-contemporary) for NARCCAP models. Ensemble (solid black line) represents normalized mean for all models used in this study.

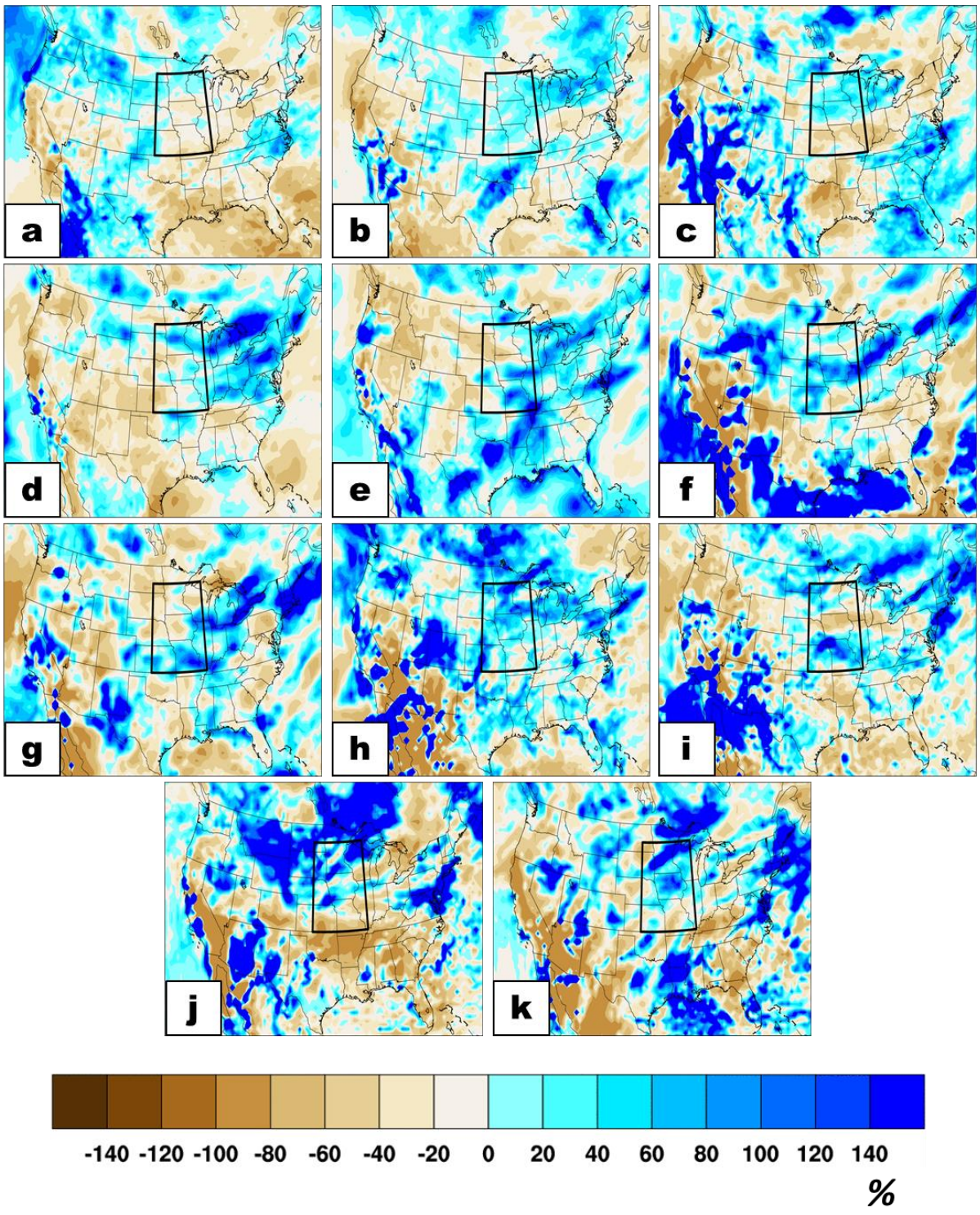

Figure 4. Scenario-minus-contemporary percent change of composite daily precipitation during widespread very heavy event days: (a) CRCMccsm, (b) CRCMcgcm3, (c) ECP2gfdl, (d) HRM3gfdl, (e) HRM3hadcm3, (f) MM5Iccsm, (g) MM5Ihadcm3, (h) RCM3cgcm3, (i) RCM3gfdl, (j) WRFGccsm, (k) WRFGcgcm3. Contour scale for all plots is in the lower right, in %.

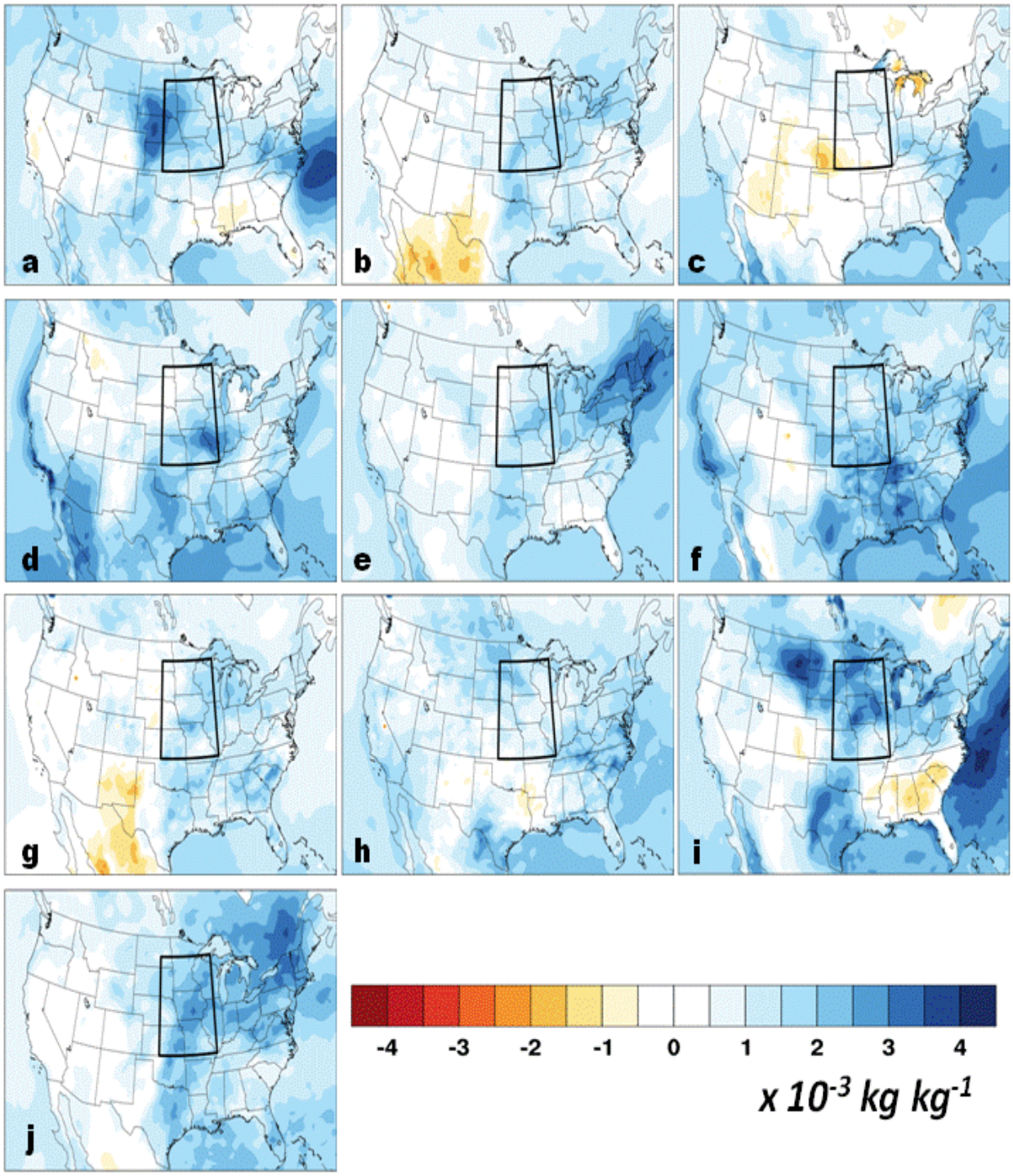

Figure 5. Scenario-minus-contemporary difference of composite 2-m specific humidity during widespread very heavy event days: (a) CRCMccsm, (b) CRCMcgcm3, (c) HRM3gfdl, (d) HRM3hadcm3, (e) MM5Iccsm, (f) MM5Ihadcm3, (g) RCM3cgcm3, (h) RCM3gfdl, (i) WRFGccsm, (j) WRFGcgcm3. Contour scale for all plots is in the lower right, in 10^{-3} kg kg^{-1}.

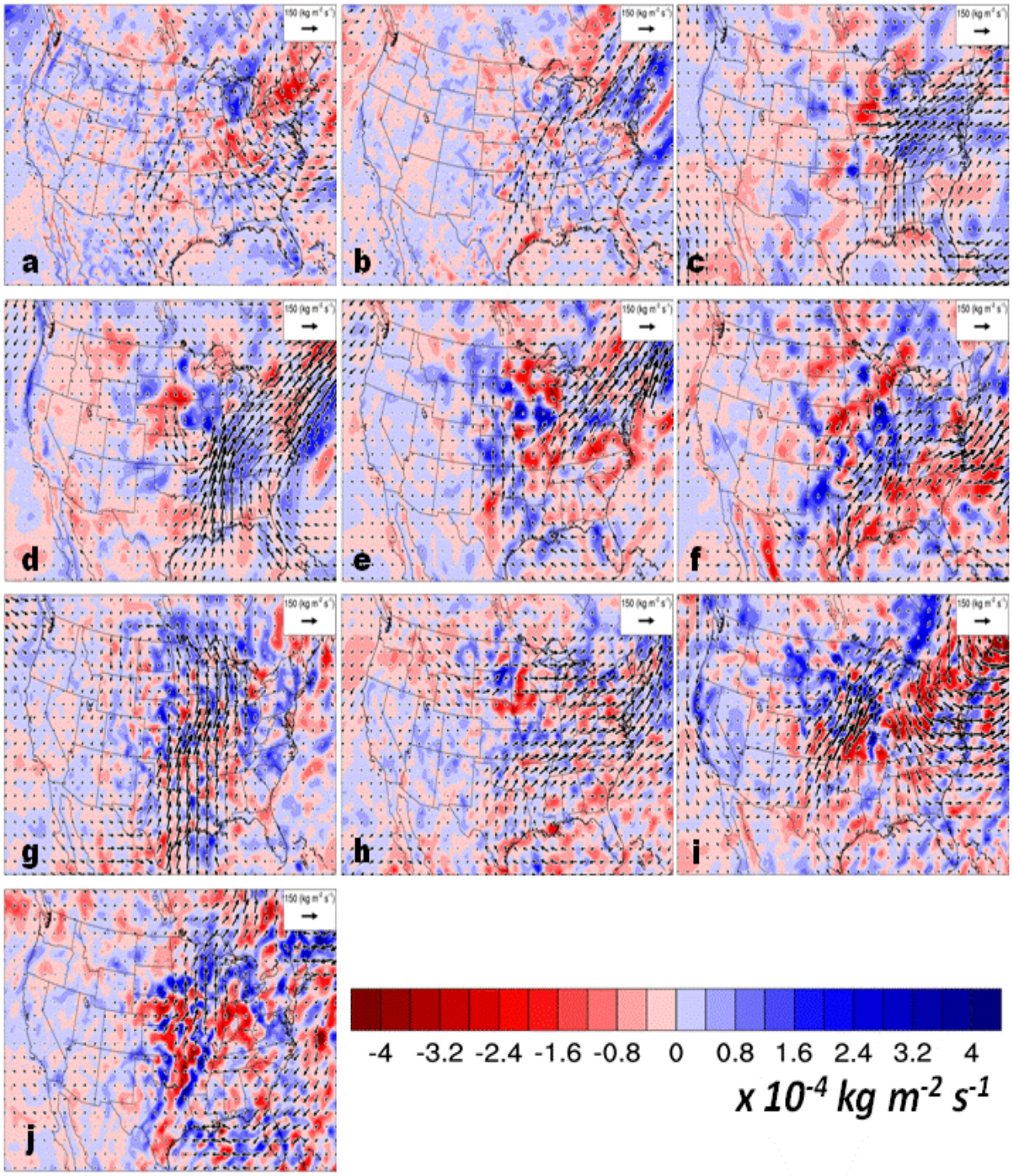

Figure 6. Scenario-minus-contemporary difference of composite VI-MFC and VI-MT during widespread very heavy event days: (a) CRCMccsm, (b) CRCMcgcm3, (c) HRM3gfdl, (d) HRM3hadcm3, (e) MM5Iccsm, (f) MM5Ihadcm3, (g) RCM3cgcm3, (h) RCM3gfdl, (i) WRFGccsm, (j) WRFGcgcm3. Vector scale and units are at the top right of each plot, representing 150 kg m^{-1} s^{-1}. Contour scale for VI-MFC is in the lower right, in 10^{-4} kg m^{-2} s^{-1}.

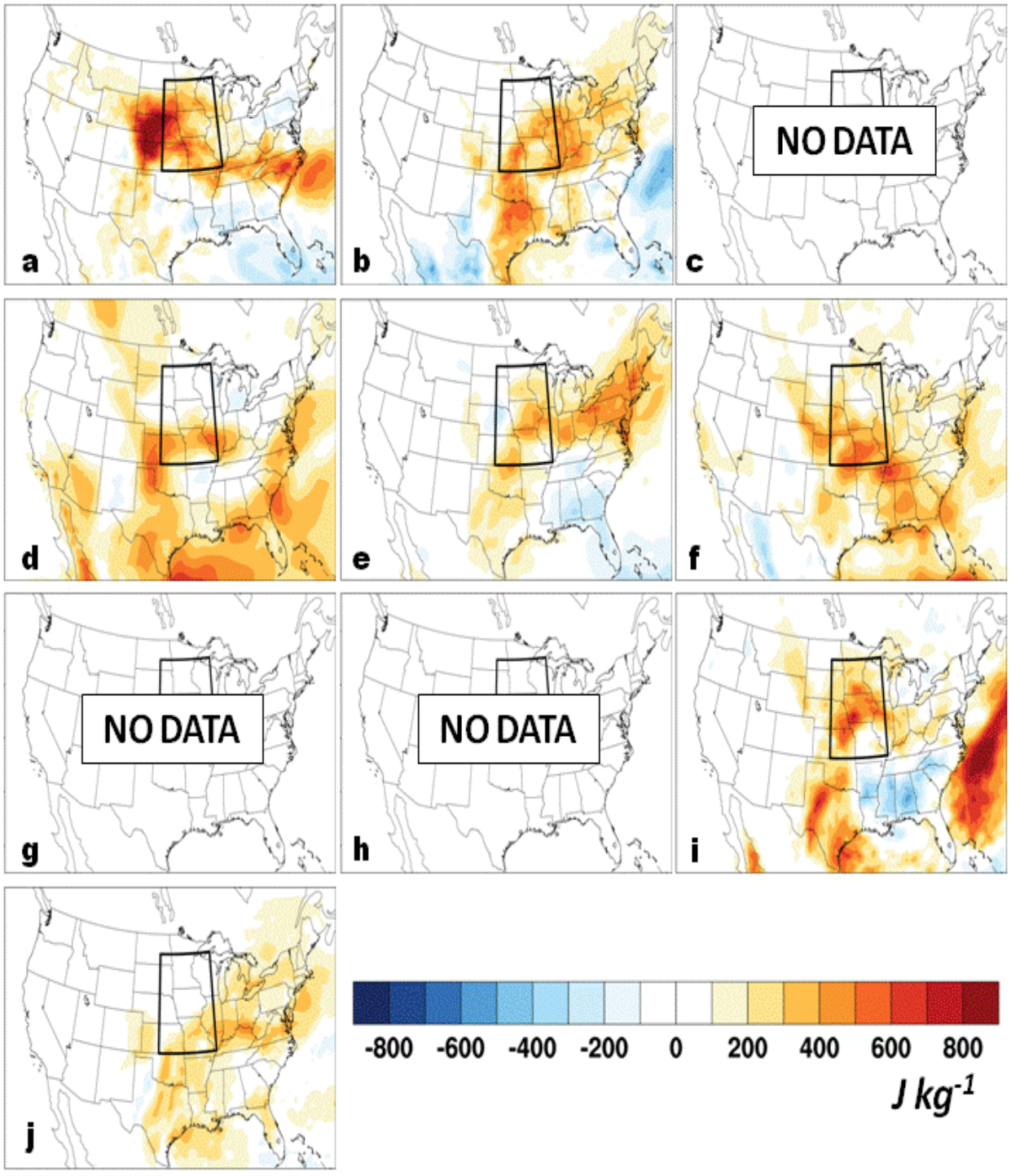

Figure 7. Scenario-minus-contemporary difference of composite CAPE during widespread very heavy event days: (a) CRCMccsm, (b) CRCMcgcm3, (c) HRM3gfdl, (d) HRM3hadcm3, (e) MM5Iccsm, (f) MM5Ihadcm3, (g) RCM3cgcm3, (h) RCM3gfdl, (i) WRFGccsm, (j) WRFGcgcm3. Contour scale for all plots is in the lower right, in J kg^{-1}.

CHAPTER 5

GENERAL CONCLUSIONS

1. Summary

Three manuscripts that make up this dissertation analyze climate model ensembles to evaluate the capability they have in replicating not only the precipitation intensity but also the supporting physical behavior seen in observations. All of the studies examine the upper Mississippi region and were guided by our study objective, which is to offer better potential for assessing the capability of climate models to produce very heavy precipitation events by combining very heavy precipitation characteristics with fields that tend to be more robustly simulated than very heavy precipitation itself. The ability of models to show characteristics similar to what occurs in the real world would support using them to assess changes in very heavy precipitation events under future climate scenarios.

Chapter 2 uses global climate models (GCMs) from the Coupled Model Intercomparison Project – Phase 5 (CMIP5) to study contemporary climate during the winter months, while Chapter 3 uses regional climate models (RCMs) from the North American Regional Climate Change Assessment Program (NARCCAP) during the summer months. The overall result is that both ensembles appear capable of producing very heavy precipitation events in the analysis region for the correct physical behavior seen in observations. Inter-model differences occur in both CMIP5 and NARCCAP contemporary simulations, but are related to horizontal resolution in the former, and which RCMs are used, instead of what the lateral boundary source, in the latter. Chapter 4 uses the NARCCAP summer simulations to examine climate change characteristics for both precipitation and the supporting environmental fields. For the climate change analysis, most models project a decrease in average precipitation but increases in

intensity and frequency of very heavy precipitation. Areas of projected precipitation increase occur in areas where conditions will become more favorable for convective storm development.

2. Future Work

For future work, a deeper examination to both Chapter 3 and Chapter 4 could be conducted. Several assumptions were made in our analysis, including the exclusion of vertical wind shear and convective inhibition, which could influence convective potential in both the contemporary and future-scenario climate. The diurnal cycle of scenario precipitation could provide clues into changes in the timing/duration of peak precipitation.

The possible connection between the North American monsoon and very heavy precipitation events in the upper Mississippi region was covered briefly in Chapter 3, but could certainly be expanded further. Do months with the least widespread very heavy events imply the onset of the North American monsoon? Does the North American monsoon begin earlier in NARCCAP models compared to observations? Are biases associated with the North American monsoon seen in past studies (e.g., Bukovsky et al. 2012) affect very heavy precipitation characteristics in our region? These points are certainly worth further investigation.

Low level jet (LLJ) analysis was also excluded from our study for two reasons. One was the timing of nocturnal jets, which, as the name implies, peak during the overnight hours. Because we chose to analyze instantaneous fields at 2100UTC, examining the LLJ 6-9 hours later could be an inconsistent comparison. The second reasoning is our use of vertically integrated moisture transport (VI-MT). Although the LLJ and the vertically integrated moisture transport may not be synonymous with each other, the time analyzed for moisture transport from the Gulf of Mexico was consistent with the time analyzed for other fields. However, the

connection of LLJ's to convective storm development is well established (e.g., Bonner 1968; Augustine et al. 1994; Arritt et al. 1997; Pan et al. 2004; Trier et al. 2014) and is examined much more frequently than VI-MT. It would be of interest in any future work to determine the behavior of LLJ for both the CMIP5 and NARRCAP ensembles during very heavy precipitation events, and how they compare with other peer-reviewed literature.

Finally, the utilization self-organizing maps (SOMs; Kohonen 2001) may be a useful diagnostic tool to examine widespread very heavy precipitation events. SOMs are similar to a cluster analysis, utilizing an unsupervised learning process to create a user determined two-dimensional array of nodes in order to segregate major pattern characteristics in the input data. The number of nodes in an array determines the strength of segregation, with a small array providing fairly general features in pattern space, and a large array potentially providing wider but somewhat unnecessary segregation of patterns (Cavazos 2000; Gutowski et al 2004; Cassano et al. 2015). Initial studies (not shown) were performed by training a 6 x 4 SOM array for models included in both the contemporary and scenario climates. Although preliminary results did provide further details on the preferred circulations patterns of both models and observations that were not seen our composite analysis, there is a need for additional diagnosis before applying our results from SOMs to this, or any future manuscripts.

References

Arritt, R. W., T. D. Rink, M. Segal, D. P. Todey, C. A. Clark, M. J. Mitchell, and K. M. Labas, 1997:The Great Plains low-level jet during the warm season of 1993. *Mon. Wea. Rev.*, **125**, 2176–2192, doi:10.1175/1520-0493(1997)125<2176:TGPLLJ>2.0.CO;2.

Augustine, J. A., and F. Caracena, 1994: Lower-tropospheric precursors to nocturnal MCS development over the central United States. *Wea. Forecasting*, **9,** 116–135, doi:10.1175/1520-0434(1994)009<0116:LTPTNM>2.0.CO;2.

Bonner, W. D., 1968: Climatology of the low level jet. *Mon. Wea. Rev.*, **96**, 833–850, doi:10.1175/1520-0493(1968)096<0833:COTLLJ>2.0.CO;2.

Bukovsky, M. S., D. J. Gochis, and L. O. Mearns, 2013: Towards assessing NARCCAP regional climate model credibility for the North American monsoon: Current climate simulations. *J. Climate*, **26**,8802–8826, doi:10.1175/JCLI-D-12-00538.1.

Cassano, E. N., J. M. Glisan, J. J. Cassano, W. J. Gutowski, and M. W. Seefeldt, 2015: Self-organizing map analysis of widespread temperature extremes in Alaska and Canada, *Climate Res.*, **62**, 199–218, doi:10.3354/cr01274.

Cavazos, T., 2000: Using self-organizing maps to investigate extreme climate events: An application to wintertime precipitation in the Balkans. *J. Climate*, **13**, 1718–1732, doi:10.1175/1520-0442(2000)013<1718:USOMTI>2.0.CO;2.

Gutowski, W. J., F. O. Otieno, R. W. Arritt, E. S. Takle, and Z. Pan, 2004: Diagnosis and attribution of a seasonal precipitation deficit in a U.S. regional climate simulation. *J. Hydrometeor.*, **5**, 230–242, doi: 10.1175/1525-7541(2004)005<0230:DAAOAS>2.0.CO;2.

Kohonen, T., 2001: *Self-Organizing Maps*. Springer Series in Information Sciences, Vol. 30, 3d ed., Springer-Verlag, 501 pp.

Pan, Z., M. Segal, and R. W. Arritt, 2004: Role of topography in forcing low-level jets in the central United States during the 1993 flood-altered terrain simulations. *Mon. Wea. Rev.*, **132**, 396–403, doi:10.1175/1520-0493(2004)132<0396:ROTIFL>2.0.CO;2.

Trier, S. B., C. A. Davis, and R. E. Carbone, 2014: Mechanisms governing the persistence and diurnal cycle of a heavy rainfall corridor. *J. Atmos. Sci.*, **71**, 4102–4126, doi:10.1175/JAS-D-14-0134.1.